NASA TN D-383

TECHNICAL NOTE

D-383

THEORETICAL CALCULATIONS OF THE PRESSURES, FORCES, AND MOMENTS DUE TO VARIOUS LATERAL MOTIONS ACTING ON TAPERED SWEPTBACK VERTICAL TAILS WITH SUPERSONIC LEADING AND TRAILING EDGES

By Kenneth Margolis and Miriam H. Elliott

Langley Research Center
Langley Field, Va.

NATIONAL AERONAUTICS AND SPACE ADMINISTRATION

WASHINGTON August 1960

NATIONAL AERONAUTICS AND SPACE ADMINISTRATION

TECHNICAL NOTE D-383

THEORETICAL CALCULATIONS OF THE PRESSURES, FORCES, AND MOMENTS DUE TO VARIOUS LATERAL MOTIONS ACTING ON TAPERED SWEPTBACK VERTICAL TAILS WITH SUPERSONIC LEADING AND TRAILING EDGES

By Kenneth Margolis and Miriam H. Elliott

SUMMARY

Based on expressions for the linearized velocity potentials and pressure distributions given in NACA Technical Report 1268, formulas for the span load distribution, forces, and moments are derived for families of thin isolated vertical tails with arbitrary aspect ratio, taper ratio, and sweepback performing the motions constant sideslip, steady rolling, steady yawing, and constant lateral acceleration. The range of Mach number considered corresponds, in general, to the condition that the tail leading and trailing edges are supersonic.

To supplement the analytical results, design-type charts are presented which enable rapid estimation of the forces and moments (expressed as stability derivatives) for given combinations of geometry parameters and Mach number.

INTRODUCTION

Formulas for the linearized velocity potentials and pressure distributions to enable the calculation of the span loading due to various motions over thin isolated vertical tails at supersonic speeds were presented in reference 1. The purpose of the present paper is to utilize these formulas to derive analytical expressions for the span load distribution and the resulting forces and moments applicable to a family of conventionally tapered vertical tails of arbitrary sweepback and aspect ratio (fig. 1). The range of Mach number considered prescribes that the tail leading and trailing edges are both supersonic subject to a relatively minor restriction that the subsonic-edged root and tip are noninteracting. Motions treated are constant sideslip, steady rolling, steady yawing, and constant lateral acceleration.

Series of design-type charts are presented which summarize the force and moment results and enable the estimation of stability derivatives for a given vertical tail at a desired Mach number. Tabulations of formulas are also included to allow calculations to be carried out for the span loading.

SYMBOLS

L
7
8
0

x,y,z	rectangular coordinates (see fig. 2(a))
$\bar{z}$	nondimensional rectangular coordinate, z/b
V	free-stream or flight velocity (see fig. 2)
ρ	density of air
q	dynamic pressure, $\frac{1}{2}\rho V^2$
ϕ	perturbation velocity potential due to particular motion under consideration, evaluated on negative y-side of tail surface (see fig. 2)
$\Delta\phi$	difference in perturbation velocity potential between two sides of tail surface, $\phi(x,0^+,z) - \phi(x,0^-,z)$
$\Delta P/q$	coefficient of pressure difference between two sides of tail surface due to particular motion under consideration, positive in sense of positive side force (see fig. 2)
M	Mach number, $\frac{V}{\text{Sonic speed}}$
B	Mach number parameter, $\sqrt{M^2 - 1}$
Γ	spanwise distribution of circulation, $\frac{V}{2}\int_{x_{le}}^{x_{te}} \frac{\Delta P}{q}\,dx$
b	span of vertical tail
c_r	root chord of vertical tail
λ	taper ratio, $\frac{\text{Tip chord}}{\text{Root chord}}$

m slope of tail leading edge, cotangent of leading-edge sweepback angle (see fig. 1)

A aspect ratio of vertical tail, b^2/S

$\bar{A}$ aspect-ratio—Mach number parameter, AB

$\bar{m}$ sweepback-Mach number parameter, mB

S area of vertical tail

L
7
8
0

β angle of sideslip

p,r angular velocities about X- and Z-axis, respectively (see fig. 2)

t time

$\dot{\beta}$ rate of change of β with time, $d\beta/dt$

F_Y side force

M_Z yawing moment

M_X rolling moment

C_Y side-force coefficient, F_Y/qS

C_n yawing-moment coefficient, M_Z/qSb

C_l rolling-moment coefficient, M_X/qSb

$$C_{Y_\beta} = \left(\frac{\partial C_Y}{\partial \beta}\right)_{\beta \to 0}$$

$$C_{n_\beta} = \left(\frac{\partial C_n}{\partial \beta}\right)_{\beta \to 0}$$

$$C_{l_\beta} = \left(\frac{\partial C_l}{\partial \beta}\right)_{\beta \to 0}$$

$$C_{Y_p} = \left(\frac{\partial C_Y}{\partial \frac{pb}{V}}\right)_{p \to 0}$$

$$C_{n_p} = \left(\frac{\partial C_n}{\partial \frac{pb}{V}}\right)_{p \to 0}$$

$$C_{l_p} = \left(\frac{\partial C_l}{\partial \frac{pb}{V}}\right)_{p \to 0}$$

$$C_{Y_r} = \left(\frac{\partial C_Y}{\partial \frac{rb}{V}}\right)_{r \to 0}$$

$$C_{n_r} = \left(\frac{\partial C_n}{\partial \frac{rb}{V}}\right)_{r \to 0}$$

$$C_{l_r} = \left(\frac{\partial C_l}{\partial \frac{rb}{V}}\right)_{r \to 0}$$

$$C_{Y_{\dot{\beta}}} = \left(\frac{\partial C_Y}{\partial \frac{\dot{\beta} b}{V}}\right)_{\dot{\beta} \to 0}$$

$$C_{n_{\dot{\beta}}} = \left(\frac{\partial C_n}{\partial \frac{\dot{\beta} b}{V}}\right)_{\dot{\beta} \to 0}$$

$$C_{l_{\dot{\beta}}} = \left(\frac{\partial C_l}{\partial \frac{\dot{\beta} b}{V}}\right)_{\dot{\beta} \to 0}$$

P_1 — specific value of $\bar{z}$ where the Mach line from the leading edge of the root section intersects the trailing edge (see fig. 1)

P_2 — specific value of $\bar{z}$ where the Mach line from the leading edge of the tip section intersects the trailing edge (see fig. 2)

$F_1, F_2, \ldots F_6$ — functions used in formulas for spanwise distribution of circulation

Subscripts:

β — due to sideslip

p — due to rolling

r — due to yawing

$\dot{\beta}$ — due to lateral acceleration

$\beta=1$ — due to unit sideslip

r=1 — due to unit yawing

1,2 — components used for $\dot{\beta}$ derivatives

le — leading edge

te — trailing edge

All angles are measured in radians.

DERIVATION OF FORMULAS

The evaluation of the spanwise loading requires a knowledge of the pressure distribution over the tail surface and is expressible in integral form as $\int_{x_{le}}^{x_{te}} \frac{\Delta P}{q}\,dx$. The spanwise distribution of circulation Γ is directly proportional to the span loading (i.e., V/2 multiplied by the span loading) and will be used in the present report in preference to the span loading in order to maintain consistency with several previously published papers dealing with plane-surface loadings. The basic relation for the spanwise distribution of circulation is thus given by

$$\Gamma(z) = \frac{V}{2} \int_{x_{le}}^{x_{te}} \frac{\Delta P}{q} (x,z) dx \tag{1}$$

The pressure-difference distribution $\frac{\Delta P}{q} (x,z)$ is expressible in terms of the perturbation-velocity-potential difference or "potential jump across the surface" $\Delta\phi$ by means of the linearized relationship

$$\frac{\Delta P}{q} = \frac{2}{V^2}\left(V \frac{\partial}{\partial x} \Delta\phi + \frac{\partial}{\partial t} \Delta\phi\right) \tag{2}$$

L780

Since the current investigation considers only thin isolated tail surfaces with no induced effects present from any neighboring surface, the perturbation velocity potentials on the two sides of the tail are equal in magnitude but are of opposite sign. Equation (2) may then be rewritten in terms of the perturbation velocity potential ϕ as follows:

$$\frac{\Delta P}{q} = - \frac{4}{V^2}\left(V \frac{\partial\phi}{\partial x} + \frac{\partial\phi}{\partial t}\right) \tag{3}$$

where ϕ is evaluated on the negative y-side of the tail surface.

For the steady motions of β, p, and r, equation (3) becomes simply

$$\frac{\Delta P}{q} = - \frac{4}{V} \frac{\partial\phi}{\partial x} \tag{4}$$

and upon substitution of equation (4) into equation (1) and direct integration there results the expression

$$\Gamma(z) = 2\phi\left(x_{te}, z\right) \tag{5}$$

For the unsteady motion $\dot{\beta}$ the analysis and procedures discussed in reference 1 yield the applicable pressure-difference formula

$$\frac{\Delta P}{q} = - \frac{\dot{\beta}}{B^2}\left[M^2\left(\frac{\Delta P}{q}\right)_{r=1} + \frac{M^2 x}{V}\left(\frac{\Delta P}{q}\right)_{\beta=1} - \frac{4}{V^2} \phi_{\beta=1}\right] \tag{6}$$

Substitution of equation (6) into equation (1) and integration through utilization of equation (4) yield the following expression for evaluating $\Gamma(z)$ for the $\dot{\beta}$ motion:

$$\Gamma(z) = 2\dot{\beta}\left[\frac{M^2}{B^2}\,\phi_{r=1}(x_{te},z) + \frac{M^2}{VB^2}\,x_{te}\phi_{\beta=1}(x_{te},z) - \frac{1}{V}\int_{x_{le}}^{x_{te}} \phi_{\beta=1}(x,z)dx\right] \tag{7}$$

where x_{le} and x_{te} are linear functions of z. (Note that $\phi_{r=1}(x_{le},z)$ and $\phi_{\beta=1}(x_{le},z)$ are both zero - see ref. 1. An analogous expression for wings undergoing constant vertical acceleration is given in ref. 2.)

L 7 8 0

Calculation of the spanwise distributions of circulation (eq. (5) for β, p, and r motions; eq. (7) for $\dot{\beta}$ motion) thus requires direct trailing-edge evaluations of previously derived velocity-potential functions (ref. 1) and an added integration for the $\dot{\beta}$ motion.

The forces and moments acting on the vertical tail due to each motion may be obtained by plan-form integrations of the appropriate pressure-distribution functions (given in ref. 1) and may be given as follows

$$F_Y = q\int_0^b \int_{x_{le}}^{x_{te}} \frac{\Delta P}{q}\,dx\,dz \tag{8}$$

$$M_Z = -q\int_0^b \int_{x_{le}}^{x_{te}} \frac{\Delta P}{q}\,x\,dx\,dz \tag{9}$$

$$M_X = q\int_0^b \int_{x_{le}}^{x_{te}} \frac{\Delta P}{q}\,z\,dx\,dz \tag{10}$$

where the moment reference is assumed to be at the leading edge of the root section. Inasmuch as for steady motions $\frac{\Delta P}{q} = -\frac{4}{V}\frac{\partial\phi}{\partial x}$, the first integration with respect to x in equations (8) and (10) directly yields ϕ (tabulated in ref. 1), and thus the derivations of F_Y and M_X for β, p, and r motions reduce to essentially a single integration involving the velocity-potential function.

The nondimensional force and moment coefficients and corresponding stability derivatives are directly obtainable from the definitions given in the list of symbols. For example,

$$C_{Y_\beta} = -C_{L_\alpha}$$

$$C_{n_\beta} = -\frac{4}{3A}\,\frac{1 + \lambda + \lambda^2}{(1 + \lambda)^2}\,C_{m_\alpha}$$

$$C_{Y_r} = \frac{2}{3A}\,\frac{1 + \lambda + \lambda^2}{(1 + \lambda)^2}\,C_{L_q}$$

$$C_{n_r} = \frac{8}{9A^2}\,\frac{\left(1 + \lambda + \lambda^2\right)^2}{(1 + \lambda)^4}\,C_{m_q}$$

L780

$$C_{Y_{\dot\beta}} = -\frac{2}{3A}\,\frac{1 + \lambda + \lambda^2}{(1 + \lambda)^2}\,C_{L_{\dot\alpha}}$$

$$C_{n_{\dot\beta}} = -\frac{8}{9A^2}\,\frac{\left(1 + \lambda + \lambda^2\right)^2}{(1 + \lambda)^4}\,C_{m_{\dot\alpha}}$$

where the wing derivatives C_{L_α}, C_{m_α}, C_{L_q}, C_{m_q}, $C_{L_{\dot\alpha}}$, and $C_{m_{\dot\alpha}}$ are defined and evaluated in references 3, 4, and 5 and should be computed for an aspect ratio twice that of the vertical tail.

In order to obtain vertical-tail derivatives applicable for other moment-reference locations (item b), the presented curves and formulas may be used in conjunction with the axes-transformation formulas presented in table II.

Relative to item (c), the magnitudes of the tail derivatives may appear to be quite large with respect to the expected tail contributions to the derivatives of a complete airplane. The following factors should be used in converting the presented analytical and numerical results to corresponding derivatives (denoted in the following relationships by subscript w) based on wing area S_w, wing span b_w, and angles $pb_w/2V$, $rb_w/2V$, and $\dot\beta b_w/2V$:

$$\left(C_{Y_\beta}\right)_w = \frac{S}{S_w} C_{Y_\beta}$$

$$\left(C_{n_\beta}\right)_w, \left(C_{l_\beta}\right)_w = \frac{S}{S_w} \frac{b}{b_w}\left(C_{n_\beta}, C_{l_\beta}\right)$$

$$\left(C_{Y_p}\right)_w, \left(C_{Y_r}\right)_w, \left(C_{Y_{\dot{\beta}}}\right)_w = 2 \frac{S}{S_w} \frac{b}{b_w}\left(C_{Y_p}, C_{Y_r}, C_{Y_{\dot{\beta}}}\right)$$

$$\left(C_{n_p}\right)_w, \left(C_{l_p}\right)_w, \left(C_{n_r}\right)_w, \left(C_{l_r}\right)_w, \left(C_{n_{\dot{\beta}}}\right)_w, \left(C_{l_{\dot{\beta}}}\right)_w = 2 \frac{S}{S_w}\left(\frac{b}{b_w}\right)^2\left(C_{n_p}, C_{l_p}, C_{n_r}, C_{l_r}, C_{n_{\dot{\beta}}}, C_{l_{\dot{\beta}}}\right)$$

L 780

CONCLUDING REMARKS

Expressions based on the application of linearized thin-airfoil theory for supersonic speeds have been derived for the span loading, forces, and moments due to various lateral motions for a family of thin isolated vertical tails of arbitrary sweepback and taper ratio. Motions considered were constant sideslip, steady rolling, steady yawing, and constant lateral acceleration. Forces and moments, expressed in the form of stability derivatives, are also presented in a series of design-type charts which facilitate evaluation for given values of Mach number and tail-geometry parameters. The results are, in general, applicable at those supersonic speeds for which both the tail leading and trailing edges are supersonic.

Langley Research Center,
National Aeronautics and Space Administration,
Langley Field, Va., February 19, 1960.

APPENDIX A

FORMULAS FOR SPANWISE DISTRIBUTION OF CIRCULATION DUE TO CONSTANT SIDESLIP

The formulas for spanwise distribution of circulation due to constant sideslip motion may be summarized for the various spanwise regions (see sketches) as follows:

L 780

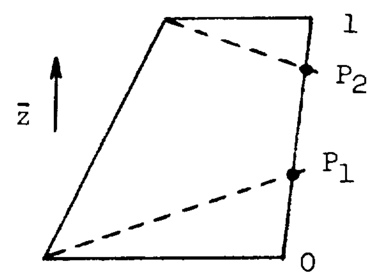

Condition	Formula for $-\frac{\Gamma}{\beta V b}$
$0 \leqq \bar{z} \leqq P_1$	F_1
$P_1 < \bar{z} \leqq P_2$	F_2
$P_2 < \bar{z} \leqq 1$	F_3

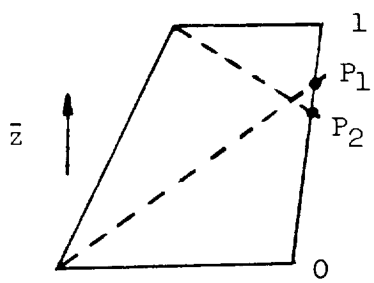

Condition	Formula for $-\frac{\Gamma}{\beta V b}$
$0 \leqq \bar{z} \leqq P_2$	F_1
$P_2 < \bar{z} \leqq P_1$	$F_1 + F_3 - F_2$
$P_1 < \bar{z} \leqq 1$	F_3

where

$$P_1 = \frac{2\bar{m}}{\bar{A}(\bar{m} - 1)(1 + \lambda) + 2\bar{m}(1 - \lambda)}$$

and

$$P_2 = \frac{\bar{A}(\bar{m} + 1)(1 + \lambda) - 2\bar{m}}{\bar{A}(\bar{m} + 1)(1 + \lambda) - 2\bar{m}(1 - \lambda)}$$

and the F functions are as follows:

L-780

$$F_1 = \frac{4}{\pi\bar{A}^{1/2}(\bar{m}+1)^{1/2}(1+\lambda)^{1/2}}\sqrt{-\left[\bar{A}(\bar{m}-1)(1+\lambda)+2\bar{m}(1-\lambda)\right]\bar{z}^2+2\bar{m}\bar{z}}$$

$$-\frac{4\bar{m}}{\pi\bar{A}(1+\lambda)(\bar{m}^2-1)^{1/2}}\left[(1-\lambda)\bar{z}-1\right]\cos^{-1}\frac{\left[\bar{A}(\bar{m}-1)(1+\lambda)+\bar{m}(1-\lambda)\right]\bar{z}-\bar{m}}{\bar{m}\left[(1-\lambda)\bar{z}-1\right]}$$

$$F_2 = \frac{-4\bar{m}}{\bar{A}(1+\lambda)(\bar{m}^2-1)^{1/2}}\left[(1-\lambda)\bar{z}-1\right]$$

$$F_3 = \frac{4}{\pi\bar{A}^{1/2}(1+\lambda)^{1/2}(\bar{m}-1)^{1/2}}\sqrt{-\left[\bar{A}(\bar{m}+1)(1+\lambda)-2\bar{m}(1-\lambda)\right]\bar{z}^2+2\left[\bar{A}(\bar{m}+1)(1+\lambda)-\bar{m}(2-\lambda)\right]\bar{z}-\left[\bar{A}(1+\lambda)(\bar{m}+1)-2\bar{m}\right]}$$

$$-\frac{4\bar{m}}{\pi\bar{A}(1+\lambda)(\bar{m}^2-1)^{1/2}}\left[(1-\lambda)\bar{z}-1\right]\cos^{-1}\frac{-\left[\bar{A}(\bar{m}+1)(1+\lambda)-\bar{m}(1-\lambda)\right]\bar{z}+\left[\bar{A}(\bar{m}+1)(1+\lambda)-\bar{m}\right]}{\bar{m}\left[(1-\lambda)\bar{z}-1\right]}$$

APPENDIX B

FORMULAS FOR SPANWISE DISTRIBUTION OF CIRCULATION DUE TO STEADY ROLLING

The formulas for spanwise distribution of circulation due to steady rolling motion may be summarized for the various spanwise regions (see sketches) as follows: L 7 8 0

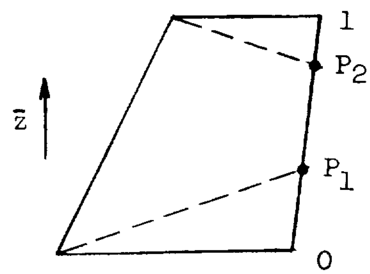

Condition	Formula for $-\frac{\Gamma}{pb^2}$
$0 \leqq \bar{z} \leqq P_1$	F_1
$P_1 < \bar{z} \leqq P_2$	F_2
$P_2 < \bar{z} \leqq 1$	F_3

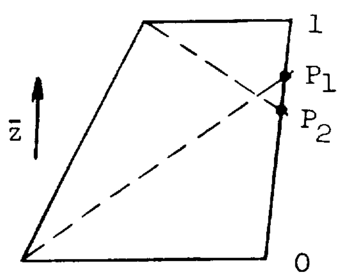

Condition	Formula for $-\frac{\Gamma}{pb^2}$
$0 \leqq \bar{z} \leqq P_2$	F_1
$P_2 < \bar{z} \leqq P_1$	$F_1 + F_3 - F_2$
$P_1 < \bar{z} \leqq 1$	F_3

where

$$P_1 = \frac{2\bar{m}}{\bar{A}(\bar{m} - 1)(1 + \lambda) + 2\bar{m}(1 - \lambda)}$$

and

$$P_2 = \frac{\bar{A}(\bar{m} + 1)(1 + \lambda) - 2\bar{m}}{\bar{A}(\bar{m} + 1)(1 + \lambda) - 2\bar{m}(1 - \lambda)}$$

and the F functions are as follows:

$$F_1 = \frac{4}{3\pi(\bar{m}+1)^{3/2}(\bar{m}-1)\bar{A}^{3/2}(1+\lambda)^{3/2}}\left\{\left[\bar{A}(\bar{m}+2)(\bar{m}-1)(1+\lambda) - \bar{m}(4\bar{m}-1)(1-\lambda)\right]\bar{z}\right.$$

$$\left. + \bar{m}(4\bar{m}-1)\right\}\sqrt{-\left[\bar{A}(\bar{m}-1)(1+\lambda) + 2\bar{m}(1-\lambda)\right]\bar{z}^2 + 2\bar{m}\bar{z}} - \frac{4\bar{m}}{\pi\bar{A}^2(\bar{m}^2-1)^{3/2}(1+\lambda)^2}\left\{\left[\bar{A}(\bar{m}^2-1)(1-\lambda^2)\right.\right.$$

$$\left.\left. + \bar{m}(1-\lambda)^2\right]\bar{z}^2 - \left[\bar{A}(\bar{m}^2-1)(1+\lambda) + 2\bar{m}(1-\lambda)\right]\bar{z} + \bar{m}\right\}\cos^{-1}\frac{\left[\bar{A}(\bar{m}-1)(1+\lambda) + \bar{m}(1-\lambda)\right]\bar{z} - \bar{m}}{\bar{m}(1-\lambda)\bar{z} - \bar{m}}$$

L-780

$$F_2 = \frac{-4\bar{m}}{\bar{A}^2(\bar{m}^2-1)^{3/2}(1+\lambda)^2}\left\{\left[\bar{A}(\bar{m}^2-1)(1-\lambda^2) + \bar{m}(1-\lambda)^2\right]\bar{z}^2 - \left[\bar{A}(\bar{m}^2-1)(1+\lambda) + 2\bar{m}(1-\lambda)\right]\bar{z} + \bar{m}\right\}$$

$$F_3 = \frac{4}{3\pi(\bar{m}+1)(\bar{m}-1)^{3/2}\bar{A}^{3/2}(1+\lambda)^{3/2}}\left\{\left[\bar{A}(\bar{m}-2)(\bar{m}+1)(1+\lambda) + \bar{m}(4\bar{m}+1)(1-\lambda)\right]\bar{z} + \bar{A}\left[(2\bar{m}-1)(\bar{m}+1)(1+\lambda)\right.\right.$$

$$\left.\left. - \bar{m}(4\bar{m}+1)\right]\right\}\sqrt{-\left[\bar{A}(\bar{m}+1)(1+\lambda) - 2\bar{m}(1-\lambda)\right]\bar{z}^2 + 2\left[\bar{A}(\bar{m}+1)(1+\lambda) - \bar{m}(2-\lambda)\right]\bar{z} - \left[\bar{A}(1+\lambda)(\bar{m}+1) - 2\bar{m}\right]}$$

$$- \frac{4\bar{m}}{\pi\bar{A}^2(\bar{m}^2-1)^{3/2}(1+\lambda)^2}\left\{\left[\bar{A}(\bar{m}^2-1)(1-\lambda^2) + \bar{m}(1-\lambda)^2\right]\bar{z}^2 - \left[\bar{A}(\bar{m}^2-1)(1+\lambda) + 2\bar{m}(1-\lambda)\right]\bar{z} + \bar{m}\right\}$$

$$\cos^{-1}\frac{-\left[\bar{A}(\bar{m}+1)(1+\lambda) - \bar{m}(1-\lambda)\right]\bar{z} + \left[\bar{A}(\bar{m}+1)(1+\lambda) - \bar{m}\right]}{\bar{m}(1-\lambda)\bar{z} - \bar{m}}$$

APPENDIX C

FORMULAS FOR SPANWISE DISTRIBUTION OF CIRCULATION DUE TO STEADY YAWING

The formulas for spanwise distribution of circulation due to steady yawing motion may be summarized for the various spanwise regions (see sketches) as follows:

L
7
8
0

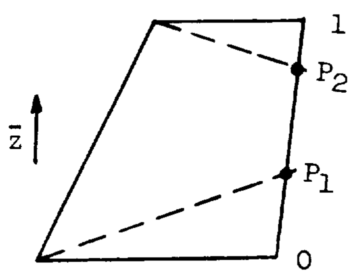

	Condition	Formula for $-\frac{\Gamma}{Brb^2}$
	$0 \leqq \bar{z} \leqq P_1$	F_1
	$P_1 < \bar{z} \leqq P_2$	F_2
	$P_2 < \bar{z} \leqq 1$	F_3

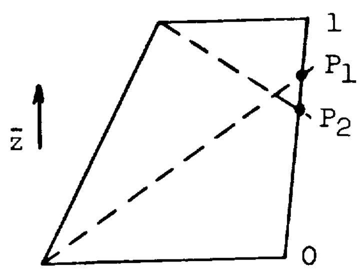

	Condition	Formula for $-\frac{\Gamma}{Brb^2}$
	$0 \leqq \bar{z} \leqq P_2$	F_1
	$P_2 < \bar{z} \leqq P_1$	$F_1 + F_3 - F_2$
	$P_1 < \bar{z} \leqq 1$	F_3

where

$$P_1 = \frac{2\bar{m}}{\bar{A}(\bar{m} - 1)(1 + \lambda) + 2\bar{m}(1 - \lambda)}$$

and

$$P_2 = \frac{\bar{A}(\bar{m} + 1)(1 + \lambda) - 2\bar{m}}{\bar{A}(\bar{m} + 1)(1 + \lambda) - 2\bar{m}(1 - \lambda)}$$

and the F functions are given as follows:

$$F_1 = \frac{4}{3\pi\bar{m}(\bar{m}+1)^{3/2}(\bar{m}-1)\bar{A}^{3/2}(1+\lambda)^{3/2}}\Bigg\{\bar{z}\left[\bar{A}(1+\lambda)(\bar{m}^3 - 2\bar{m}^2 - 2\bar{m} + 3) + \bar{m}(1-\lambda)(5\bar{m}^2 + 4\bar{m} - 6)\right] - \bar{m}(5\bar{m}^2$$

$$+ 4\bar{m} - 6)\Bigg\}\sqrt{-\left[\bar{A}(\bar{m}-1)(1+\lambda) + 2\bar{m}(1-\lambda)\right]\bar{z}^2 + 2\bar{m}\bar{z}} + \frac{4}{\pi(\bar{m}^2-1)^{3/2}\bar{A}^2(1+\lambda)^2}\Bigg\{\bar{z}^2\Big[\bar{A}(1-\lambda^2)(\bar{m}^2-1)$$

$$- \bar{m}(\bar{m}^2-2)(1-\lambda)^2\Big] - \bar{z}\left[\bar{A}(1+\lambda)(\bar{m}^2-1) - 2\bar{m}(1-\lambda)(\bar{m}^2-2)\right]$$

$$- \bar{m}(\bar{m}^2-2)\Bigg\}\cos^{-1}\frac{\left[\bar{A}(1+\lambda)(\bar{m}-1) + \bar{m}(1-\lambda)\right]\bar{z} - \bar{m}}{\bar{m}(1-\lambda)\bar{z} - \bar{m}}$$

$$F_2 = \frac{4}{(\bar{m}^2-1)^{3/2}\bar{A}^2(1+\lambda)^2}\left\{\bar{z}^2\left[\bar{A}(1-\lambda^2)(\bar{m}^2-1) - \bar{m}(\bar{m}^2-2)(1-\lambda)^2\right] - \bar{z}\left[\bar{A}(1+\lambda)(\bar{m}^2-1) - 2\bar{m}(1-\lambda)(\bar{m}^2-2)\right] - \bar{m}(\bar{m}^2-2)\right\}$$

$$F_3 = \frac{4}{3\pi\bar{m}(\bar{m}+1)(\bar{m}-1)^{3/2}\bar{A}^{3/2}(1+\lambda)^{3/2}}\Bigg\{-\bar{z}\left[\bar{A}(1+\lambda)(\bar{m}^3 + 2\bar{m}^2 - 2\bar{m} - 3) - \bar{m}(1-\lambda)(5\bar{m}^2 - 4\bar{m} - 6)\right] + \bar{A}(1+\lambda)(\bar{m}^3 - \bar{m}^2 - 2\bar{m})$$

$$- \bar{m}(5\bar{m}^2 - 4\bar{m} - 6)\Bigg\}\sqrt{-\left[\bar{A}(\bar{m}+1)(1+\lambda) - 2\bar{m}(1-\lambda)\right]\bar{z}^2 + \left[2\bar{A}(\bar{m}+1)(1+\lambda) - 2\bar{m}(2-\lambda)\right]\bar{z} - \left[\bar{A}(1+\lambda)(\bar{m}+1) - 2\bar{m}\right]}$$

$$+ \frac{4}{\pi(\bar{m}^2-1)^{3/2}\bar{A}^2(1+\lambda)^2}\Bigg\{\bar{z}^2\left[\bar{A}(1-\lambda^2)(\bar{m}^2-1) - \bar{m}(\bar{m}^2-2)(1-\lambda)^2\right] - \bar{z}\left[\bar{A}(1+\lambda)(\bar{m}^2-1) - 2\bar{m}(1-\lambda)(\bar{m}^2-2)\right]$$

$$- \bar{m}(\bar{m}^2-2)\Bigg\}\cos^{-1}\frac{-\left[\bar{A}(1+\lambda)(\bar{m}+1) - \bar{m}(1-\lambda)\right]\bar{z} + \left[\bar{A}(1+\lambda)(\bar{m}+1) - \bar{m}\right]}{\bar{m}(1-\lambda)\bar{z} - \bar{m}}$$

APPENDIX D

FORMULAS FOR SPANWISE DISTRIBUTION OF CIRCULATION DUE TO CONSTANT LATERAL ACCELERATION

The formulas for spanwise distribution of circulation due to constant lateral acceleration motion may be summarized for the various spanwise regions (see sketches) as follows: L780

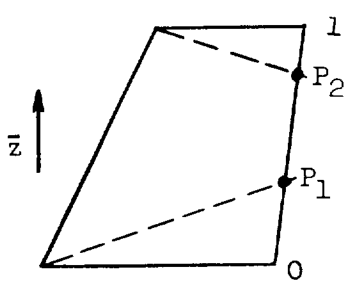

Condition	Formula for $\frac{\Gamma}{\dot{\beta} b^2}$
$0 \leqq \bar{z} \leqq P_1$	$F_1 + F_2$
$P_1 < \bar{z} \leqq P_2$	$F_3 + F_4$
$P_2 < \bar{z} \leqq 1$	$F_5 + F_6$

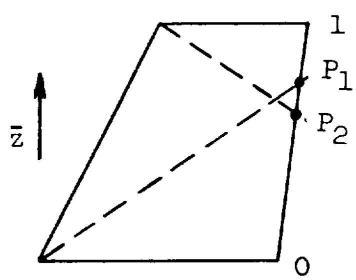

Condition	Formula for $\frac{\Gamma}{\dot{\beta} b^2}$
$0 \leqq \bar{z} \leqq P_2$	$F_1 + F_2$
$P_2 < \bar{z} \leqq P_1$	$F_1 + F_2 + F_5 + F_6 - F_3 - F_4$
$P_1 < \bar{z} \leqq 1$	$F_5 + F_6$

where

$$P_1 = \frac{2\bar{m}}{\bar{A}(\bar{m} - 1)(1 + \lambda) + 2\bar{m}(1 - \lambda)}$$

and

$$P_2 = \frac{\bar{A}(\bar{m} + 1)(1 + \lambda) - 2\bar{m}}{\bar{A}(\bar{m} + 1)(1 + \lambda) - 2\bar{m}(1 - \lambda)}$$

and the F functions are given as follows:

L-780

$$\frac{1}{B}F_1 = \frac{4\bar{m}}{\pi\bar{A}^2(1+\lambda)^2(\bar{m}^2-1)^{3/2}}\left[(1-\lambda)\bar{z}-1\right]^2\cos^{-1}\frac{\left[\bar{A}(\bar{m}-1)(1+\lambda)+\bar{m}(1-\lambda)\right]\bar{z}-\bar{m}}{\bar{m}(1-\lambda)\bar{z}-\bar{m}}$$

$$+\frac{4}{3\pi\bar{m}(\bar{m}+1)^{3/2}(\bar{m}-1)\bar{A}^{3/2}(1+\lambda)^{3/2}}\left\{\left[\bar{A}(\bar{m}-1)(1+\lambda)-\bar{m}(1-\lambda)\right]\bar{z}+\bar{m}\right\}\sqrt{-\left[\bar{A}(\bar{m}-1)(1+\lambda)+2\bar{m}(1-\lambda)\right]\bar{z}^2+2\bar{m}\bar{z}}$$

$$-\frac{8(\bar{m}^2+\bar{m}-1)}{3\pi\bar{m}(\bar{m}+1)^{3/2}(\bar{m}-1)\bar{A}^{3/2}(1+\lambda)^{3/2}}\frac{\left\{-\left[\bar{A}(\bar{m}-1)(1+\lambda)+2\bar{m}(1-\lambda)\right]\bar{z}^2+2\bar{m}\bar{z}\right\}^{3/2}}{\bar{z}}$$

$$BF_2 = \frac{4\bar{m}^3}{\pi\bar{A}^2(1+\lambda)^2(\bar{m}^2-1)^{3/2}}\left[(1-\lambda)\bar{z}-1\right]^2\cos^{-1}\frac{\left[\bar{A}(\bar{m}-1)(1+\lambda)+\bar{m}(1-\lambda)\right]\bar{z}-\bar{m}}{\bar{m}(1-\lambda)\bar{z}-\bar{m}}$$

$$+\frac{4\bar{m}}{3\pi(\bar{m}+1)^{3/2}(\bar{m}-1)\bar{A}^{3/2}(1+\lambda)^{3/2}}\left\{\left[\bar{A}(\bar{m}-1)(1+\lambda)-\bar{m}(1-\lambda)\right]\bar{z}+\bar{m}\right\}\sqrt{-\left[\bar{A}(\bar{m}-1)(1+\lambda)+2\bar{m}(1-\lambda)\right]\bar{z}^2+2\bar{m}\bar{z}}$$

$$-\frac{8}{3\pi(\bar{m}+1)^{3/2}(\bar{m}-1)\bar{A}^{3/2}(1+\lambda)^{3/2}}\frac{\left\{-\left[\bar{A}(\bar{m}-1)(1+\lambda)+2\bar{m}(1-\lambda)\right]\bar{z}^2+2\bar{m}\bar{z}\right\}^{3/2}}{\bar{z}}$$

$$\frac{1}{B}F_3 = \frac{4\bar{m}}{(\bar{m}^2-1)^{3/2}\bar{A}^2(1+\lambda)^2}\left[(1-\lambda)\bar{z}-1\right]^2$$

$$BF_4 = \frac{4\bar{m}^3}{(\bar{m}^2-1)^{3/2}\bar{A}^2(1+\lambda)^2}\left[(1-\lambda)\bar{z}-1\right]^2$$

$$\frac{1}{B}F_5 = \frac{4\bar{m}}{\pi\bar{A}^2(1+\lambda)^2(\bar{m}^2-1)^{3/2}}\left[(1-\lambda)\bar{z}-1\right]^2\cos^{-1}\frac{-\left[\bar{A}(\bar{m}+1)(1+\lambda)-\bar{m}(1-\lambda)\right]\bar{z}+\left[\bar{A}(\bar{m}+1)(1+\lambda)-\bar{m}\right]}{\bar{m}(1-\lambda)\bar{z}-\bar{m}}+\frac{4}{3\pi\bar{m}(\bar{m}+1)(\bar{m}-1)^{3/2}\bar{A}^{3/2}(1+\lambda)^{3/2}}\left\{-\left[\bar{A}(\bar{m}+1)(1+\lambda)\right.\right.$$

$$\left.\left.+\bar{m}(1-\lambda)\right]\bar{z}+\left[\bar{A}(\bar{m}+1)(1+\lambda)+\bar{m}\right]\right\}\sqrt{-\left[\bar{A}(\bar{m}+1)(1+\lambda)-2\bar{m}(1-\lambda)\right]\bar{z}^2+2\left[\bar{A}(\bar{m}+1)(1+\lambda)-\bar{m}(2-\lambda)\right]\bar{z}-\left[\bar{A}(\bar{m}+1)(1+\lambda)-2\bar{m}\right]}$$

$$-\frac{8(\bar{m}^2-\bar{m}-1)}{3\pi\bar{m}(\bar{m}+1)(\bar{m}-1)^{3/2}\bar{A}^{3/2}(1+\lambda)^{3/2}}\frac{\left\{-\left[\bar{A}(\bar{m}+1)(1+\lambda)-2\bar{m}(1-\lambda)\right]\bar{z}^2+2\left[\bar{A}(\bar{m}+1)(1+\lambda)-\bar{m}(2-\lambda)\right]\bar{z}-\left[\bar{A}(\bar{m}+1)(1+\lambda)-2\bar{m}\right]\right\}^{3/2}}{(1-\bar{z})}$$

$$BF_6 = \frac{4\bar{m}^3}{\pi\bar{A}^2(1+\lambda)^2(\bar{m}^2-1)^{3/2}}\left[(1-\lambda)\bar{z}-1\right]^2\cos^{-1}\frac{-\left[\bar{A}(\bar{m}+1)(1+\lambda)-\bar{m}(1-\lambda)\right]\bar{z}+\left[\bar{A}(\bar{m}+1)(1+\lambda)-\bar{m}\right]}{\bar{m}(1-\lambda)\bar{z}-\bar{m}}+\frac{4\bar{m}}{3\pi(\bar{m}+1)(\bar{m}-1)^{3/2}\bar{A}^{3/2}(1+\lambda)^{3/2}}\left\{-\left[\bar{A}(\bar{m}+1)(1+\lambda)\right.\right.$$

$$\left.\left.+\bar{m}(1-\lambda)\right]\bar{z}+\left[\bar{A}(\bar{m}+1)(1+\lambda)+\bar{m}\right]\right\}\sqrt{-\left[\bar{A}(\bar{m}+1)(1+\lambda)-2\bar{m}(1-\lambda)\right]\bar{z}^2+2\left[\bar{A}(\bar{m}+1)(1+\lambda)-\bar{m}(2-\lambda)\right]\bar{z}-\left[\bar{A}(\bar{m}+1)(1+\lambda)-2\bar{m}\right]}$$

$$+\frac{8}{3\pi(\bar{m}+1)(\bar{m}-1)^{3/2}\bar{A}^{3/2}(1+\lambda)^{3/2}}\frac{\left\{-\left[\bar{A}(\bar{m}+1)(1+\lambda)-2\bar{m}(1-\lambda)\right]\bar{z}^2+2\left[\bar{A}(\bar{m}+1)(1+\lambda)-\bar{m}(2-\lambda)\right]\bar{z}-\left[\bar{A}(\bar{m}+1)(1+\lambda)-2\bar{m}\right]\right\}^{3/2}}{(1-\bar{z})}$$

$$\lim_{\bar{A}\to\infty} BC_{l_\beta} = \frac{-4\bar{m}}{3(\bar{m}^2 - 1)^{1/2}}\left(\frac{1 + 2\lambda}{1 + \lambda}\right) \qquad \text{(E11)}$$

$$\lim_{\bar{A}\to\infty} C_{n_\beta} = \frac{4}{3(\bar{m}^2 - 1)^{1/2}}\left(\frac{1 + 2\lambda}{1 + \lambda}\right) \qquad \text{(E12)}$$

L
7
8
0

$$\lim_{\lambda\to 1} BC_{Y_\beta} = \frac{-2\bar{m}}{\bar{A}(\bar{m}^2 - 1)^{3/2}}\left[-\bar{m}^2 + 2\bar{A}(\bar{m}^2 - 1)\right] \qquad \text{(E13)}$$

$$\lim_{\lambda\to 1} BC_{l_\beta} = \frac{-\bar{m}}{\bar{A}^2(\bar{m}^2 - 1)^{5/2}}\left[-\bar{m}^3 - \bar{A}\bar{m}(\bar{m} - 1)^2(\bar{m} + 1) + 2\bar{A}^2(\bar{m} - 1)^2\right] \qquad \text{(E14)}$$

$$\lim_{\lambda\to 1} C_{n_\beta} = \frac{1}{3\bar{A}^2(\bar{m}^2 - 1)^{5/2}}\left[\bar{m}^3(-4\bar{m}^2 + 1) + 3\bar{A}\bar{m}(2\bar{m} + 1)(\bar{m} - 1)^2(\bar{m} + 1) + 6\bar{A}^2(\bar{m} + 1)^2(\bar{m} - 1)^2\right] \qquad \text{(E15)}$$

APPENDIX F

FORMULAS FOR STABILITY DERIVATIVES DUE TO STEADY ROLLING MOTION

L780

The formulas for the stability derivatives associated with steady rolling motion are as follows:

$$BC_{Y_p} = \frac{-4\bar{m}}{3\bar{A}^{1/2}(1+\lambda)^{3/2}(1-\lambda)^2}\left\{\frac{\bar{A}(\bar{m}+1)(1+\lambda)+\bar{m}(1-\lambda)}{(\bar{m}+1)^{3/2}\left[\bar{A}(\bar{m}-1)(1+\lambda)+2\bar{m}(1-\lambda)\right]^{1/2}} + \frac{\lambda^2\left[\bar{A}(\bar{m}-1)(1+\lambda)(2\lambda-3)+\bar{m}\lambda(1-\lambda)\right]}{(\bar{m}-1)^{3/2}\left[\bar{A}(\bar{m}+1)(1+\lambda)-2\bar{m}(1-\lambda)\right]^{1/2}}\right\} \tag{F1}$$

$$BC_{l_p} = \frac{-\bar{m}}{3\bar{A}^{1/2}(1+\lambda)^{3/2}(1-\lambda)^3}\left(\frac{2\bar{A}^2(\bar{m}^2-1)(1+\lambda)^2+2\bar{A}\bar{m}(3\bar{m}+2)(1-\lambda^2)+3\bar{m}^2(1-\lambda)^2}{(\bar{m}+1)^{3/2}\left[\bar{A}(\bar{m}-1)(1+\lambda)+2\bar{m}(1-\lambda)\right]^{3/2}} - \frac{\lambda^2\left\{2\bar{A}^2(3\lambda^2-8\lambda+6)(\bar{m}^2-1)(1+\lambda)^2-2\bar{A}\bar{m}\left[3\lambda^2(\bar{m}-2)-4\lambda(3\bar{m}-4)+12(\bar{m}-1)\right](1-\lambda^2)-\bar{m}^2\lambda(5\lambda-8)(1-\lambda)^2\right\}}{(\bar{m}-1)^{3/2}\left[\bar{A}(\bar{m}+1)(1+\lambda)-2\bar{m}(1-\lambda)\right]^{3/2}}\right) \tag{F2}$$

$$C_{n_p} = \frac{1}{3\bar{A}^{3/2}(1+\lambda)^{5/2}(1-\lambda)^3}\left[\frac{2\bar{A}^3(\bar{m}^2-1)(1+\lambda)^3+2\bar{A}^2\bar{m}(\bar{m}^2+3\bar{m}+1)(1+\lambda)^2(1-\lambda)+\bar{A}\bar{m}^2(6\bar{m}+1)(1+\lambda)(1-\lambda)^2+6\bar{m}^3(1-\lambda)^3}{(\bar{m}+1)^{3/2}\left[\bar{A}(\bar{m}-1)(1+\lambda)+2\bar{m}(1-\lambda)\right]^{3/2}} - \frac{\left(\lambda^2\left\{2\bar{A}^3(3\lambda^2-8\lambda+6)(\bar{m}^2-1)(1+\lambda)^3-2\bar{A}^2\bar{m}(1+\lambda)^2(1-\lambda)\left[3\lambda^2(\bar{m}^2+\bar{m}-3)-4\lambda(\bar{m}^2+3\bar{m}-5)+12(\bar{m}-1)\right] + \bar{A}\bar{m}^2\lambda(1+\lambda)(1-\lambda)^2\left[\lambda(2\bar{m}-15)-8(\bar{m}-2)\right]+6\bar{m}^3\lambda^2(1-\lambda)^3\right\}\right)}{(\bar{m}-1)^{3/2}\left[\bar{A}(\bar{m}+1)(1+\lambda)-2\bar{m}(1-\lambda)\right]^{3/2}}\right] \tag{F3}$$

$$\lim_{\bar{m}\to\infty} BC_{Y_p} = \frac{-4}{3\bar{A}^{1/2}(1-\lambda)^2(1+\lambda)^{3/2}}\left\{\frac{\bar{A}(1+\lambda)+(1-\lambda)}{\left[\bar{A}(1+\lambda)+2(1-\lambda)\right]^{1/2}}+\frac{\lambda^2\left[\bar{A}(1+\lambda)(2\lambda-3)+\lambda(1-\lambda)\right]}{\left[\bar{A}(1+\lambda)-2(1-\lambda)\right]^{1/2}}\right\} \tag{F4}$$

$$\lim_{\bar{m}\to\infty} BC_{l_p} = \frac{-1}{3\bar{A}^{1/2}(1-\lambda)^3(1+\lambda)^{3/2}}\left\{\frac{2\bar{A}^2(1+\lambda)^2+6\bar{A}(1-\lambda^2)+3(1-\lambda)^2}{\left[\bar{A}(1+\lambda)+2(1-\lambda)\right]^{3/2}} - \frac{\lambda^2\left[2\bar{A}^2(3\lambda^2-8\lambda+6)(1+\lambda)^2-2\bar{A}(3\lambda^2-12\lambda+12)(1-\lambda^2)-\lambda(5\lambda-8)(1-\lambda)^2\right]}{\left[\bar{A}(1+\lambda)-2(1-\lambda)\right]^{3/2}}\right\} \tag{F5}$$

$$\lim_{\bar{m}\to\infty} C_{n_p} = \frac{2}{3\bar{A}^{3/2}(1-\lambda)^2(1+\lambda)^{5/2}}\left\{\frac{\bar{A}^2(1+\lambda)^2 + 3\bar{A}(1-\lambda^2) + 3(1-\lambda)^2}{\left[\bar{A}(1+\lambda) + 2(1-\lambda)\right]^{3/2}} + \frac{\lambda^2\left[\bar{A}^2\lambda(3\lambda-4)(1+\lambda)^2 - \bar{A}\lambda(\lambda-4)(1-\lambda^2) - 3\lambda^2(1-\lambda)^2\right]}{\left[\bar{A}(1+\lambda) - 2(1-\lambda)\right]^{3/2}}\right\} \tag{F6}$$

L
7
8
0

$$\lim_{\substack{\bar{A}\to\infty \\ \bar{m}\to\infty}} BC_{Y_p} = \frac{-4(2\lambda^3 - 3\lambda^2 + 1)}{3(1+\lambda)(1-\lambda)^2} \tag{F7}$$

$$\lim_{\substack{\bar{A}\to\infty \\ \bar{m}\to\infty}} BC_{l_p} = \frac{-2(1+3\lambda)}{3(1+\lambda)} \tag{F8}$$

$$\lim_{\substack{\bar{A}\to\infty \\ \bar{m}\to\infty}} C_{n_p} = 0 \tag{F9}$$

$$\lim_{\bar{A}\to\infty} BC_{Y_p} = \frac{-4\bar{m}(2\lambda^3 - 3\lambda^2 + 1)}{3(1+\lambda)(1-\lambda)^2(\bar{m}^2-1)^{1/2}} \tag{F10}$$

$$\lim_{\bar{A}\to\infty} BC_{l_p} = \frac{\bar{m}(6\lambda^4 - 16\lambda^3 + 12\lambda^2 - 2)}{3(1+\lambda)(1-\lambda)^3(\bar{m}^2-1)^{1/2}} \tag{F11}$$

$$\lim_{\bar{A}\to\infty} C_{n_p} = \frac{-(6\lambda^4 - 16\lambda^3 + 12\lambda^2 - 2)}{3(1+\lambda)(1-\lambda)^3(\bar{m}^2-1)^{1/2}} \tag{F12}$$

W

L780

$$\lim_{\lambda \to 1} BC_{Y_p} = \frac{\bar{m}}{\bar{A}^2(\bar{m}^2 - 1)^{5/2}}\left[\bar{m}^3 - \bar{A}\bar{m}(\bar{m}+1)^2(\bar{m}-1) + 2\bar{A}^2(\bar{m}+1)^2(\bar{m}-1)^2\right] \tag{F13}$$

$$\begin{aligned}\lim_{\lambda \to 1} BC_{l_p} = \frac{-\bar{m}}{24\bar{A}^3(\bar{m}^2 - 1)^{7/2}}\Big[&\bar{m}^4(\bar{m}^2 + 9) + 4\bar{A}\bar{m}^2(\bar{m}+1)^2(\bar{m}-1)^2 \\ &- 24\bar{A}^2\bar{m}^2(\bar{m}+1)^2(\bar{m}-1)^2 + 32\bar{A}^3(\bar{m}+1)^3(\bar{m}-1)^3\Big]\end{aligned} \tag{F14}$$

$$\begin{aligned}\lim_{\lambda \to 1} C_{n_p} = \frac{1}{24\bar{A}^3(\bar{m}^2 - 1)^{7/2}}\Big[&\bar{m}^4(19\bar{m}^2 - 9) - 4\bar{A}\bar{m}^2(\bar{m}+1)(\bar{m}-1)^2(4\bar{m}^2 + 7\bar{m} + 3) \\ &+ 24\bar{A}^2\bar{m}(\bar{m}+1)^2(\bar{m}-1)^2(\bar{m}^2 - \bar{m} - 1) + 32\bar{A}^3(\bar{m}+1)^3(\bar{m}-1)^3\Big]\end{aligned} \tag{F15}$$

APPENDIX G

FORMULAS FOR STABILITY DERIVATIVES DUE TO STEADY YAWING MOTION

The formulas for the stability derivatives associated with steady yawing motion are as follows:

$$C_{Y_r} = \frac{4}{3\bar{A}^{1/2}(1+\lambda)^{3/2}(1-\lambda)^2}\left\{\frac{\bar{A}(\bar{m}+1)(1+\lambda)+\bar{m}(2\bar{m}+3)(1-\lambda)}{(\bar{m}+1)^{3/2}\left[\bar{A}(\bar{m}-1)(1+\lambda)+2\bar{m}(1-\lambda)\right]^{1/2}} + \frac{\lambda^2\left[\bar{A}(\bar{m}-1)(1+\lambda)(2\lambda-3)-\bar{m}(2\bar{m}-3)\lambda(1-\lambda)\right]}{(\bar{m}-1)^{3/2}\left[\bar{A}(\bar{m}+1)(1+\lambda)-2\bar{m}(1-\lambda)\right]^{1/2}}\right\} \tag{G1}$$

$$C_{l_r} = \frac{1}{3\bar{A}^{1/2}(1+\lambda)^{3/2}(1-\lambda)^3}\left(\frac{2\bar{A}^2(\bar{m}^2-1)(1+\lambda)^2+2\bar{A}\bar{m}(\bar{m}^2+3\bar{m}+1)(1-\lambda^2)+3\bar{m}^2(2\bar{m}+3)(1-\lambda)^2}{(\bar{m}+1)^{3/2}\left[\bar{A}(\bar{m}-1)(1+\lambda)+2\bar{m}(1-\lambda)\right]^{3/2}}\right.$$
$$\left.-\frac{\lambda^2\left\{2\bar{A}^2(\bar{m}^2-1)(1+\lambda)^2(3\lambda^2-8\lambda+6)-2\bar{A}\bar{m}(1-\lambda^2)\left[3\lambda^2(\bar{m}^2+\bar{m}-3)-4\lambda(\bar{m}^2+3\bar{m}-5)+12(\bar{m}-1)\right]+\bar{m}^2\lambda(5\lambda-8)(2\bar{m}-3)(1-\lambda)^2\right\}}{(\bar{m}-1)^{3/2}\left[\bar{A}(\bar{m}+1)(1+\lambda)-2\bar{m}(1-\lambda)\right]^{3/2}}\right) \tag{G2}$$

$$\frac{1}{B}C_{n_r} = \frac{-1}{3\bar{m}\bar{A}^{3/2}(1+\lambda)^{5/2}(1-\lambda)^3}\left(\frac{\begin{gathered}2\bar{A}^3(\bar{m}^2-1)(1+\lambda)^3+2\bar{A}^2\bar{m}^2(2\bar{m}+3)(1+\lambda)^2(1-\lambda)+\bar{A}\bar{m}^2(8\bar{m}+12\bar{m}-1)(1+\lambda)(1-\lambda)^2 \\ +6\bar{m}^3(2\bar{m}+3)(1-\lambda)^3-\lambda^2\Big\{2\bar{A}^3(3\lambda^2-8\lambda+6)(\bar{m}^2-1)(1+\lambda)^3 \\ -2\bar{A}^2\bar{m}(1+\lambda)^2(1-\lambda)\left[3\lambda^2(2\bar{m}^2+\bar{m}-4)-4\lambda(2\bar{m}^2+3\bar{m}-6)+12(\bar{m}-1)\right] \\ +\lambda\bar{A}\bar{m}^2(1+\lambda)(1-\lambda)^2\left[\lambda(8\bar{m}^2+12\bar{m}-33)-8(3\bar{m}-4)\right]-6\lambda^2\bar{m}^3(2\bar{m}-3)(1-\lambda)^3\Big\}\end{gathered}}{(\bar{m}-1)^{3/2}\left[\bar{A}(\bar{m}+1)(1+\lambda)-2\bar{m}(1-\lambda)\right]^{3/2}}\right) \tag{G3}$$

$$\lim_{\bar{m}\to\infty} C_{Y_r} = \frac{8}{3\bar{A}^{1/2}(1+\lambda)^{3/2}(1-\lambda)}\left\{\frac{1}{\left[\bar{A}(1+\lambda)+2(1-\lambda)\right]^{1/2}} - \frac{\lambda^3}{\left[\bar{A}(1+\lambda)-2(1-\lambda)\right]^{1/2}}\right\} \tag{G4}$$

$$\lim_{\bar{m}\to\infty} C_{l_r} = \frac{2}{3\bar{A}^{1/2}(1+\lambda)^{3/2}(1-\lambda)^2}\left\{\frac{\bar{A}(1+\lambda)+3(1-\lambda)}{\left[\bar{A}(1+\lambda)+2(1-\lambda)\right]^{3/2}} - \frac{\lambda^3\left[-\bar{A}(3\lambda-4)(1+\lambda)+(5\lambda-8)(1-\lambda)\right]}{\left[\bar{A}(1+\lambda)-2(1-\lambda)\right]^{3/2}}\right\} \tag{G5}$$

$$\lim_{\bar{m}\to\infty} \frac{1}{B}C_{n_r} = \frac{-4}{3\bar{A}^{3/2}(1+\lambda)^{5/2}(1-\lambda)}\left\{\frac{2\bar{A}(1+\lambda)+3(1-\lambda)}{\left[\bar{A}(1+\lambda)+2(1-\lambda)\right]^{3/2}} - \frac{\lambda^4\left[2\bar{A}(1+\lambda)-3(1-\lambda)\right]}{\left[\bar{A}(1+\lambda)-2(1-\lambda)\right]^{3/2}}\right\} \tag{G6}$$

$$\lim_{\substack{\bar{m}\to\infty \\ \bar{A}\to\infty}} C_{Y_r} = 0 \tag{G7}$$

$$\lim_{\substack{\bar{m}\to\infty \\ \bar{A}\to\infty}} C_{l_r} = 0 \tag{G8}$$

$$\lim_{\substack{\bar{m}\to\infty \\ \bar{A}\to\infty}} \frac{1}{B} C_{n_r} = 0 \tag{G9}$$

$$\lim_{\bar{A}\to\infty} C_{Y_r} = \frac{4(2\lambda^3 - 3\lambda^2 + 1)}{3(1+\lambda)(1-\lambda)^2(\bar{m}^2 - 1)^{1/2}} \tag{G10}$$

$$\lim_{\bar{A}\to\infty} C_{l_r} = \frac{-2(3\lambda^4 - 8\lambda^3 + 6\lambda^2 - 1)}{3(1+\lambda)(1-\lambda)^3(\bar{m}^2 - 1)^{1/2}} \tag{G11}$$

$$\lim_{\bar{A}\to\infty} \frac{1}{B} C_{n_r} = \frac{2(3\lambda^4 - 8\lambda^3 + 6\lambda^2 - 1)}{3\bar{m}(1+\lambda)(1-\lambda)^3(\bar{m}^2 - 1)^{1/2}} \tag{G12}$$

$$\lim_{\lambda\to 1} C_{Y_r} = \frac{-1}{3\bar{A}^2(\bar{m}^2 - 1)^{5/2}}\left[\bar{m}^3(2\bar{m}^2 - 5) - 3\bar{A}\bar{m}(\bar{m}^2 - 1)(2\bar{m}^2 - \bar{m} - 3) - 6\bar{A}^2(\bar{m}^2 - 1)^2\right] \tag{G13}$$

$$\lim_{\lambda \to 1} C_{l_r} = \frac{-1}{24\bar{A}^3(\bar{m}^2 - 1)^{7/2}}\left[5\bar{m}^4(\bar{m}^2 - 3) + 4\bar{A}\bar{m}^2(\bar{m} + 1)(\bar{m} - 1)^2(2\bar{m}^2 - \bar{m} - 3)\right.$$

$$\left. - 24\bar{A}^2\bar{m}(\bar{m} + 1)^2(\bar{m} - 1)^2(\bar{m}^2 - \bar{m} - 1) - 32\bar{A}^3(\bar{m} + 1)^3(\bar{m} - 1)^3\right] \tag{G14}$$

$$\lim_{\lambda \to 1} \frac{1}{B} C_{n_r} = \frac{-1}{24\bar{A}^3\bar{m}(\bar{m}^2 - 1)^{7/2}}\left[\bar{m}^4(-12\bar{m}^4 + 37\bar{m}^2 - 15)\right.$$

$$+ 4\bar{A}\bar{m}^2(\bar{m} + 1)(\bar{m} - 1)^2(8\bar{m}^3 + 2\bar{m}^2 - 7\bar{m} - 1)$$

$$+ 24\bar{A}^2\bar{m}(\bar{m} + 1)^2(\bar{m} - 1)^2(2\bar{m}^2 - \bar{m} - 2)$$

$$\left. + 32\bar{A}^3(\bar{m} + 1)^3(\bar{m} - 1)^3\right] \tag{G15}$$

L
7
8
0

APPENDIX H

FORMULAS FOR STABILITY DERIVATIVES DUE TO CONSTANT LATERAL ACCELERATION

L-780

The formulas for the stability derivatives associated with constant lateral acceleration motion are as follows:

$$C_{Y_{\dot{\beta}}} = \frac{8\bar{m}}{3\bar{A}^{1/2}(1+\lambda)^{3/2}(1-\lambda)}\left(\frac{\bar{A}(1+\lambda)(1+\bar{m}^2) + \left[\bar{m}^2 - \bar{m}(\bar{m}+2)\right](1-\lambda)}{(\bar{m}+1)^{3/2}\left[\bar{A}(\bar{m}-1)(1+\lambda) + 2\bar{m}(1-\lambda)\right]^{3/2}} - \frac{\lambda^3\left\{\bar{A}(1+\lambda)(1+\bar{m}^2) - \left[\bar{m}^2 - \bar{m}(\bar{m}-2)\right](1-\lambda)\right\}}{(\bar{m}-1)^{3/2}\left[\bar{A}(\bar{m}+1)(1+\lambda) - 2\bar{m}(1-\lambda)\right]^{3/2}}\right) \qquad \text{(H1)}$$

$$\begin{aligned} C_{l_{\dot{\beta}}} = \frac{2\bar{m}}{3\bar{A}^{1/2}(1+\lambda)^{3/2}(1-\lambda)^2}\Bigg[& \frac{\bar{A}^2(1+\bar{m}^2)(\bar{m}-1)(1+\lambda)^2 + 5\bar{A}\bar{m}(1+\bar{m}^2)(1-\lambda)(1+\lambda) + 3\bar{m}(1-\lambda)^2\left[\bar{m}^2 - \bar{m}(\bar{m}+2)\right]}{(\bar{m}+1)^{3/2}\left[\bar{A}(\bar{m}-1)(1+\lambda) + 2\bar{m}(1-\lambda)\right]^{5/2}} \\ & + \lambda^3 \frac{\left(\begin{aligned} & \bar{A}^2(3\lambda-4)(1+\bar{m}^2)(\bar{m}+1)(1+\lambda)^2 - \Big\{\lambda\left[\bar{m}^2(7\bar{m}+4) - \bar{m}(4\bar{m}^2 - 4\bar{m} - 11)\right] - 4\Big[\bar{m}^2(3\bar{m}+1) \\ & - \bar{m}(\bar{m}^2 - \bar{m} - 4)\Big]\Big\}\bar{A}(1+\lambda)(1-\lambda) + \bar{m}(5\lambda-8)(1-\lambda)^2\left[\bar{m}^2 - \bar{m}(\bar{m}-2)\right] \end{aligned}\right)}{(\bar{m}-1)^{3/2}\left[\bar{A}(\bar{m}+1)(1+\lambda) - 2\bar{m}(1-\lambda)\right]^{5/2}}\Bigg] \end{aligned} \qquad \text{(H2)}$$

$$\begin{aligned} C_{n_{\dot{\beta}}} = \frac{-2B}{3\bar{A}^{3/2}(1+\lambda)^{5/2}(1-\lambda)^2}\Bigg[& \frac{\left\{\begin{aligned} & \bar{A}^3(1+\lambda)^3(\bar{m}-1) + \bar{A}^2\bar{m}(1+\lambda)^2(1-\lambda)(4\bar{m}+1) - \bar{A}\bar{m}^2(1+\lambda)(1-\lambda)^2(6\bar{m}^2 \\ & + 9\bar{m} - 8) - 6\bar{m}^3(1-\lambda)^3(\bar{m}+2) + \bar{m}^2\Big[\bar{A}^3(1+\lambda)^3(\bar{m}-1) \\ & + \bar{A}^2\bar{m}(1+\lambda)^2(1-\lambda)(4\bar{m}+1) + \bar{A}\bar{m}(1+\lambda)(1-\lambda)^2(8\bar{m}-3) + 6\bar{m}^2(1-\lambda)^3\Big] \end{aligned}\right\}}{(\bar{m}+1)^{3/2}\left[\bar{A}(\bar{m}-1)(1+\lambda) + 2\bar{m}(1-\lambda)\right]^{5/2}} \\ & + \lambda^3 \frac{\left(\begin{aligned} & \bar{A}^3(1+\lambda)^3(3\lambda-4)(\bar{m}+1) + \bar{A}^2\bar{m}(1+\lambda)^2(1-\lambda)\left[\lambda(4\bar{m}^2 - 8\bar{m} - 15) - 4(\bar{m}^2 - \bar{m} - 4)\right] \\ & - \bar{A}\bar{m}^2(1+\lambda)(1-\lambda)^2\left[\lambda(6\bar{m}^2 - \bar{m} - 24) - 8(\bar{m}-2)\right] + 6\lambda\bar{m}^3(1-\lambda)^3(\bar{m}-2) \\ & + \bar{m}^2\Big\{\bar{A}^3(1+\lambda)^3(3\lambda-4)(\bar{m}+1) - \bar{A}^2(1+\lambda)^2(1-\lambda)\left[\lambda(4\bar{m}^2 + 11\bar{m} + 4) - 4(3\bar{m}+1)\right] \\ & + \bar{A}\bar{m}(1+\lambda)(1-\lambda)^2\left[\lambda(8\bar{m}+11) - 8\right] - 6\lambda\bar{m}^2(1-\lambda)^3\Big\} \end{aligned}\right)}{(\bar{m}-1)^{3/2}\left[\bar{A}(\bar{m}+1)(1+\lambda) - 2\bar{m}(1-\lambda)\right]^{5/2}}\Bigg] \end{aligned} \qquad \text{(H3)}$$

$$\lim_{m \to \infty} C_{Y_{\dot{\beta}}} = \frac{8}{3B^2\bar{A}^{1/2}(1+\lambda)^{3/2}(1-\lambda)}\left\{\frac{\bar{A}(1+\lambda)+(1-B^2)(1-\lambda)}{\left[\bar{A}(1+\lambda)+2(1-\lambda)\right]^{3/2}} - \frac{\lambda^3\left[\bar{A}(1+\lambda)-(1-B^2)(1-\lambda)\right]}{\left[\bar{A}(1+\lambda)-2(1-\lambda)\right]^{3/2}}\right\} \quad \text{(H4)}$$

$$\lim_{m \to \infty} C_{l_{\dot{\beta}}} = \frac{2}{3B^2\bar{A}^{1/2}(1+\lambda)^{3/2}(1-\lambda)^2}\left(\frac{3(1-B^2)(1-\lambda)^2+5\bar{A}(1-\lambda)(1+\lambda)+\bar{A}^2(1+\lambda)^2}{\left[\bar{A}(1+\lambda)+2(1-\lambda)\right]^{5/2}}\right.$$

$$\left. + \frac{\lambda^3\left\{(5\lambda-8)(1-\lambda)^2(1-B^2)-\bar{A}(1+\lambda)(1-\lambda)\left[(7-4B^2)\lambda-4(3-B^2)\right]+\bar{A}^2(1+\lambda)^2(3\lambda-4)\right\}}{\left[\bar{A}(1+\lambda)-2(1-\lambda)\right]^{5/2}}\right) \quad \text{(H5)}$$

$$\lim_{m \to \infty} C_{n_{\dot{\beta}}} = \frac{-2}{3B\bar{A}^{3/2}(1+\lambda)^{5/2}(1-\lambda)}\left(\frac{-6B^2(1-\lambda)\left[\bar{A}(1+\lambda)+(1-\lambda)\right]+4\bar{A}(1+\lambda)\left[\bar{A}(1+\lambda)+2(1-\lambda)\right]+6(1-\lambda)^2}{\left[\bar{A}(1+\lambda)+2(1-\lambda)\right]^{5/2}}\right.$$

$$\left. + \frac{\lambda^4\left\{-6B^2(1-\lambda)\left[\bar{A}(1+\lambda)-(1-\lambda)\right]-4\bar{A}(1+\lambda)\left[\bar{A}(1+\lambda)-2(1-\lambda)\right]-6(1-\lambda)^2\right\}}{\left[\bar{A}(1+\lambda)-2(1-\lambda)\right]^{5/2}}\right) \quad \text{(H6)}$$

$$\lim_{\bar{A} \to \infty} C_{Y_{\dot{\beta}}} = 0 \quad \text{(H7)}$$

$$\lim_{\bar{A} \to \infty} C_{l_{\dot{\beta}}} = 0 \quad \text{(H8)}$$

$$\lim_{\bar{A} \to \infty} C_{n_{\dot{\beta}}} = 0 \quad \text{(H9)}$$

$$\lim_{\lambda \to 1} C_{Y_{\dot{\beta}}} = \frac{2\bar{m}}{3\bar{A}^2(\bar{m}^2-1)^{5/2}}\left[-\bar{m}^2(\bar{m}^2+2)+3\bar{A}(\bar{m}^2-1)\right] + \frac{2\bar{m}^3}{3\bar{A}^2(\bar{m}^2-1)^{5/2}}\left[-(2\bar{m}^2+1)+3\bar{A}(\bar{m}^2-1)\right] \quad \text{(H10)}$$

$$\lim_{\lambda \to 1} C_{l_{\dot{\beta}}} = \frac{\bar{m}}{12\bar{A}^3(\bar{m}^2-1)^{7/2}}\left[-3\bar{m}^3(3\bar{m}^2+2)+4\bar{m}\bar{A}(\bar{m}+1)(\bar{m}-1)^2(-\bar{m}^2+\bar{m}-1)+12\bar{A}^2(\bar{m}+1)^2(\bar{m}-1)^2\right]$$

$$+ \frac{B\bar{m}^3}{12\bar{A}^3(\bar{m}^2-1)^{7/2}}\left[-3\bar{m}(4\bar{m}^2+1)+4\bar{A}(\bar{m}+1)(\bar{m}-1)^2(-2\bar{m}+1)+12\bar{A}^2(\bar{m}+1)^2(\bar{m}-1)^2\right] \quad \text{(H11)}$$

L-780

$$\lim_{\lambda \to 1} C_{n_{\dot{\beta}}} = \frac{-B}{12\bar{A}^3(\bar{m}^2 - 1)^{7/2}} \Big[-3\bar{m}^3(2\bar{m}^4 + 5\bar{m}^2 - 2) + 4\bar{m}\bar{A}(\bar{m} + 1)(\bar{m} - 1)^2(-\bar{m}^2 + 5\bar{m} + 3)$$

$$+ 12\bar{A}^2(\bar{m} + 1)^2(\bar{m} - 1)^2 \Big] - \frac{-B\bar{m}^2}{12\bar{A}^3(\bar{m} \;\; - 1)^{7/2}} \Big[-3\bar{m}(4\bar{m}^4 + 2\bar{m}^2 - 1)$$

$$+ 4\bar{A}(\bar{m} + 1)(\bar{m} - 1)^2(4\bar{m}^2 + 2\bar{m} + 1) + 12\bar{A}^2(\bar{m} + 1)^2(\bar{m} - 1)^2 \Big] \qquad \text{(H12)}$$

L 7 8 0

REFERENCES

1. Margolis, Kenneth, and Bobbitt, Percy J.: Theoretical Calculations of the Pressures, Forces, and Moments at Supersonic Speeds Due to Various Lateral Motions Acting on Thin Isolated Vertical Tails. NACA Rep. 1268, 1956. (Supersedes NACA TN 3373 by Margolis and NACA TN 3240 by Bobbitt.)

2. Cole, Isabella J., and Margolis, Kenneth: Span Load Distributions Resulting From Constant Vertical Acceleration for Thin Sweptback Tapered Wings With Streamwise Tips - Supersonic Leading and Trailing Edges. NACA TN 3120, 1954.

3. Martin, John C., Margolis, Kenneth, and Jeffreys, Isabella: Calculation of Lift and Pitching Moments Due to Angle of Attack and Steady Pitching Velocity at Supersonic Speeds for Thin Sweptback Tapered Wings With Streamwise Tips and Supersonic Leading and Trailing Edges. NACA TN 2699, 1952.

4. Harmon, Sidney M., and Jeffreys, Isabella: Theoretical Lift and Damping in Roll of Thin Wings With Arbitrary Sweep and Taper at Supersonic Speeds - Supersonic Leading and Trailing Edges. NACA TN 2114, 1950.

5. Cole, Isabella J., and Margolis, Kenneth: Lift and Pitching Moment at Supersonic Speeds Due to Constant Vertical Acceleration for Thin Sweptback Tapered Wings With Streamwise Tips - Supersonic Leading and Trailing Edges. NACA TN 3196, 1954.

TABLE I

INDEX TO DESIGN CHARTS FOR STABILITY DERIVATIVES

Stability derivative	Taper ratio	Figure number	Page number	Stability derivative	Taper ratio	Figure number	Page number	Stability derivative	Taper ratio	Figure number	Page number
C_{Y_β}	0	3(a)	37	C_{Y_r}	0	9(a)	73	$C_{n_{\dot\beta}}$	0	13(a)	103
	.2	3(b)	38		.2	9(b)	74		0	13(b)	104
	.4	3(c)	39		.4	9(c)	75		.2	13(c)	105
	.6	3(d)	40		.6	9(d)	76		.2	13(d)	106
	.8	3(e)	41		.8	9(e)	77		.4	13(e)	107
	1.0	3(f)	42		1.0	9(f)	78		.4	13(f)	108
$C_{n_{\dot\beta}}$	0	4(a)	43	C_{n_r}	0	10(a)	79		.6	13(g)	109
	.2	4(b)	44		.2	10(b)	80		.6	13(h)	110
	.4	4(c)	45		.4	10(c)	81		.8	13(i)	111
	.6	4(d)	46		.6	10(d)	82		.8	13(j)	112
	.8	4(e)	47		.8	10(e)	83		1.0	13(k)	113
	1.0	4(f)	48		1.0	10(f)	84		1.0	13(l)	114
C_{l_β}	0	5(a)	49	C_{l_r}	0	11(a)	85	$C_{l_{\dot\beta}}$	0	14(a)	115
	.2	5(b)	50		.2	11(b)	86		0	14(b)	116
	.4	5(c)	51		.4	11(c)	87		.2	14(c)	117
	.6	5(d)	52		.6	11(d)	88		.2	14(d)	118
	.8	5(e)	53		.8	11(e)	89		.4	14(e)	119
	1.0	5(f)	54		1.0	11(f)	90		.4	14(f)	120
C_{Y_p}	0	6(a)	55	$C_{Y_{\dot\beta}}$	0	12(a)	91		.6	14(g)	121
	.2	6(b)	56		0	12(b)	92		.6	14(h)	122
	.4	6(c)	57		.2	12(c)	93		.8	14(i)	123
	.6	6(d)	58		.2	12(d)	94		.8	14(j)	124
	.8	6(e)	59		.4	12(e)	95		1.0	14(k)	125
	1.0	6(f)	60		.4	12(f)	96		1.0	14(l)	126
C_{n_p}	0	7(a)	61		.6	12(g)	97				
	.2	7(b)	62		.6	12(h)	98				
	.4	7(c)	63		.8	12(i)	99				
	.6	7(d)	64		.8	12(j)	100				
	.8	7(e)	65		1.0	12(k)	101				
	1.0	7(f)	66		1.0	12(l)	102				
C_{l_p}	0	8(a)	67								
	.2	8(b)	68								
	.4	8(c)	69								
	.6	8(d)	70								
	.8	8(e)	71								
	1.0	8(f)	72								

TABLE II

TRANSFER-OF-AXES FORMULAS

Stability derivatives in a body system of axes with origin at tail apex (see fig. 2(b))	Formulas for transfer to a body system of axes with origin displaced distances x_o (positive forward) and z_o (positive downward) from the tail apex (see fig. 2(c))
C_{Y_β}	C_{Y_β}
C_{n_β}	$C_{n_\beta} - \frac{x_o}{b} C_{Y_\beta}$
C_{l_β}	$C_{l_\beta} + \frac{z_o}{b} C_{Y_\beta}$
C_{Y_p}	C_{Y_p}
C_{n_p}	$C_{n_p} - \frac{x_o}{b} C_{Y_p}$
C_{l_p}	$C_{l_p} + \frac{z_o}{b} C_{Y_p}$
C_{Y_r}	$C_{Y_r} - \frac{x_o}{b} C_{Y_\beta}$
C_{n_r}	$C_{n_r} - \frac{x_o}{b}\left(C_{n_\beta} + C_{Y_r}\right) + \left(\frac{x_o}{b}\right)^2 C_{Y_\beta}$
C_{l_r}	$C_{l_r} + \frac{z_o}{b} C_{Y_r} - \frac{x_o}{b} C_{l_\beta} - \left(\frac{z_o}{b}\right)\left(\frac{x_o}{b}\right) C_{Y_\beta}$
$C_{Y_{\dot\beta}}$	$C_{Y_{\dot\beta}}$
$C_{n_{\dot\beta}}$	$C_{n_{\dot\beta}} - \frac{x_o}{b} C_{Y_{\dot\beta}}$
$C_{l_{\dot\beta}}$	$C_{l_{\dot\beta}} + \frac{z_o}{b} C_{Y_{\dot\beta}}$

L780

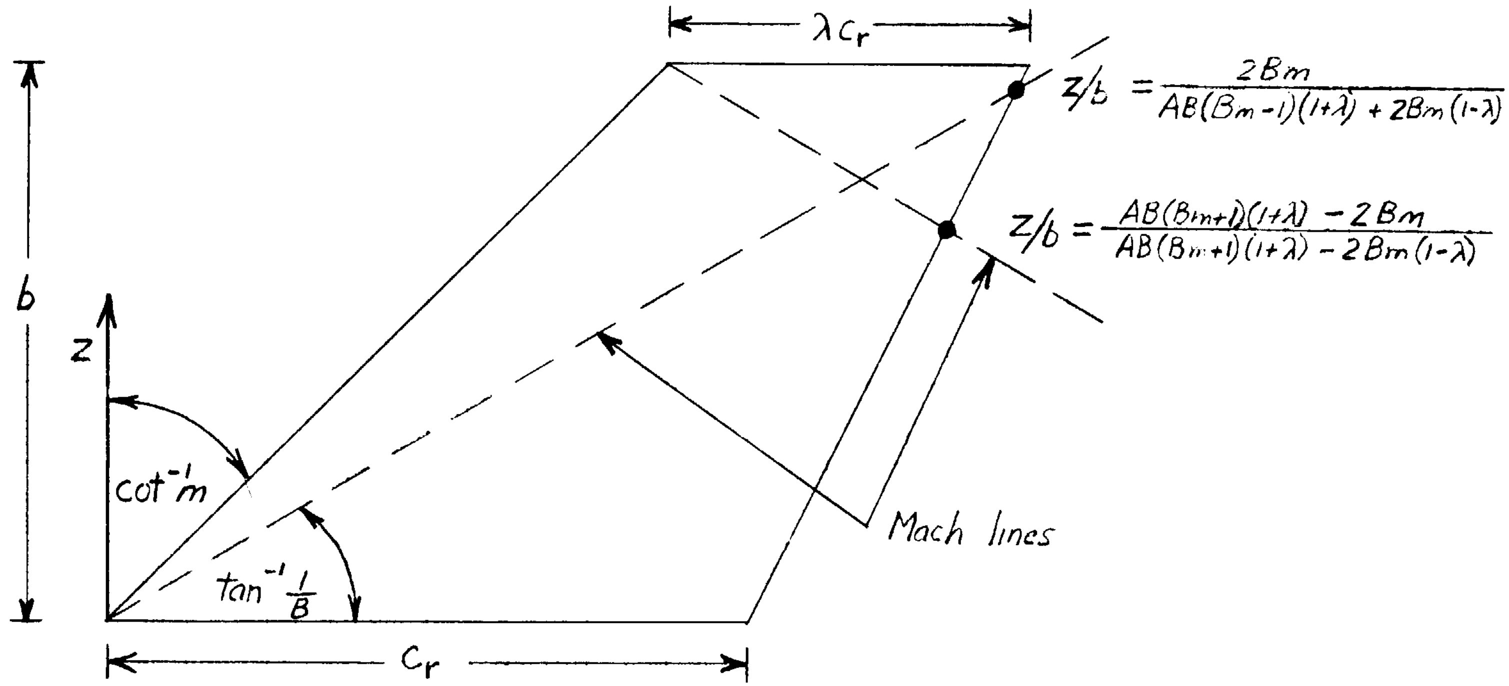

Figure 1.- General plan form of vertical tail with pertinent symbols and associated data. (Note that tail aspect ratio $A = \frac{2b}{c_r(1 + \lambda)}$.)

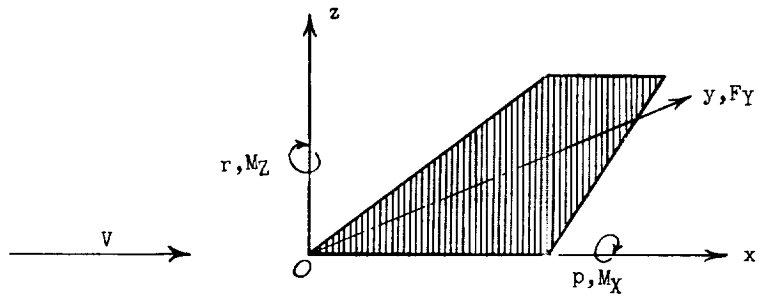

(a) Body-axes system used for analysis. Free-stream velocity V.

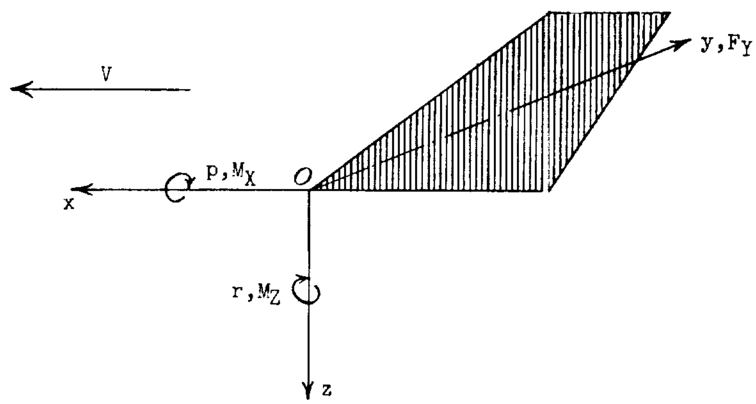

(b) Principal body-axes system used for presentation of stability derivatives. Entire system moving with flight velocity V.

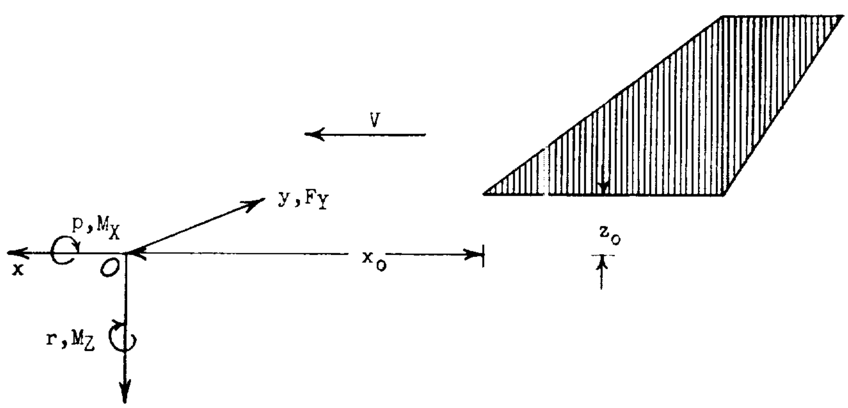

(c) Same type of axes system as (b) with origin translated.

Figure 2.- Systems of body axes. Positive directions of axes, forces, and moments indicated by arrows.

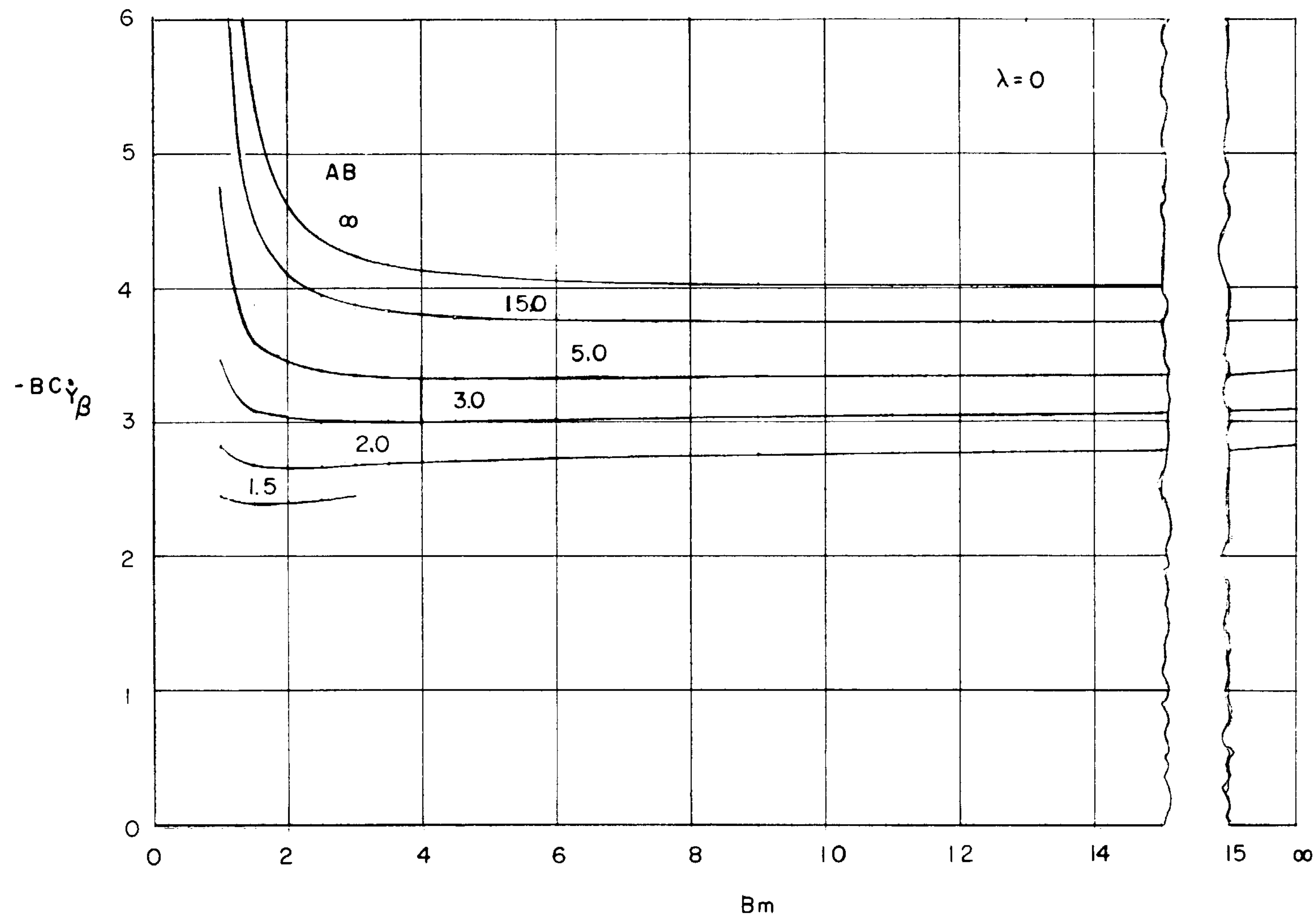

(a) Taper ratio, 0.

Figure 3.- Variation of $-BC_{Y_\beta}$ with Mach number-geometry parameters.

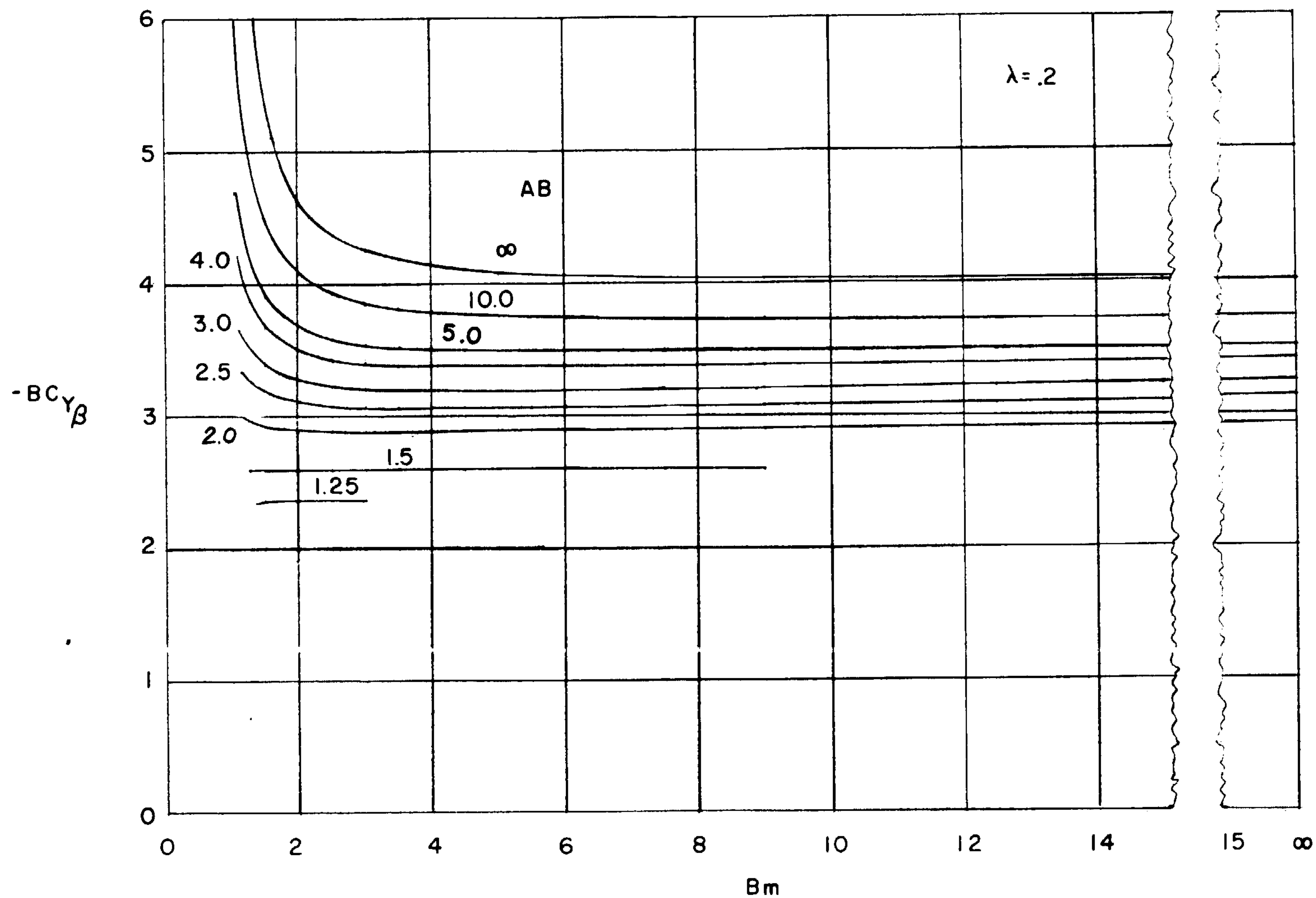

(b) Taper ratio, 0.2.

Figure 3.- Continued.

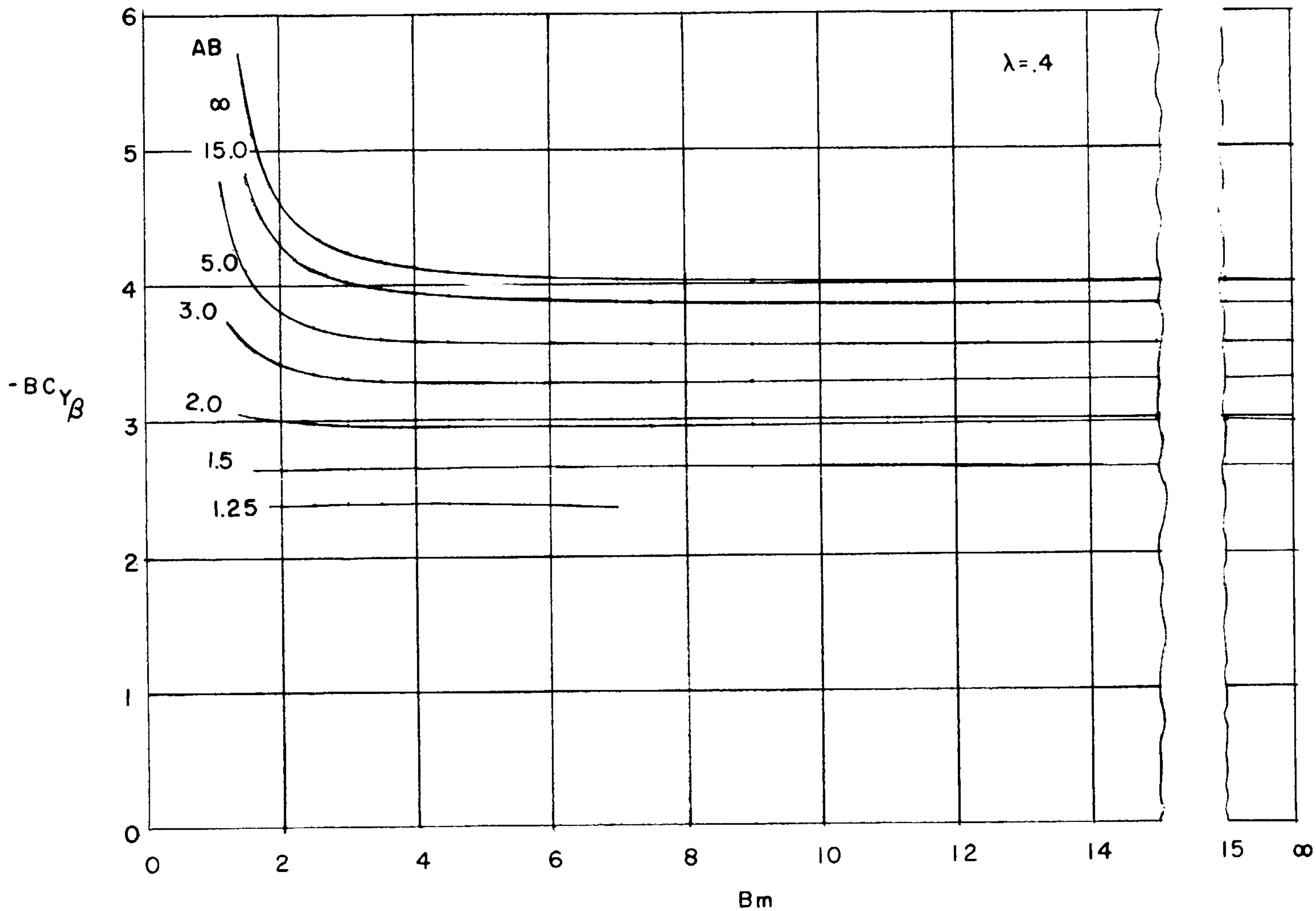

(c) Taper ratio, 0.4.

Figure 3.- Continued.

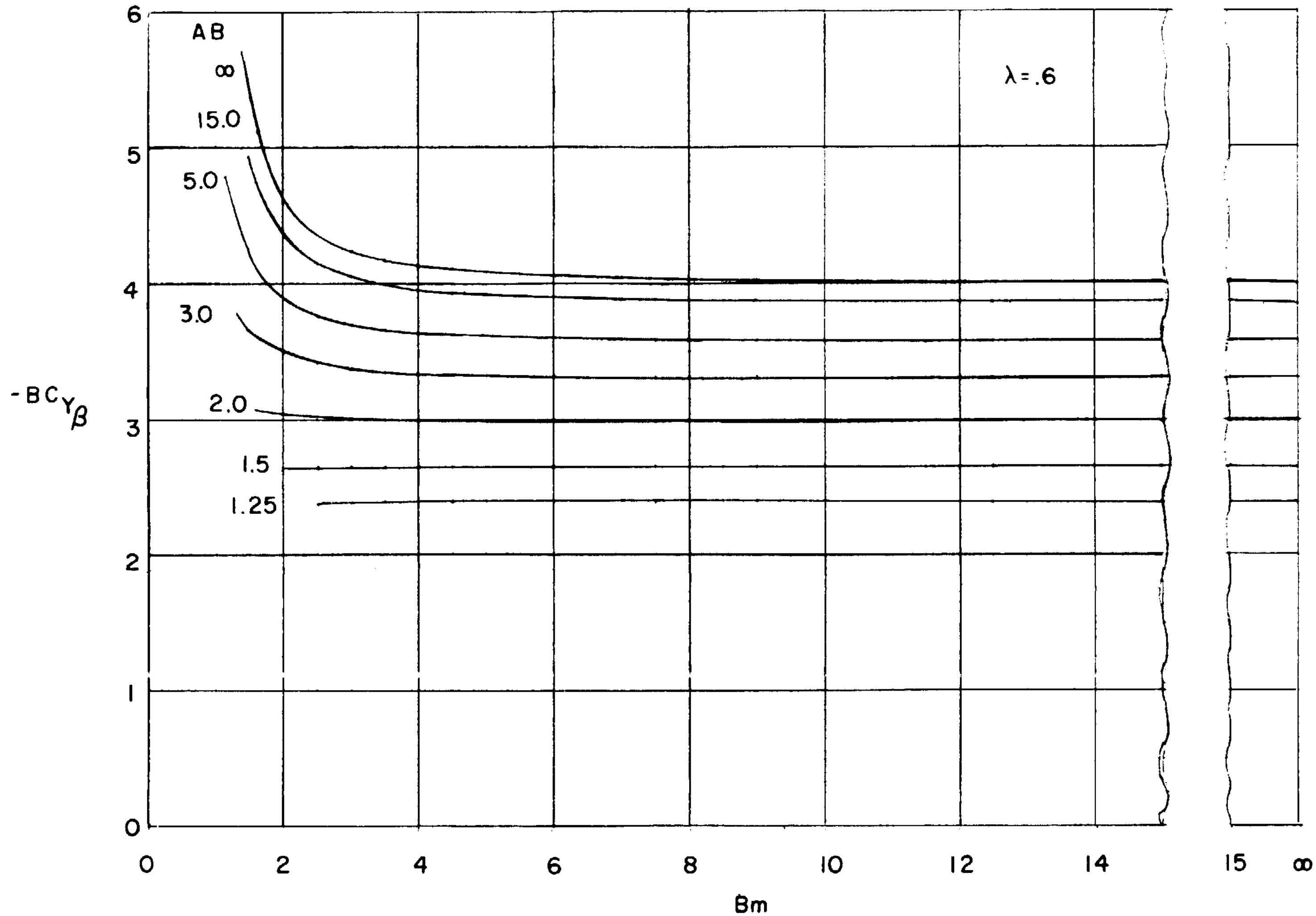

(d) Taper ratio, 0.6.

Figure 3.- Continued.

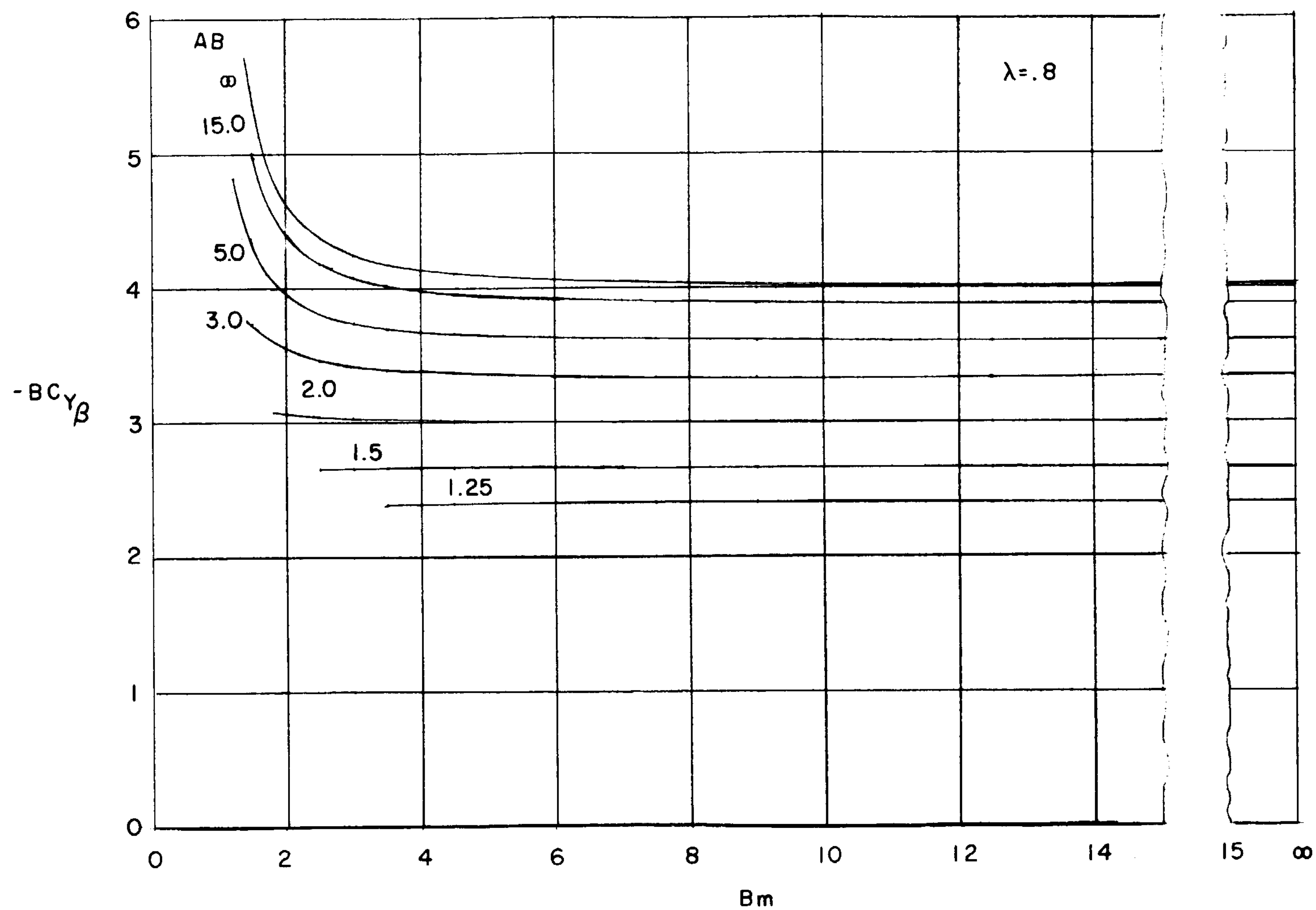

(e) Taper ratio, 0.8.

Figure 3.- Continued.

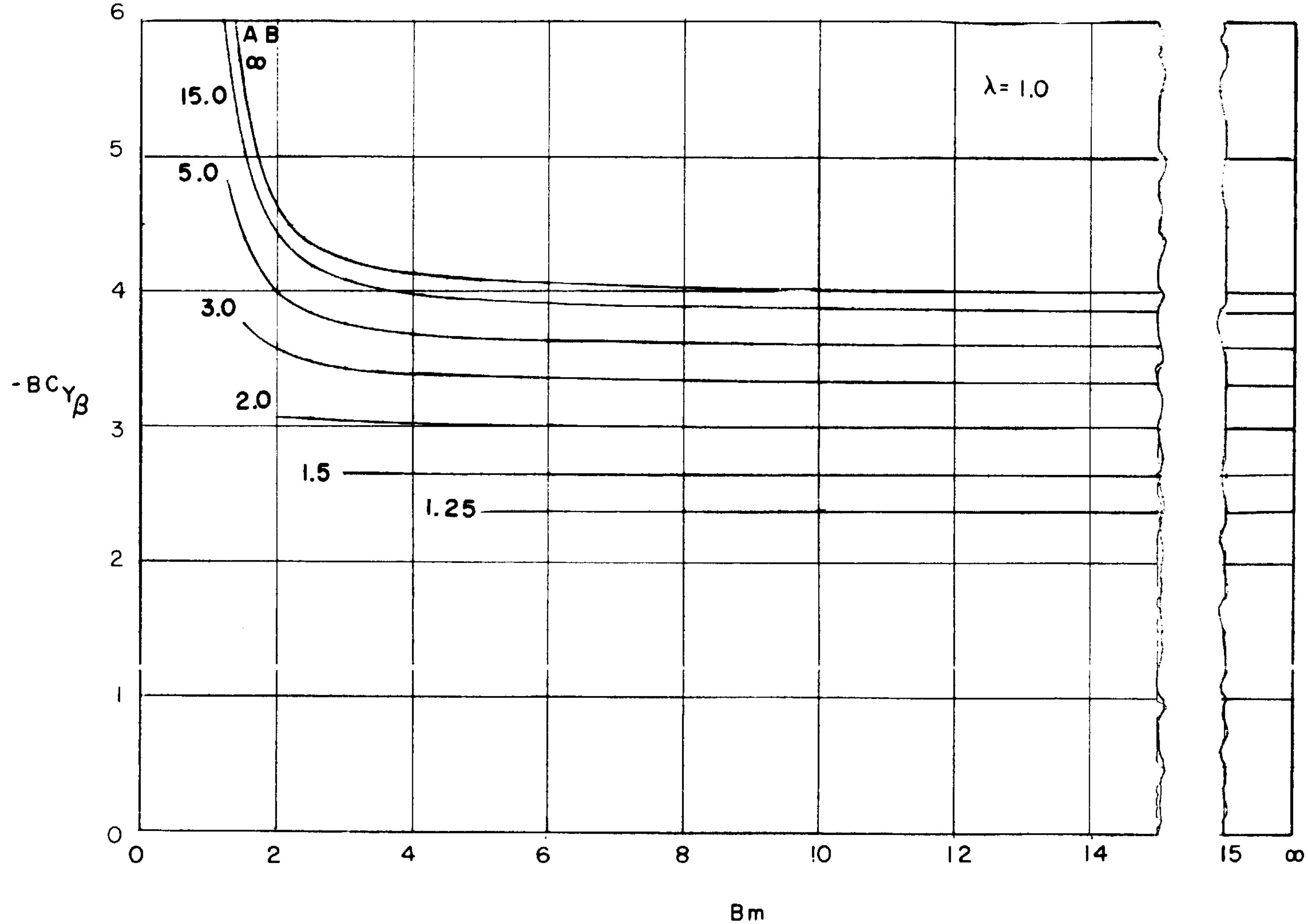

(f) Taper ratio, 1.0.

Figure 3.- Concluded.

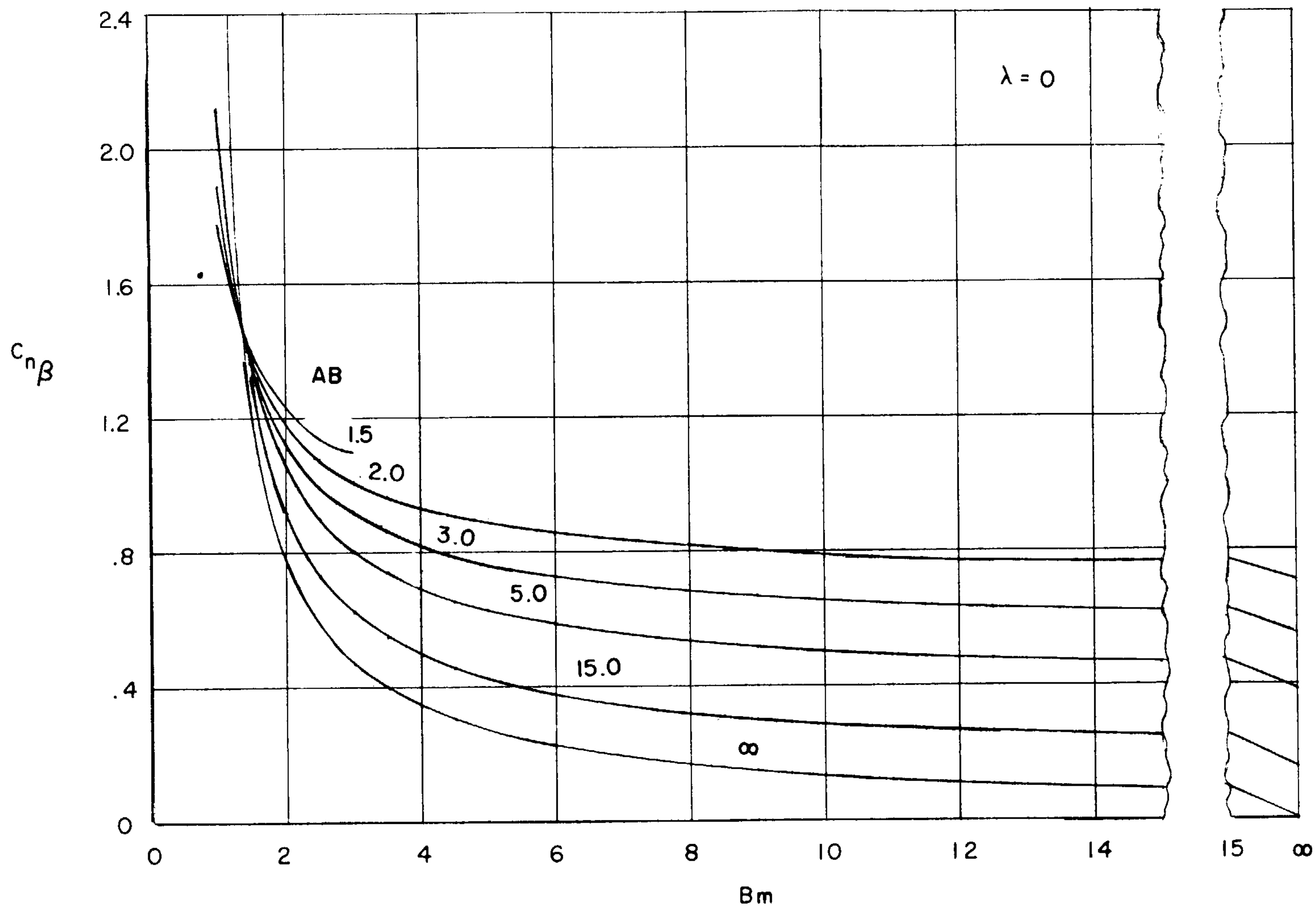

(a) Taper ratio, 0.

Figure 4.- Variation of C_{n_β} with Mach number-geometry parameters.

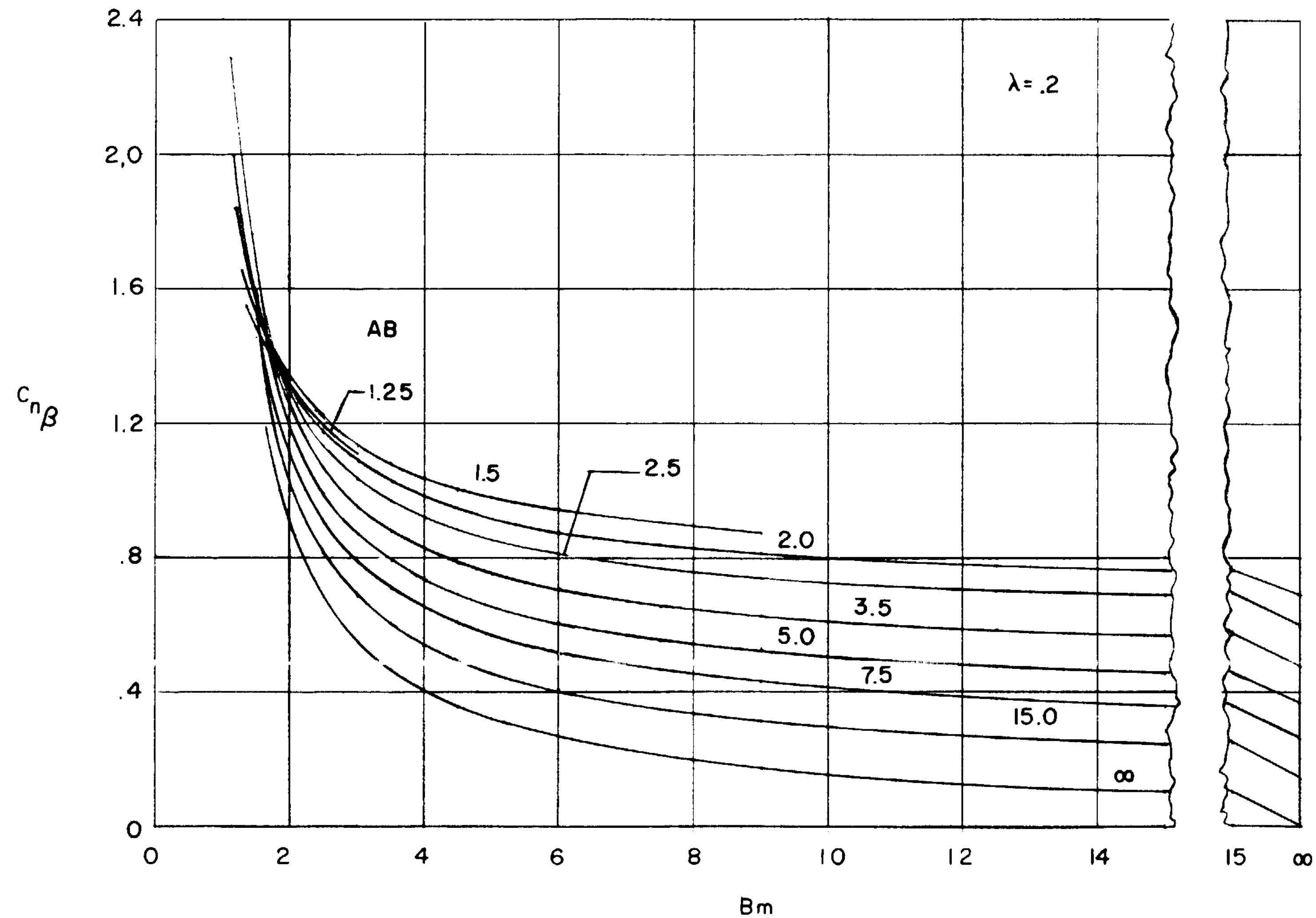

(b) Taper ratio, 0.2.

Figure 4.- Continued.

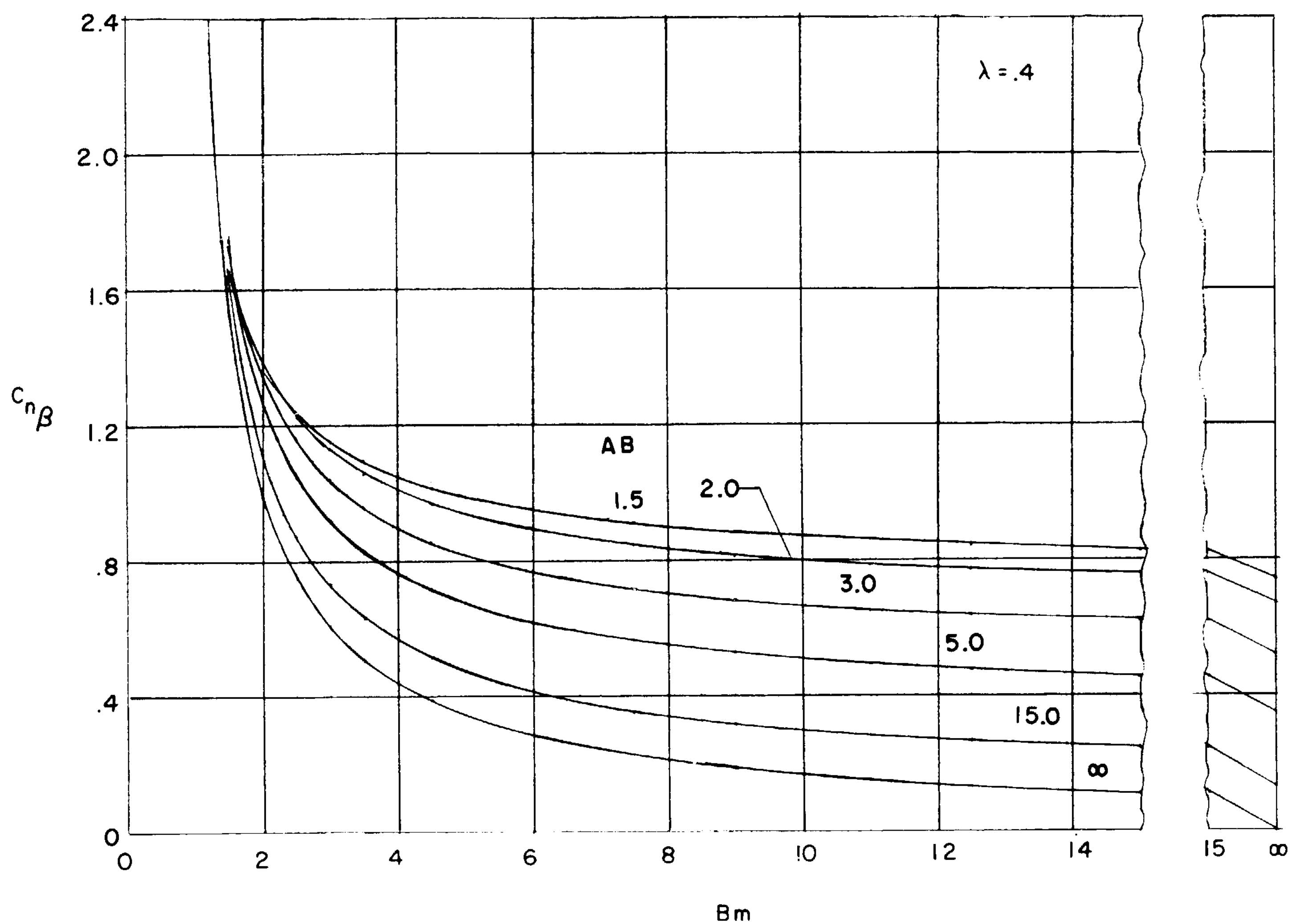

(c) Taper ratio, 0.4.

Figure 4.- Continued.

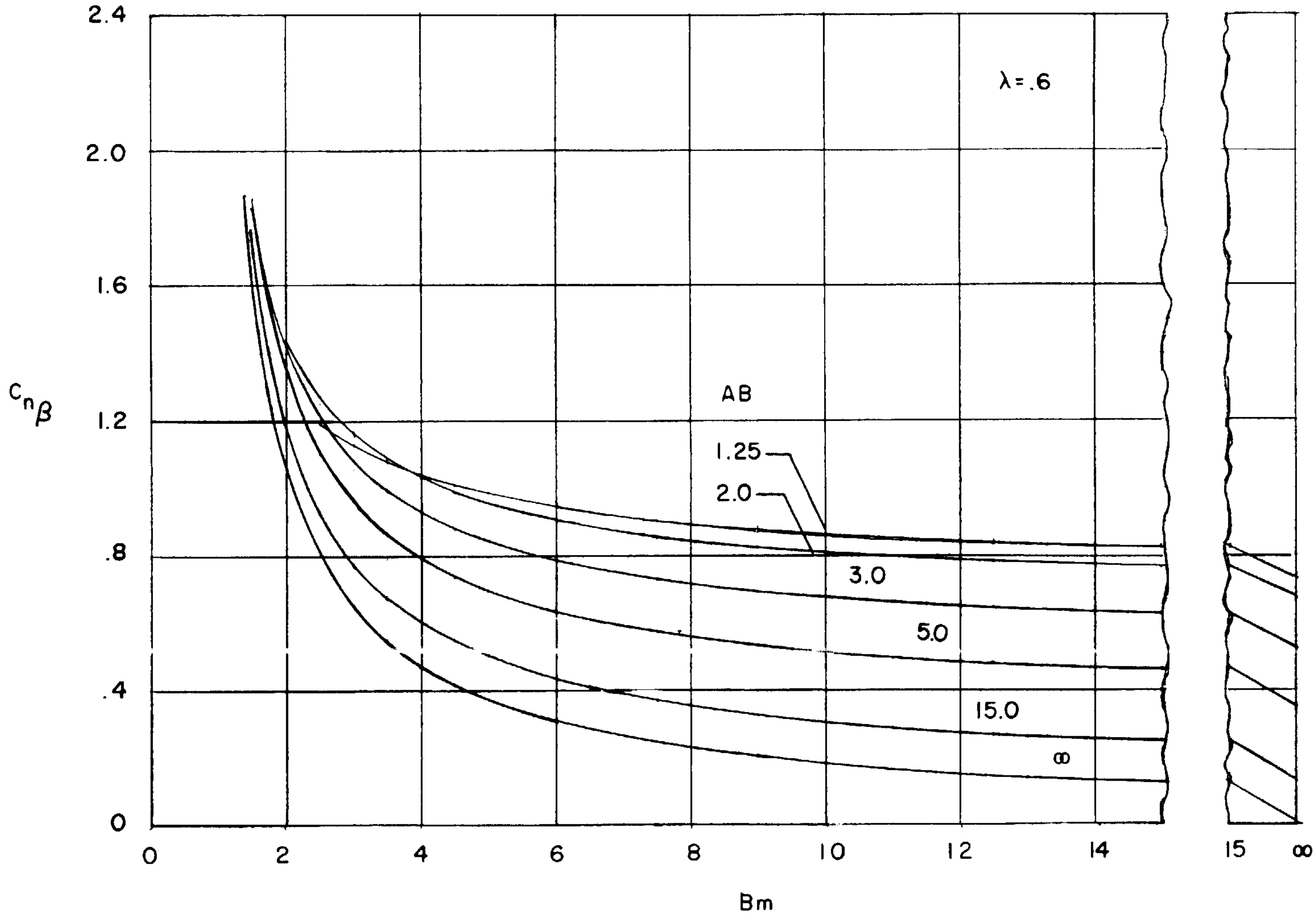

(d) Taper ratio, 0.6.

Figure 4.- Continued.

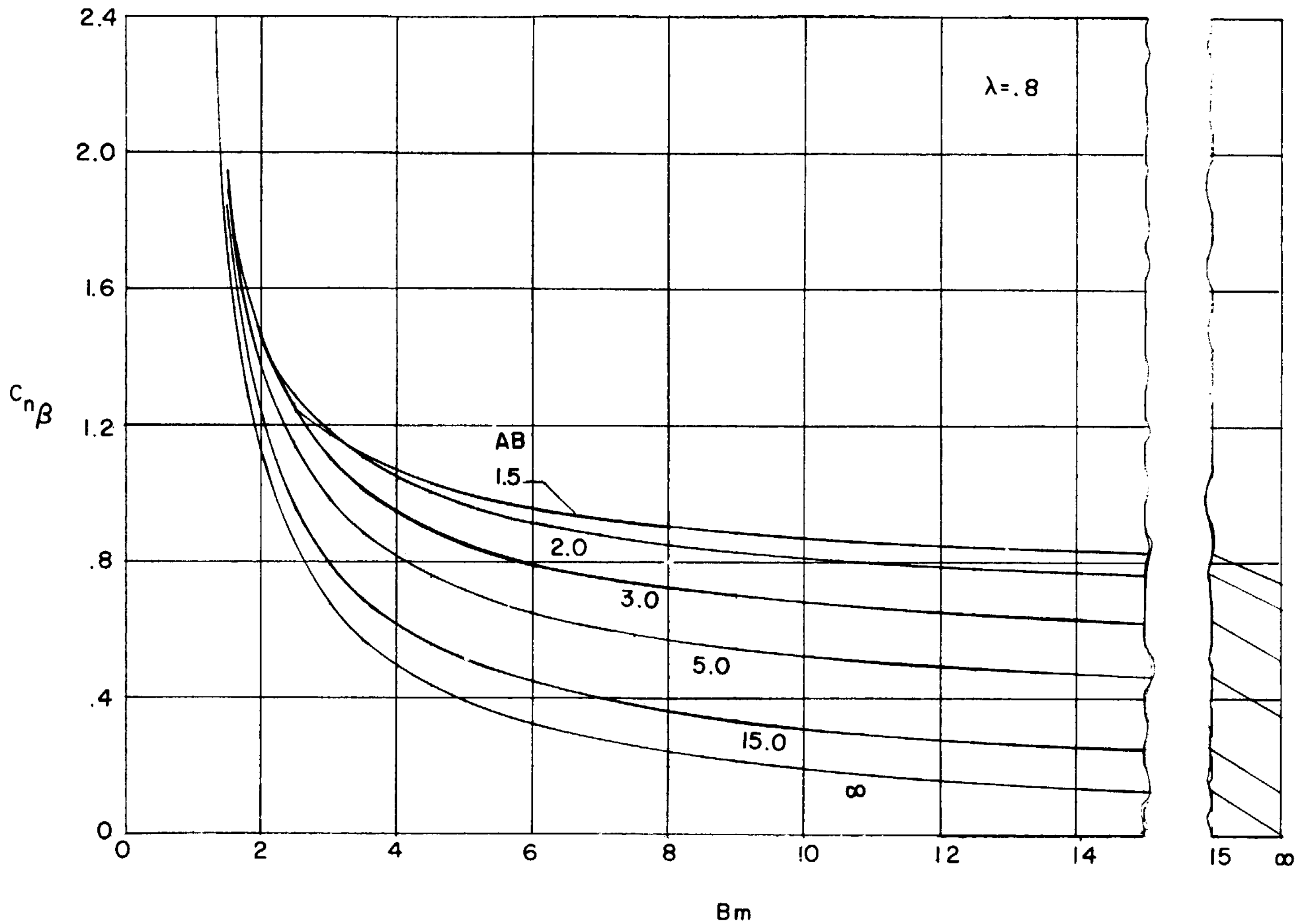

(e) Taper ratio, 0.8.

Figure 4.- Continued.

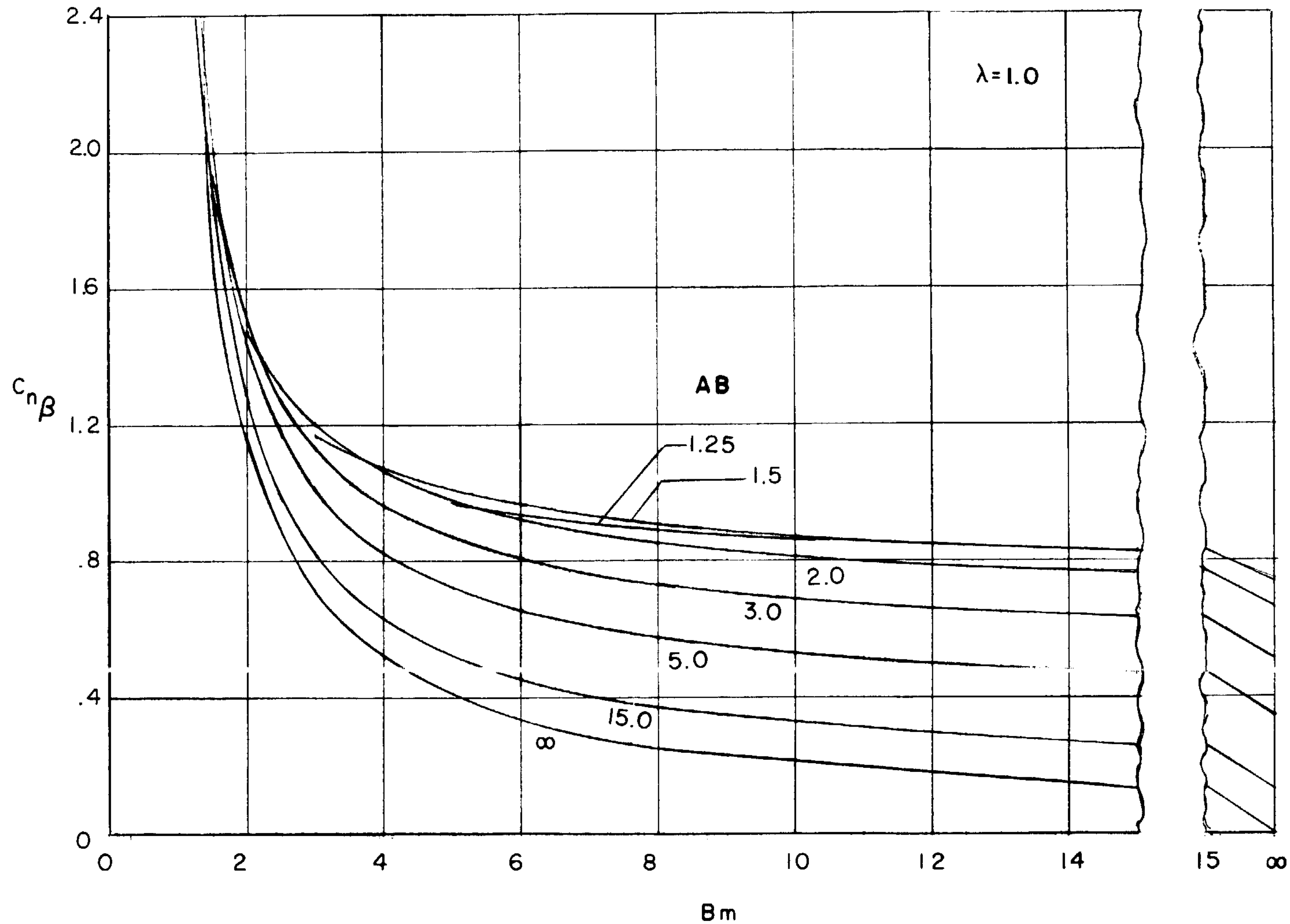

(f) Taper ratio, 1.0.

Figure 4.- Concluded.

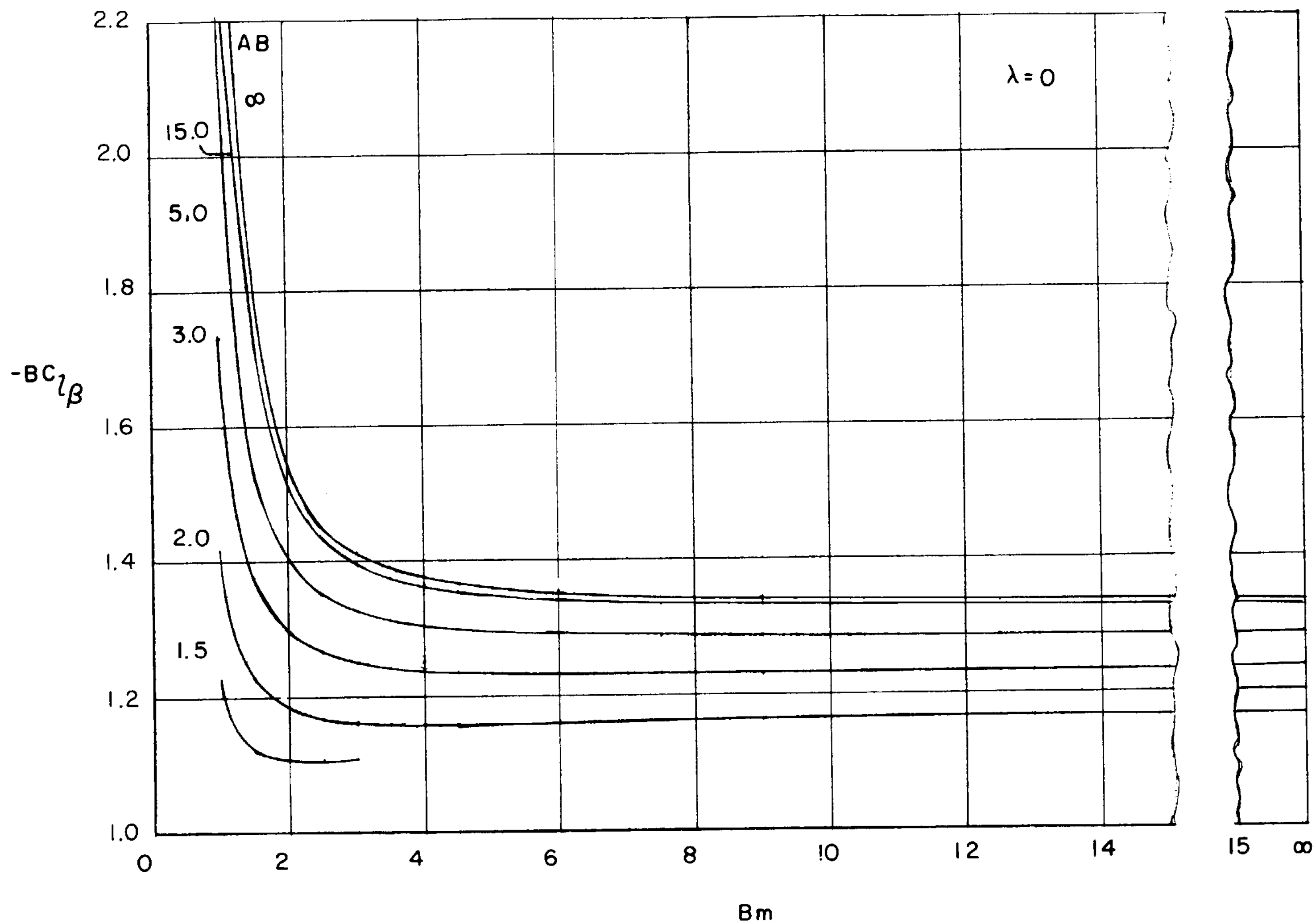

(a) Taper ratio, 0.

Figure 5.- Variation of $-BC_{l_\beta}$ with Mach number-geometry parameters.

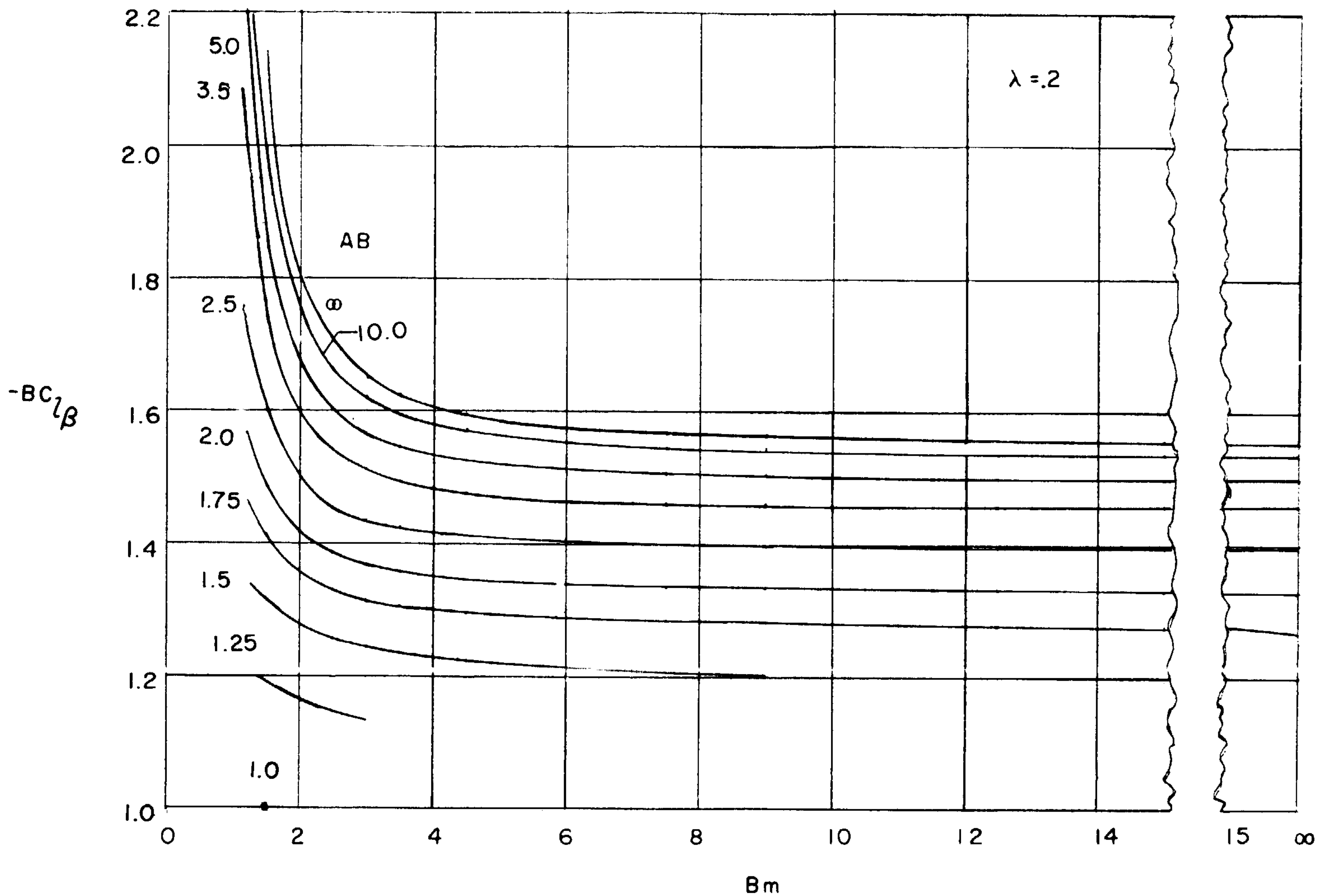

(b) Taper ratio, 0.2.

Figure 5.- Continued.

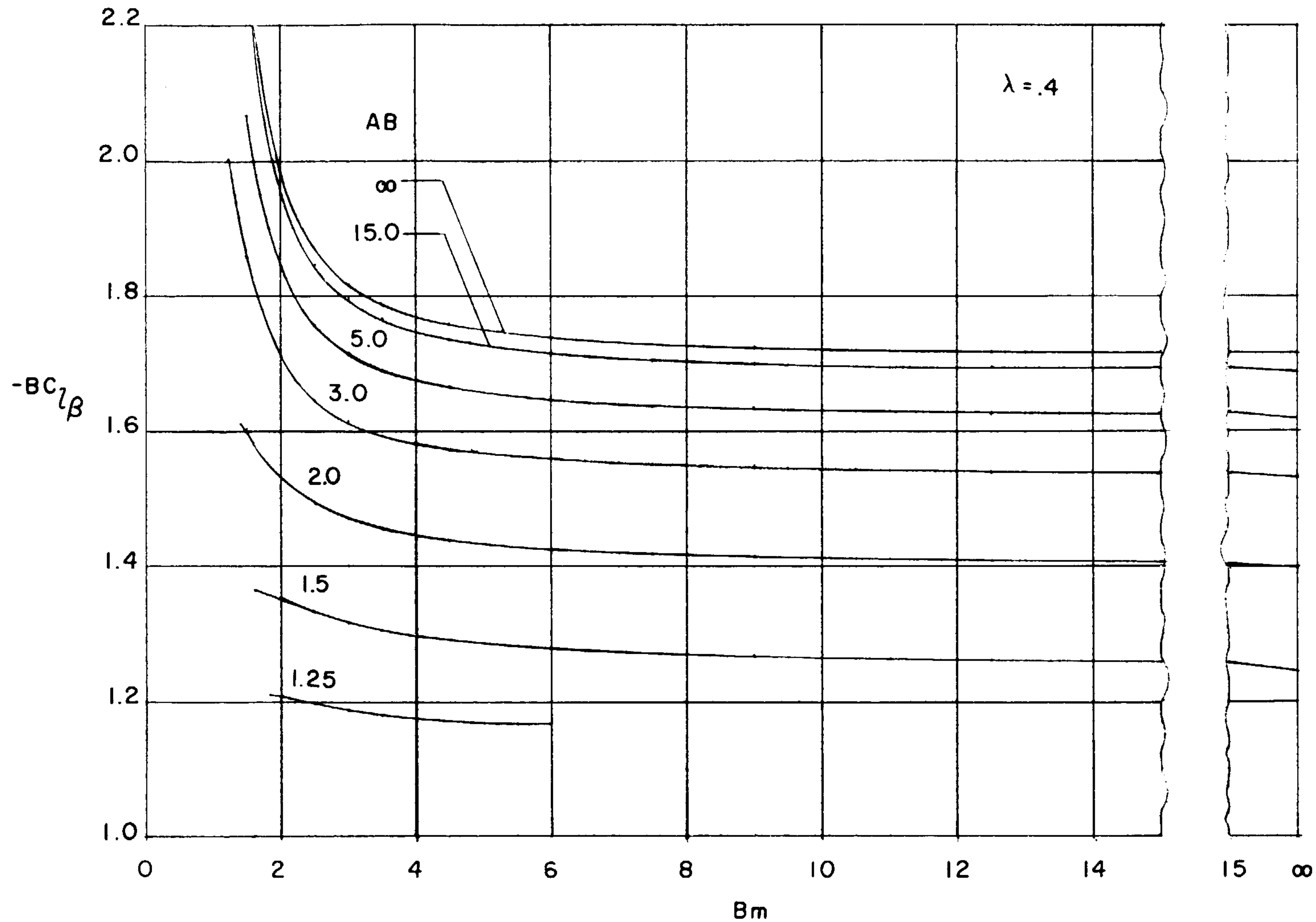

(c) Taper ratio, 0.4.

Figure 5.- Continued.

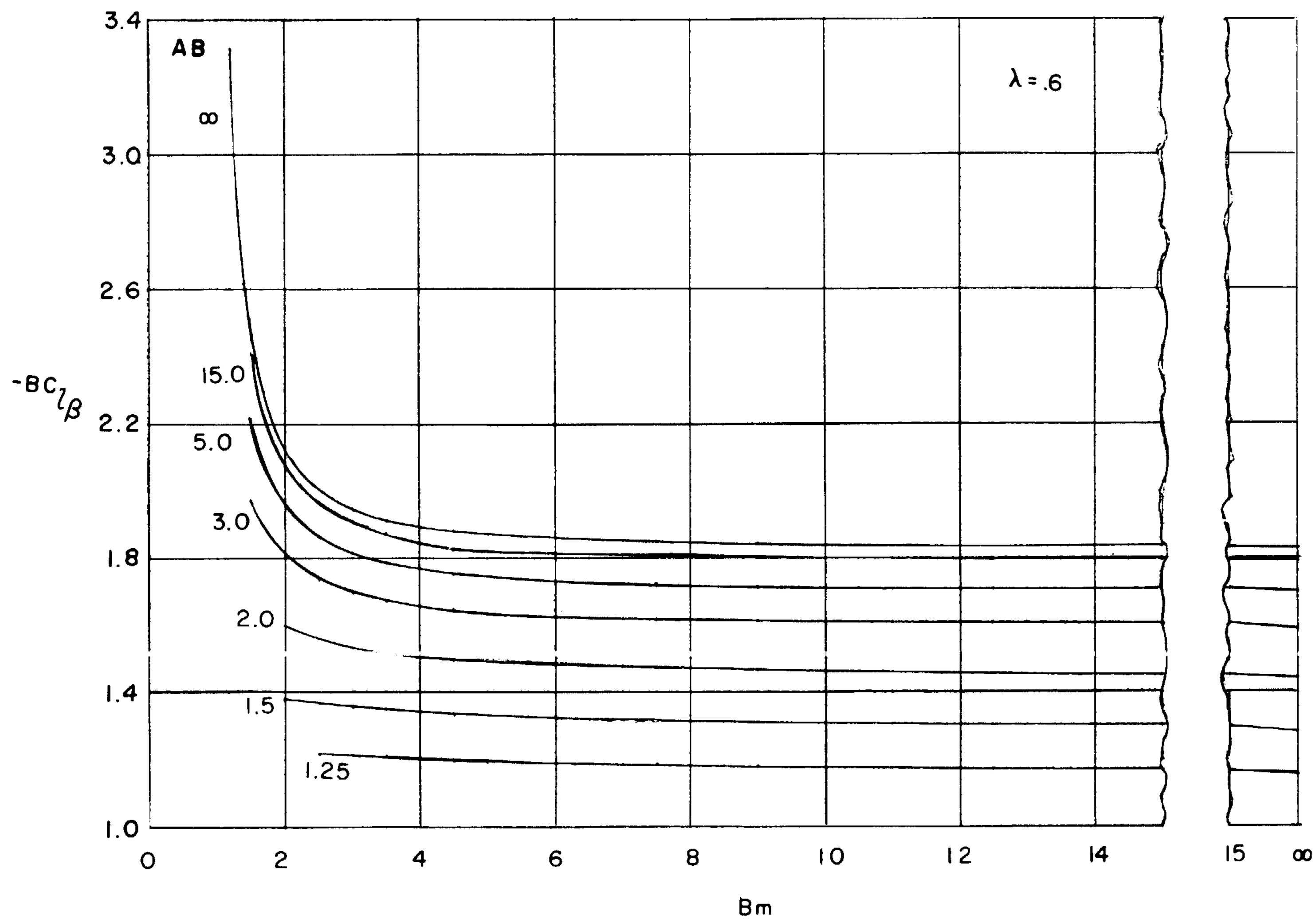

(d) Taper ratio, 0.6.

Figure 5.- Continued.

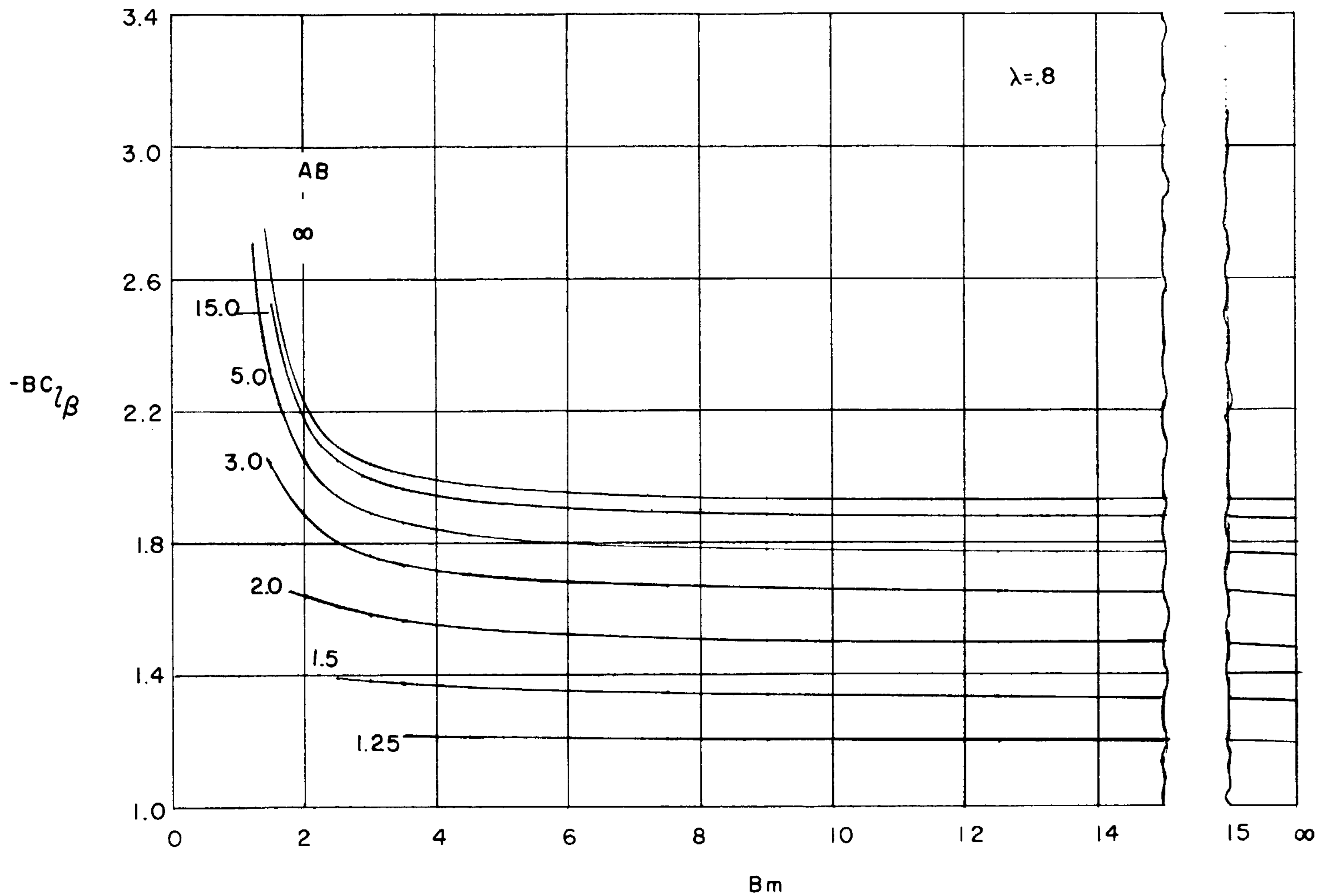

(e) Taper ratio, 0.8.

Figure 5.- Continued.

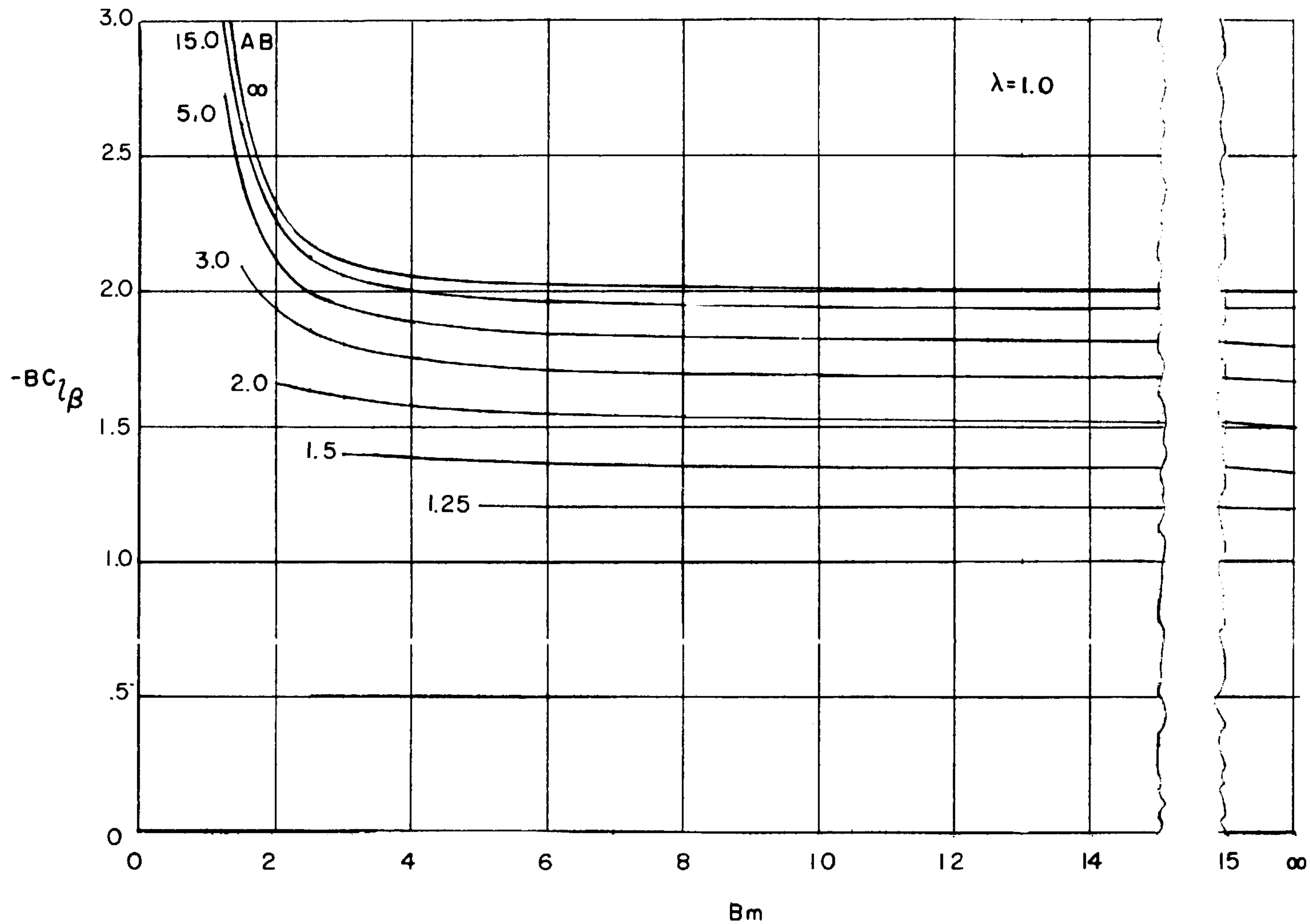

(f) Taper ratio, 1.0.

Figure 5.- Concluded.

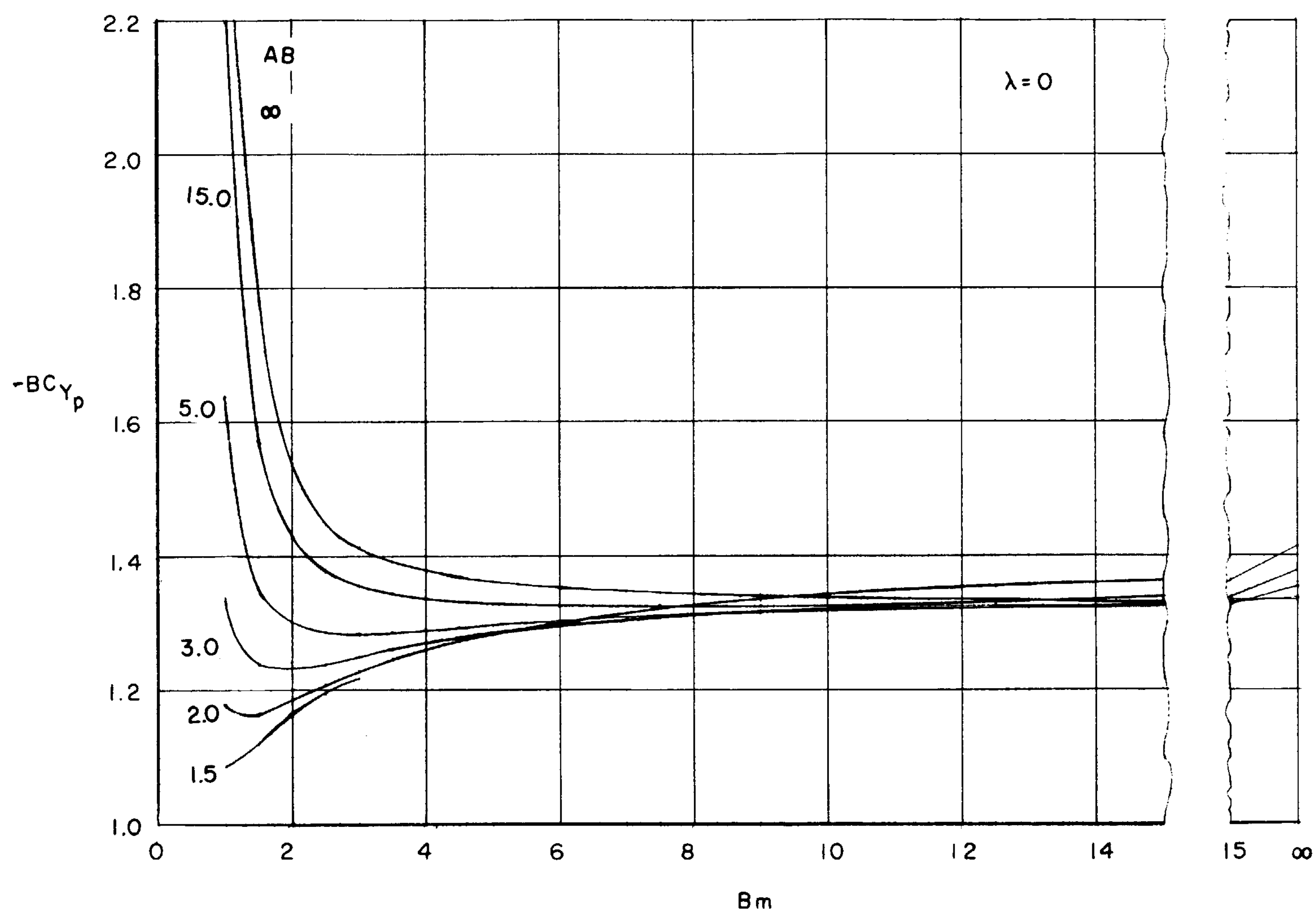

(a) Taper ratio, 0.

Figure 6.- Variation of $-BC_{Y_p}$ with Mach number-geometry parameters.

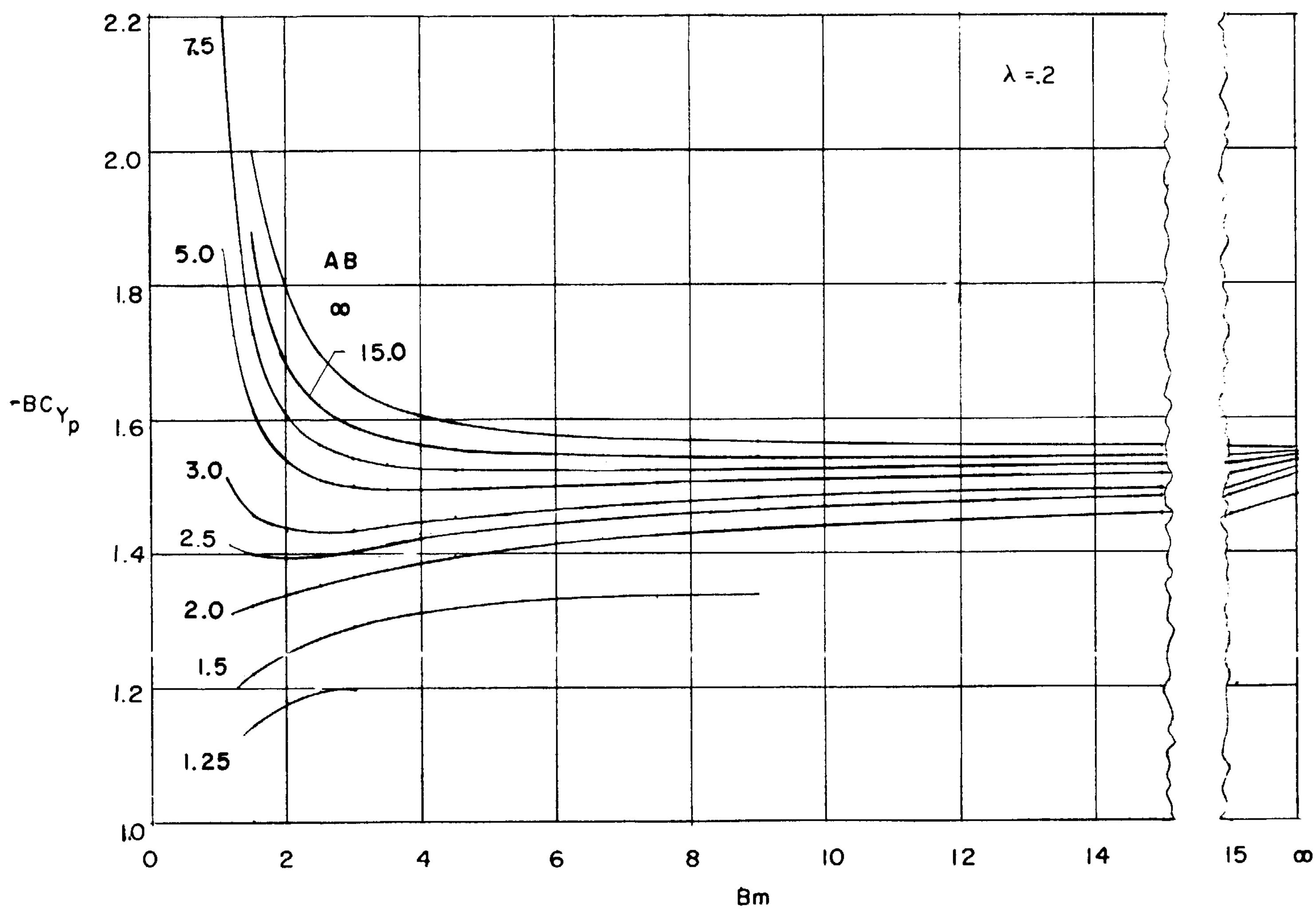

(b) Taper ratio, 0.2.

Figure 6.- Continued.

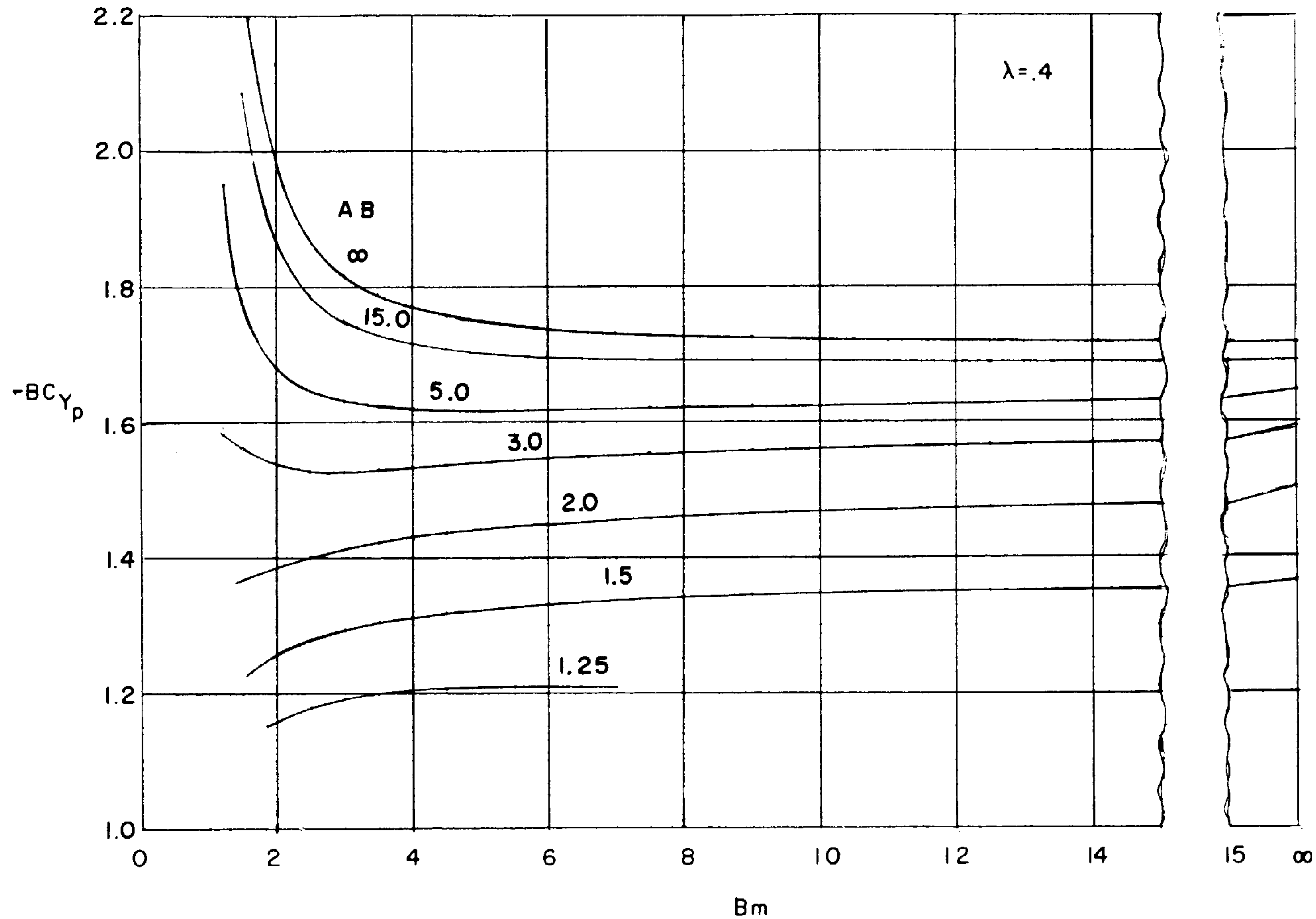

(c) Taper ratio, 0.4.

Figure 6.- Continued.

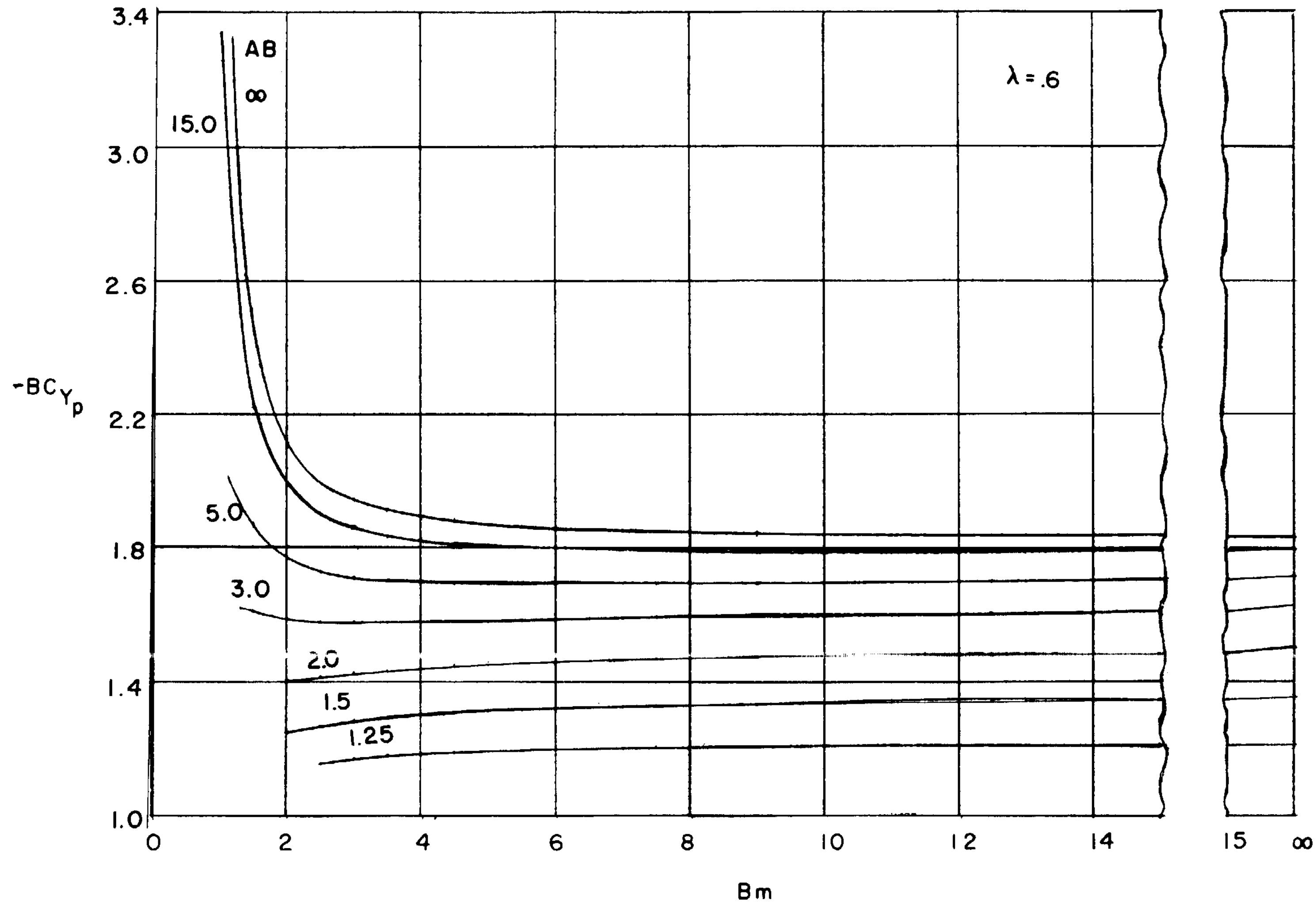

(d) Taper ratio, 0.6.

Figure 6.- Continued.

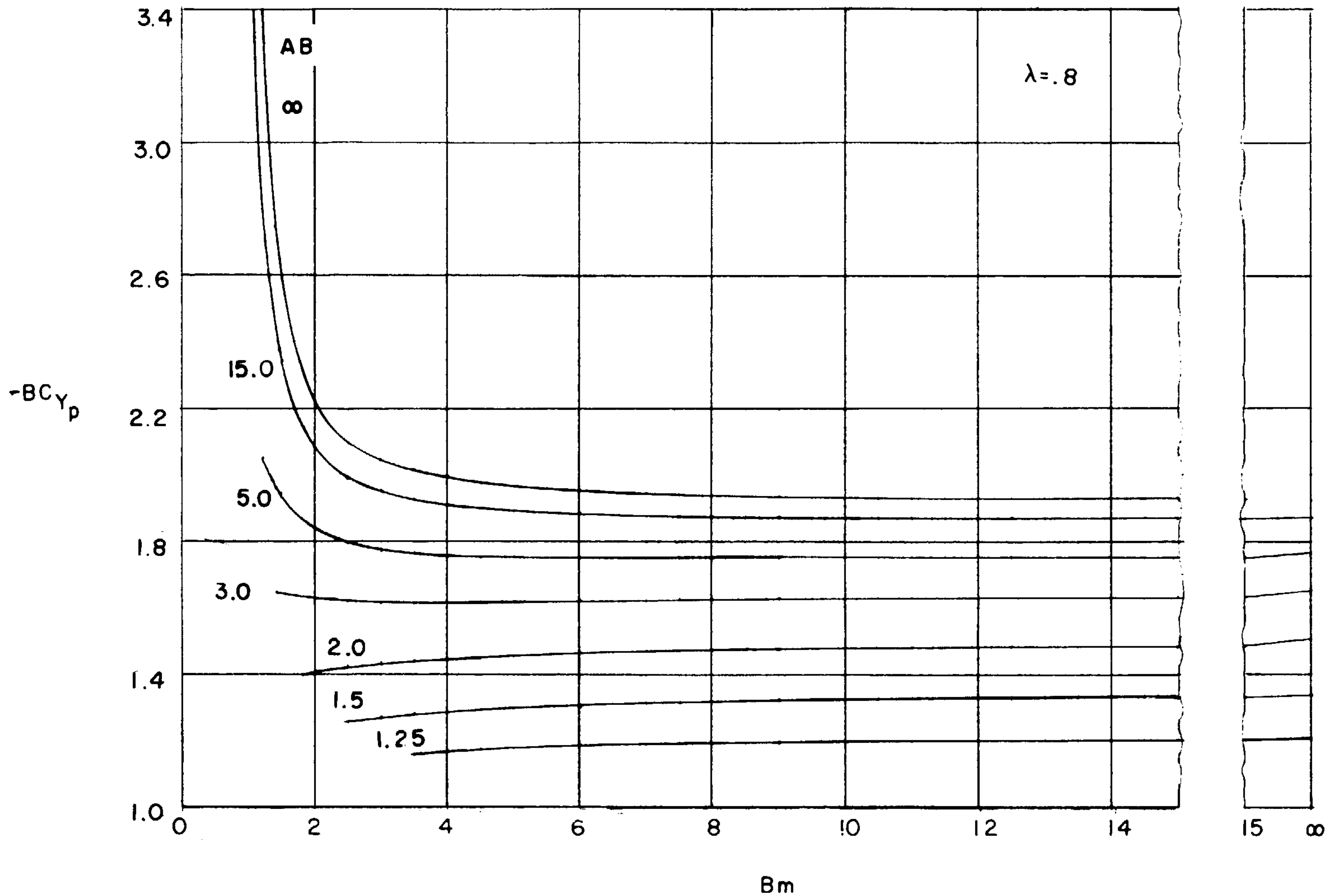

(e) Taper ratio, 0.8.

Figure 6.- Continued.

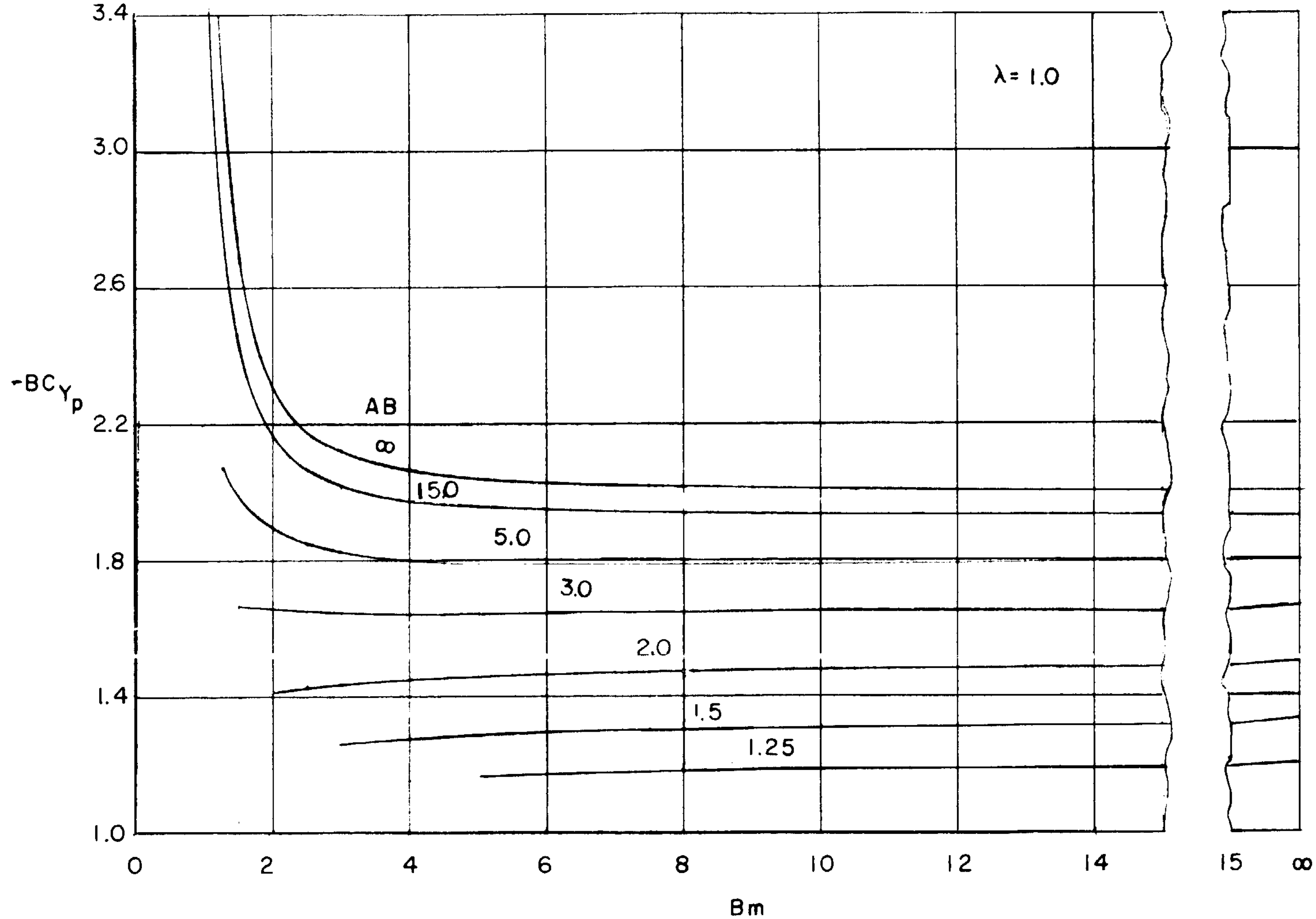

(f) Taper ratio, 1.0.

Figure 6.- Concluded.

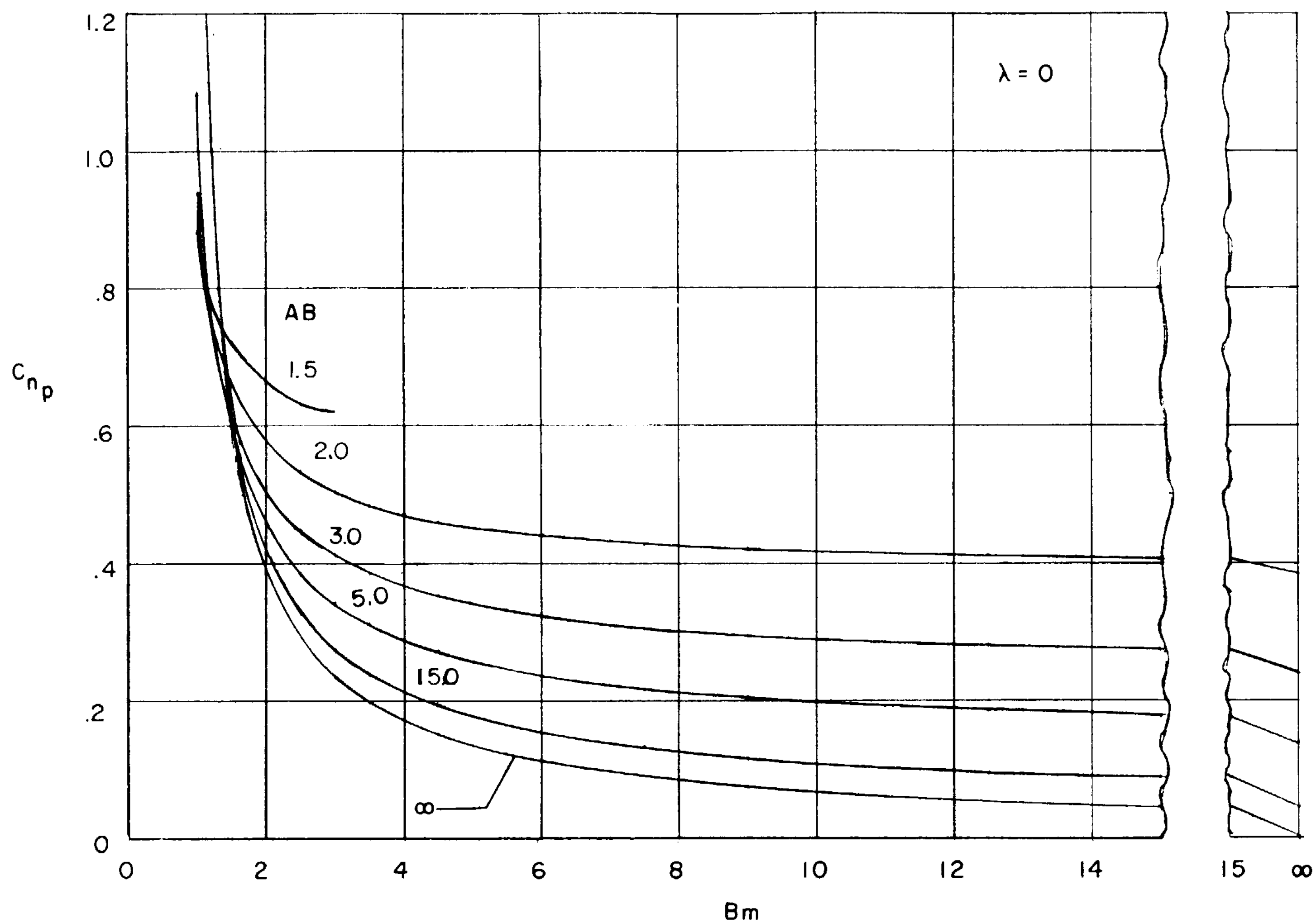

(a) Taper ratio, 0.

Figure 7.- Variation of C_{n_p} with Mach number-geometry parameters.

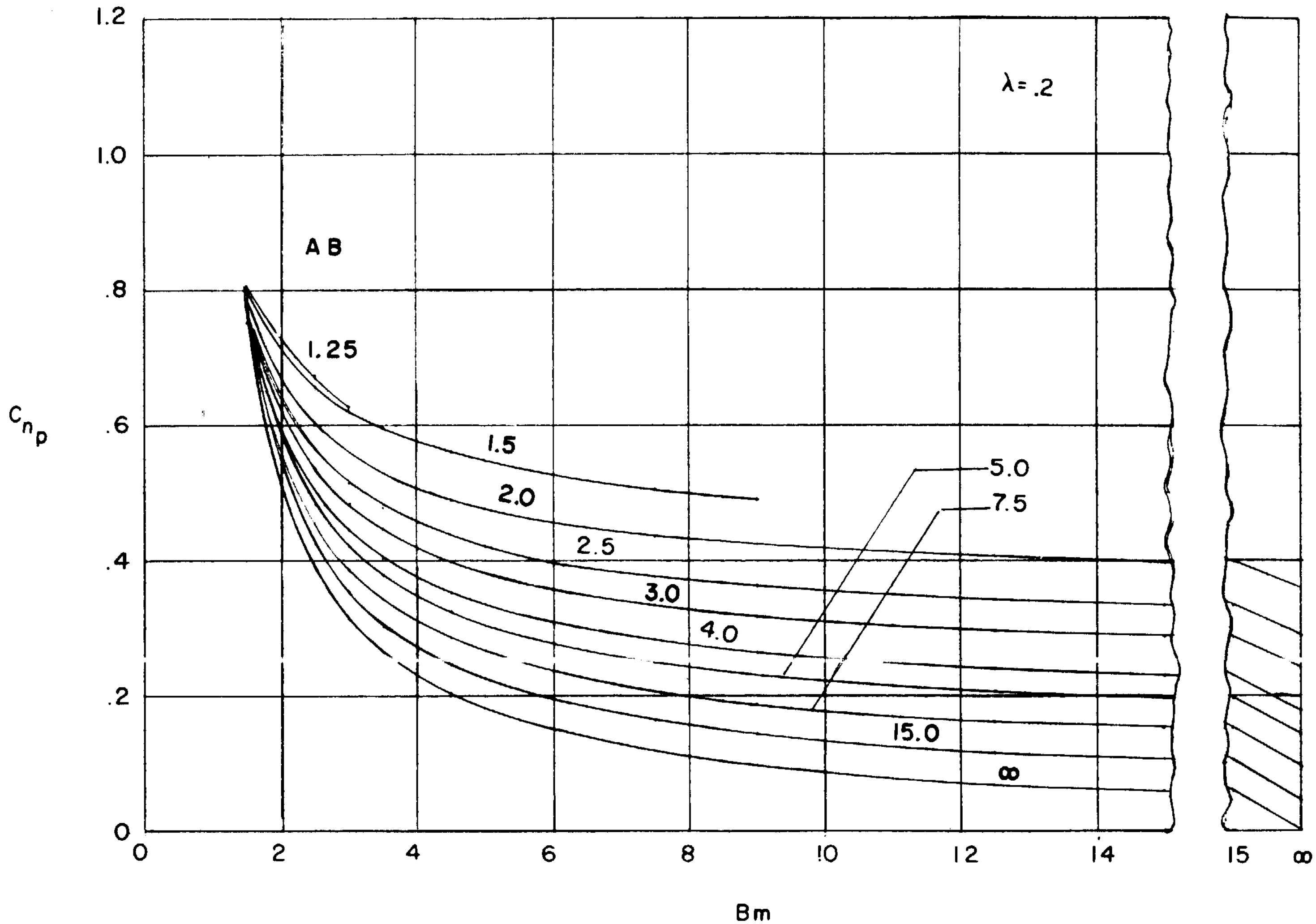

(b) Taper ratio, 0.2.

Figure 7.- Continued.

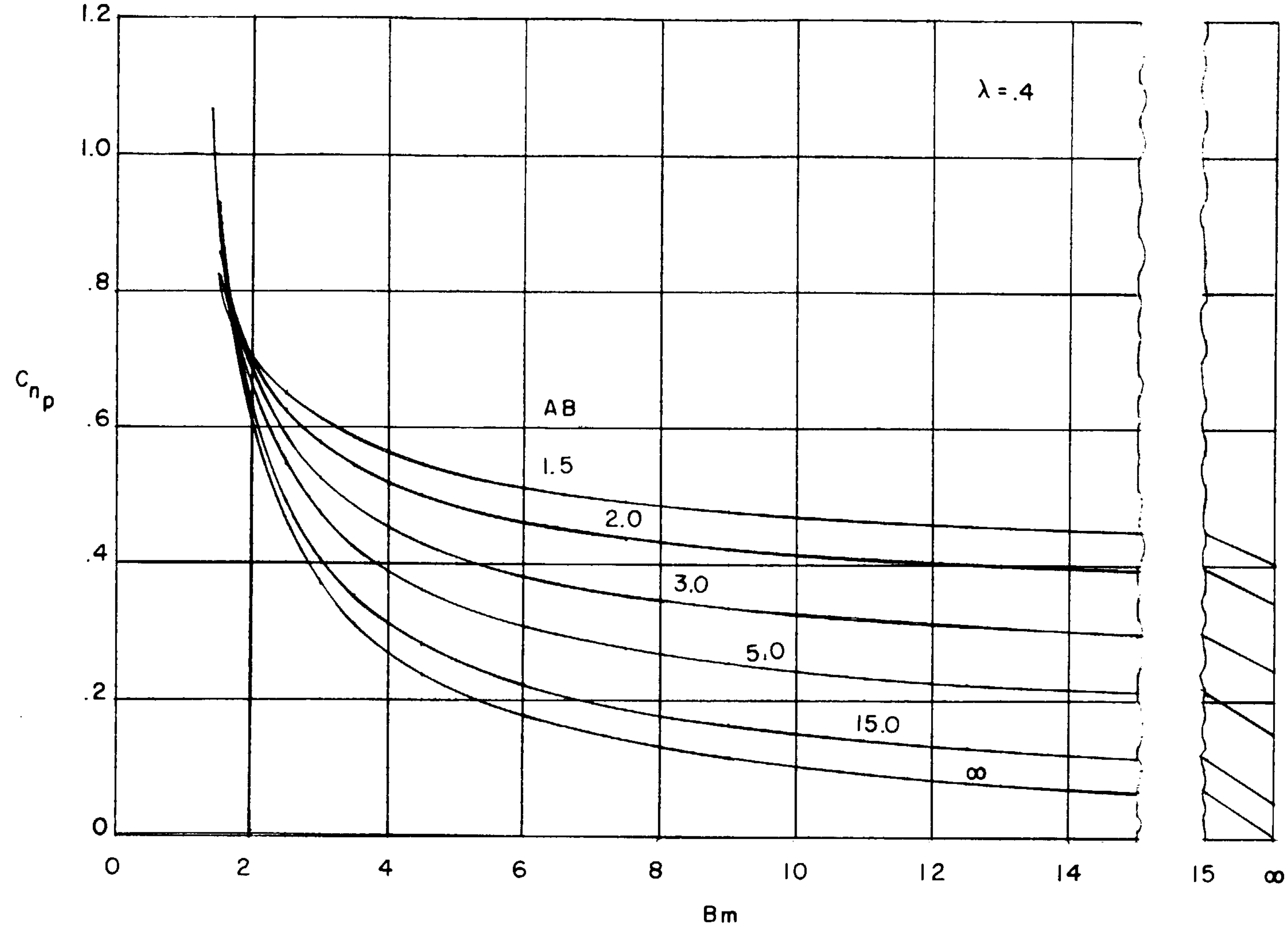

(c) Taper ratio, 0.4.

Figure 7.- Continued.

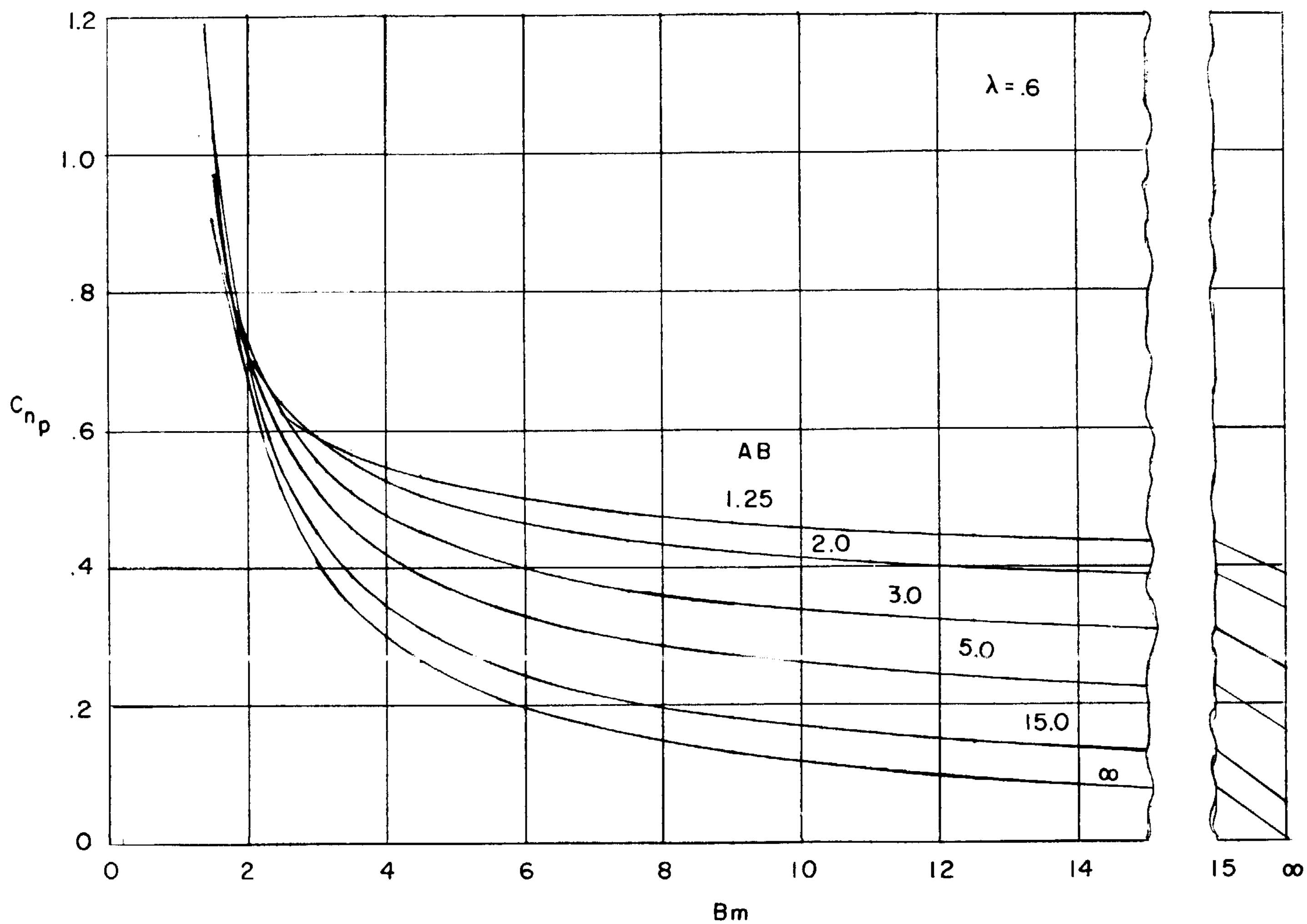

(d) Taper ratio, 0.6.

Figure 7.- Continued.

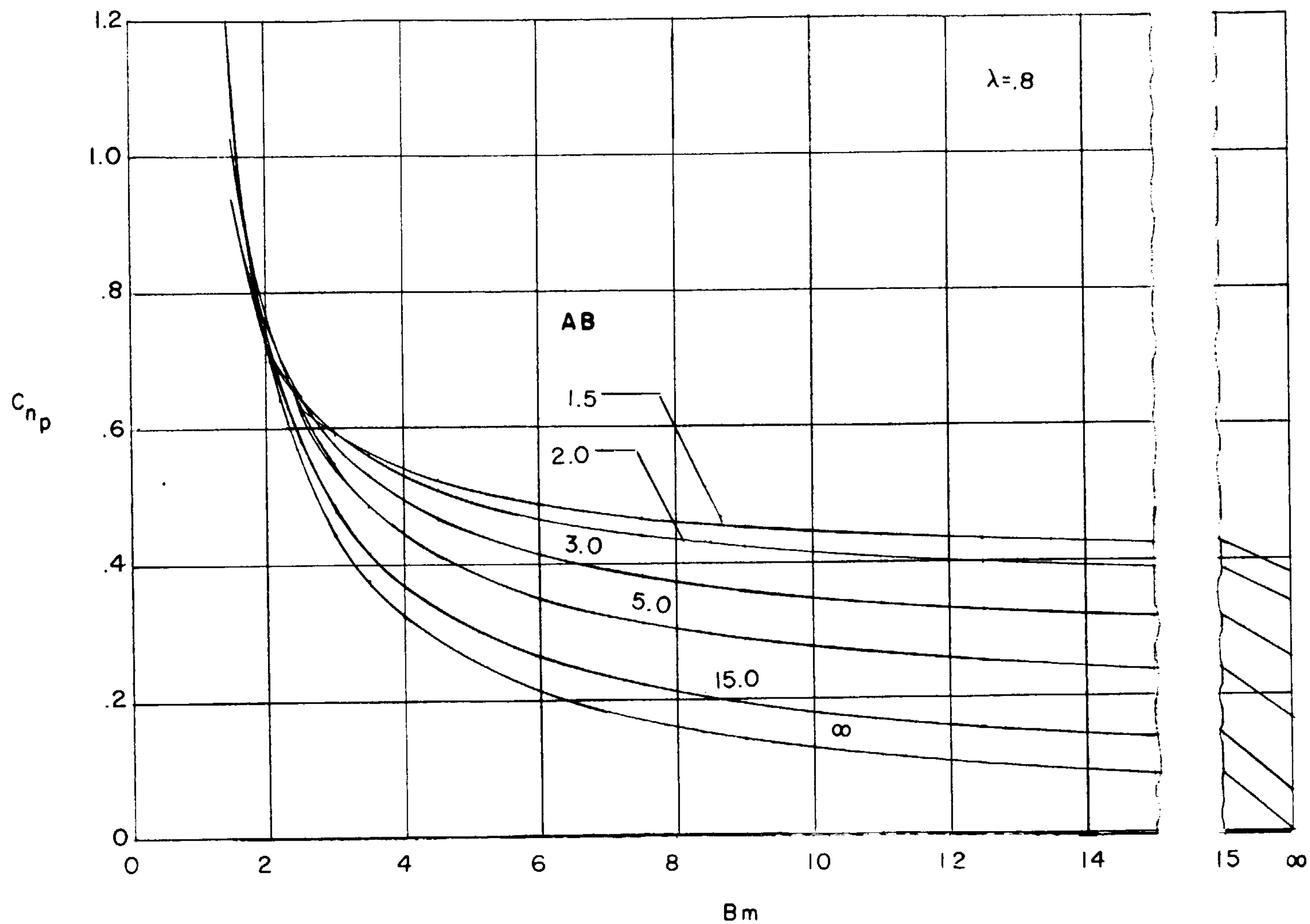

(e) Taper ratio, 0.8.

Figure 7.- Continued.

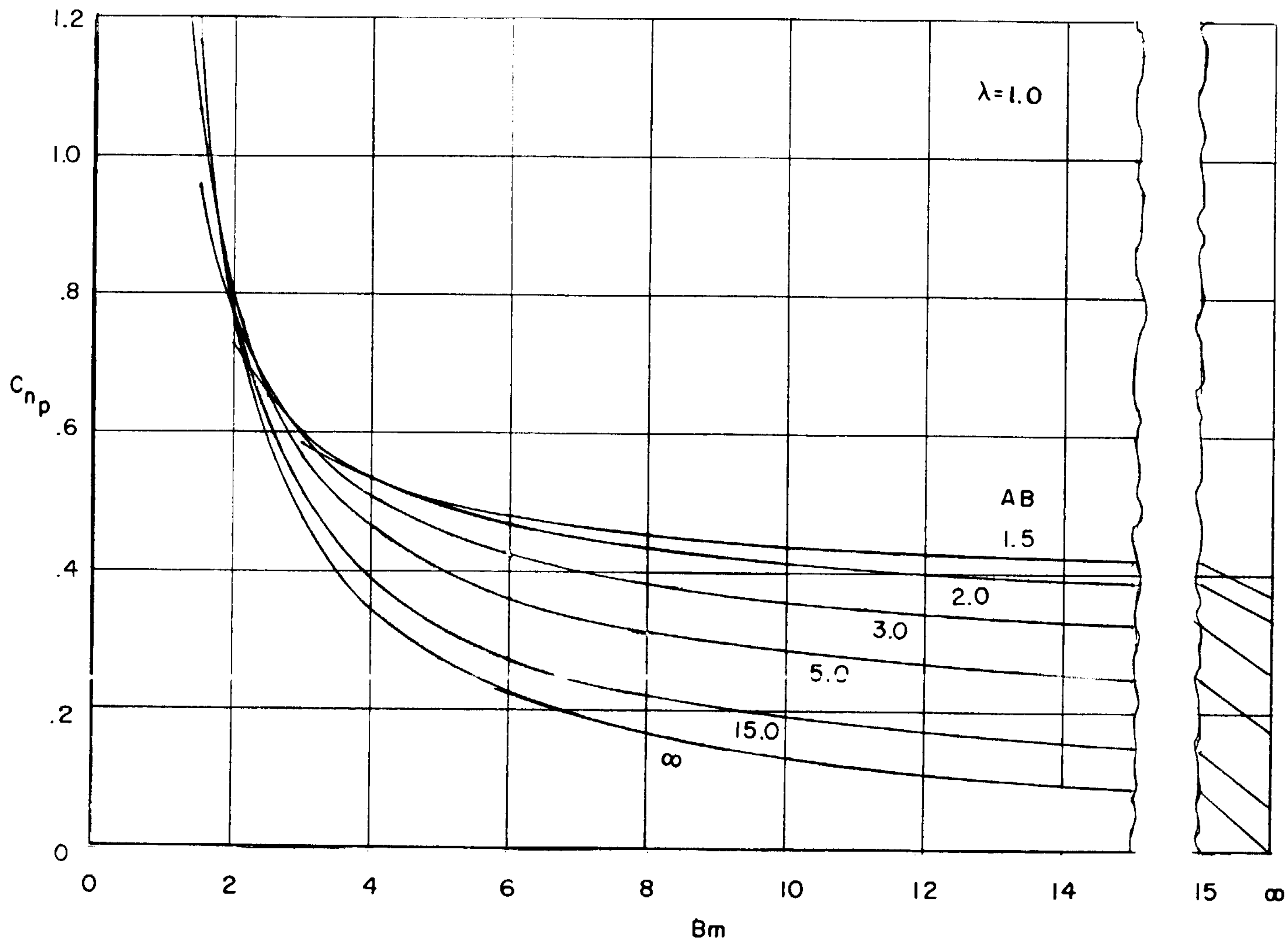

(f) Taper ratio, 1.0.

Figure 7.- Concluded.

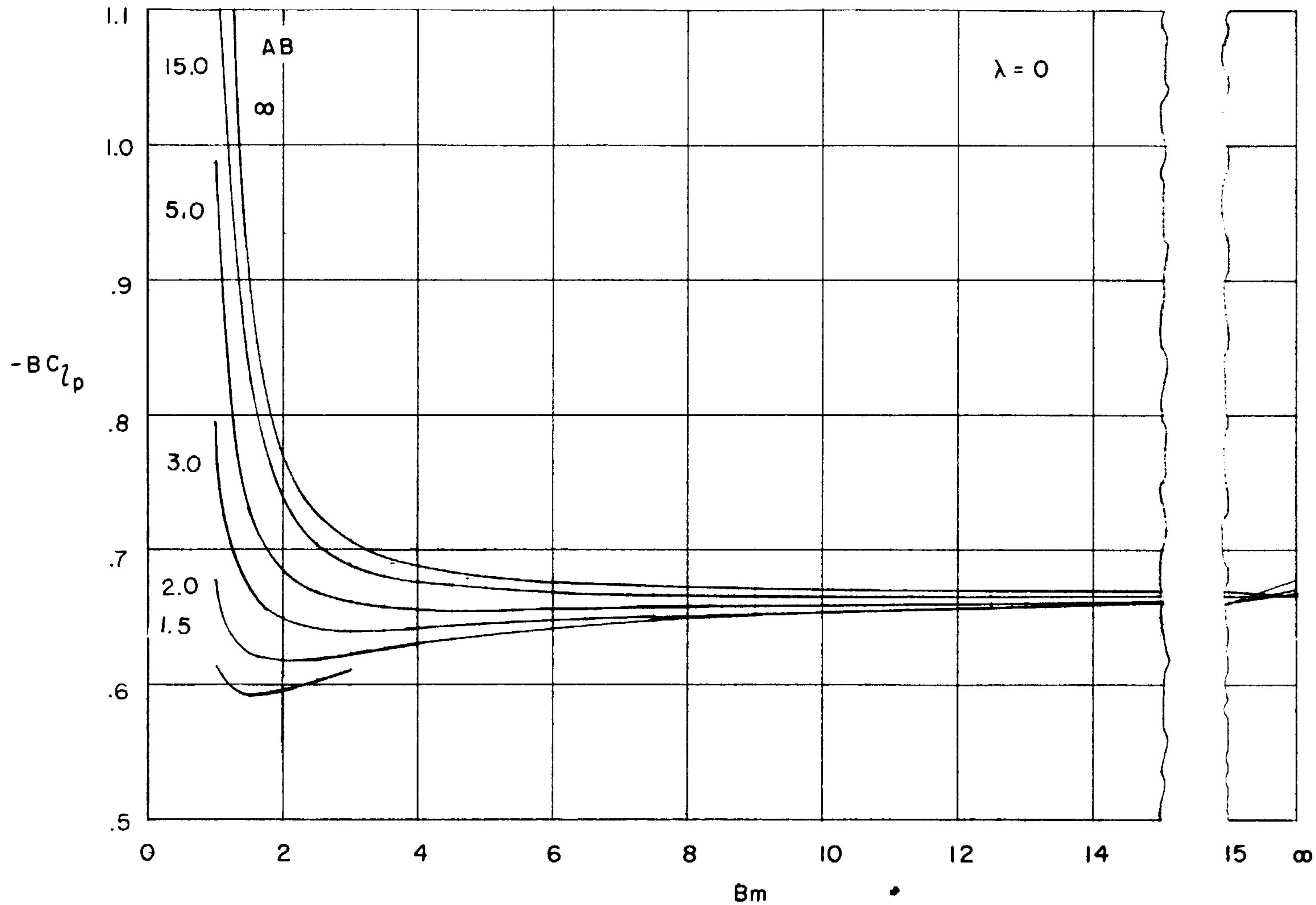

(a) Taper ratio, 0.

Figure 8.- Variation of $-BC_{l_p}$ with Mach number-geometry parameters.

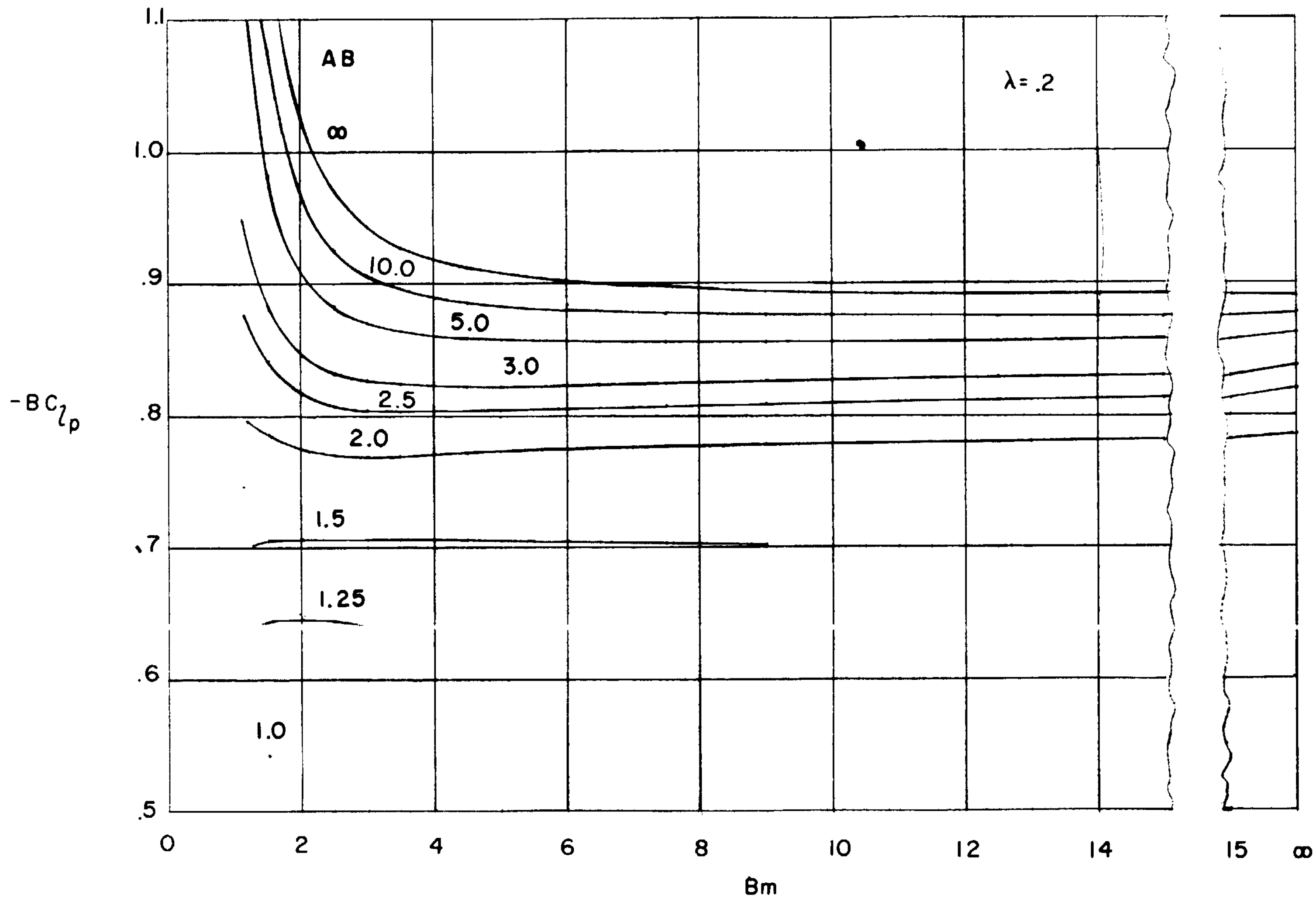

(b) Taper ratio, 0.2.

Figure 8.- Continued.

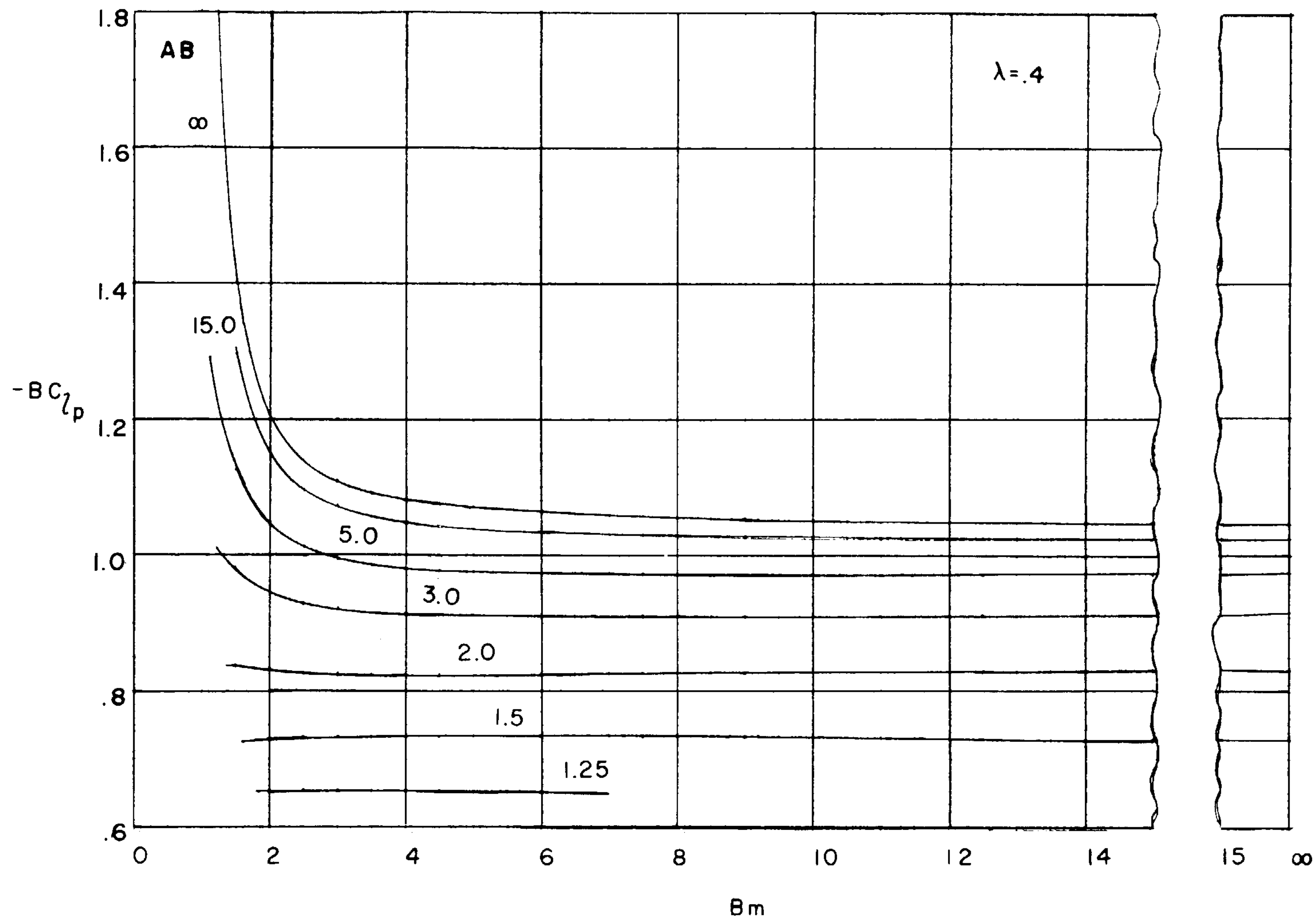

(c) Taper ratio, 0.4.

Figure 8.- Continued.

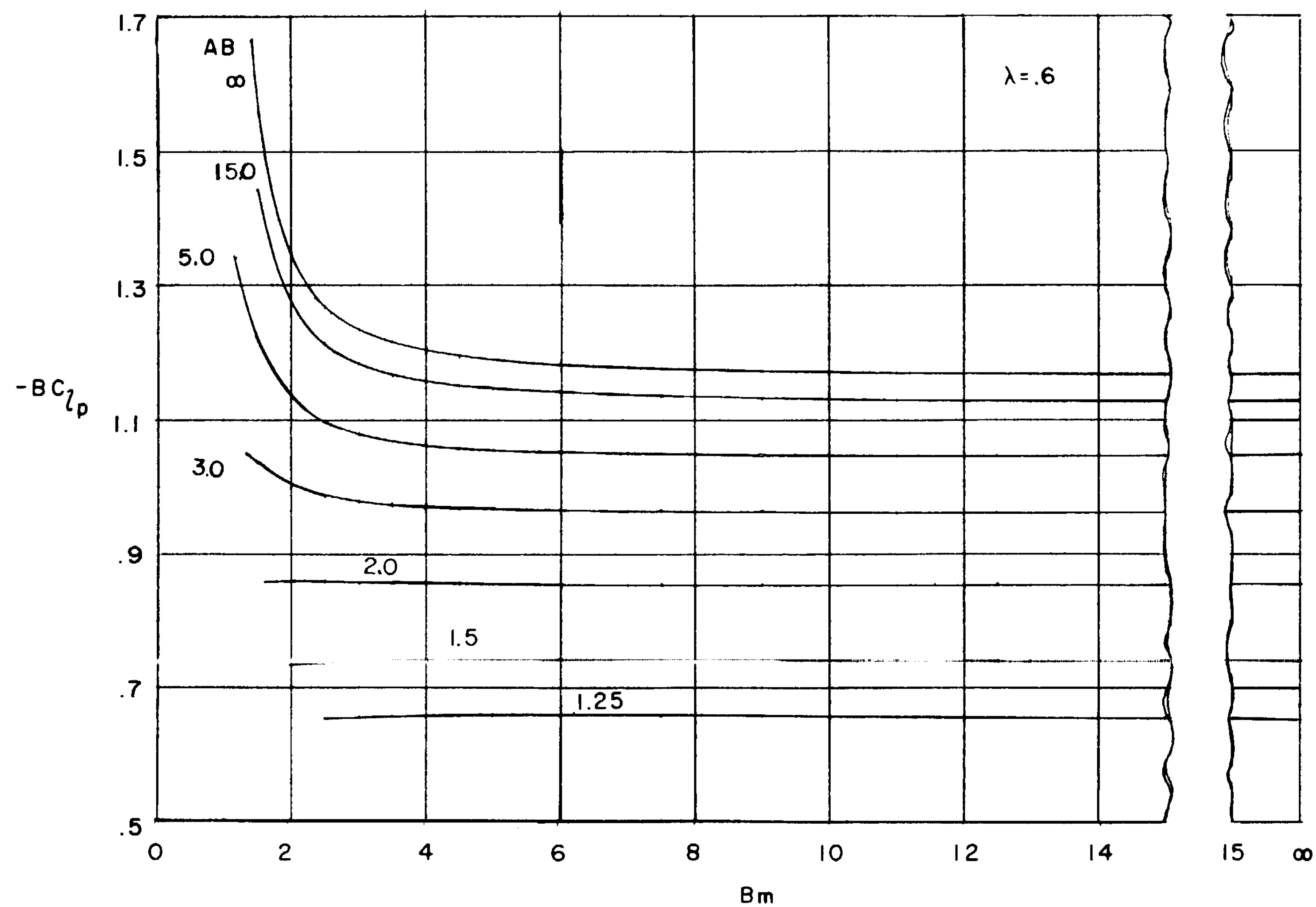

(d) Taper ratio, 0.6.

Figure 8.- Continued.

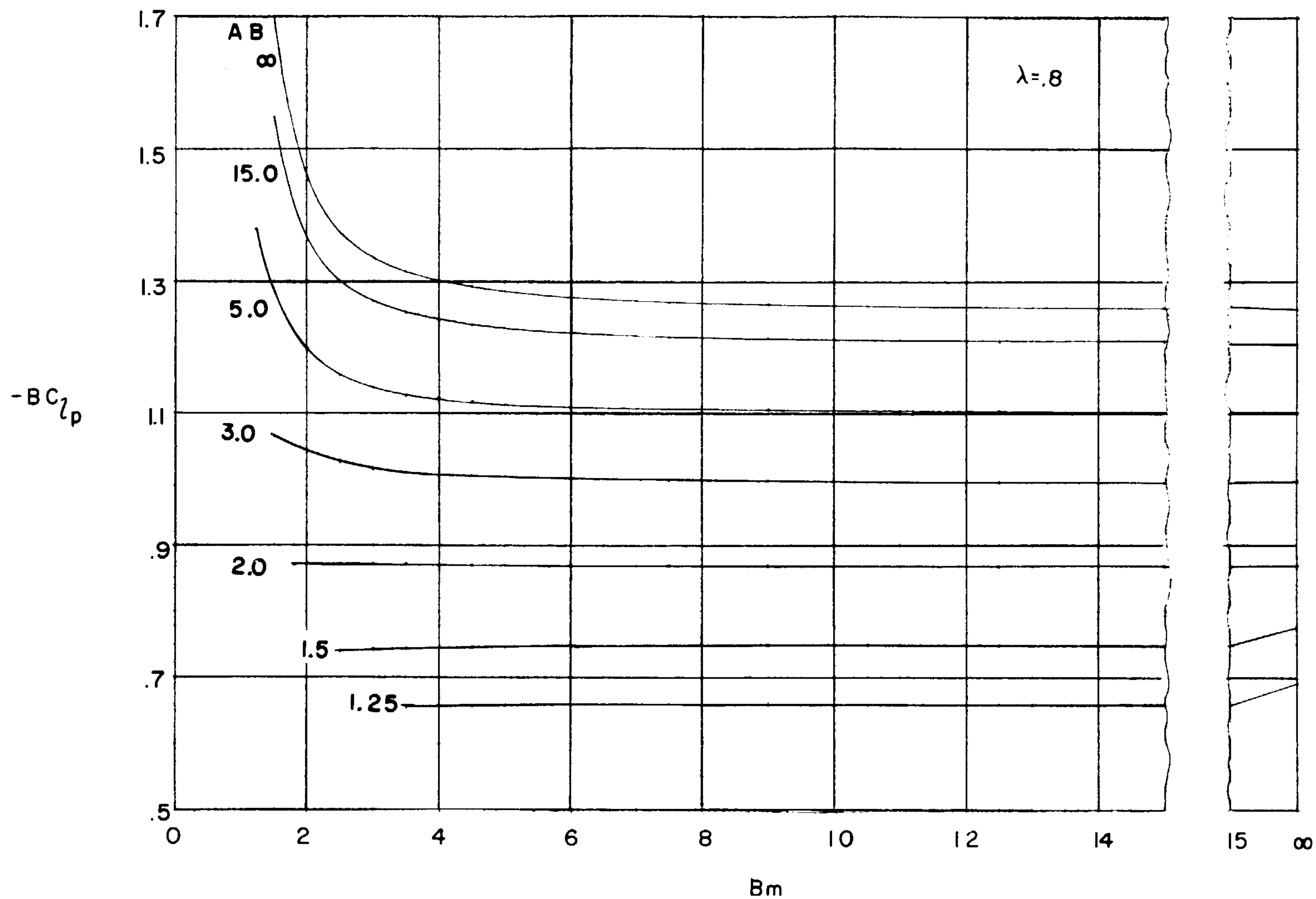

(e) Taper ratio, 0.8.

Figure 8.- Continued.

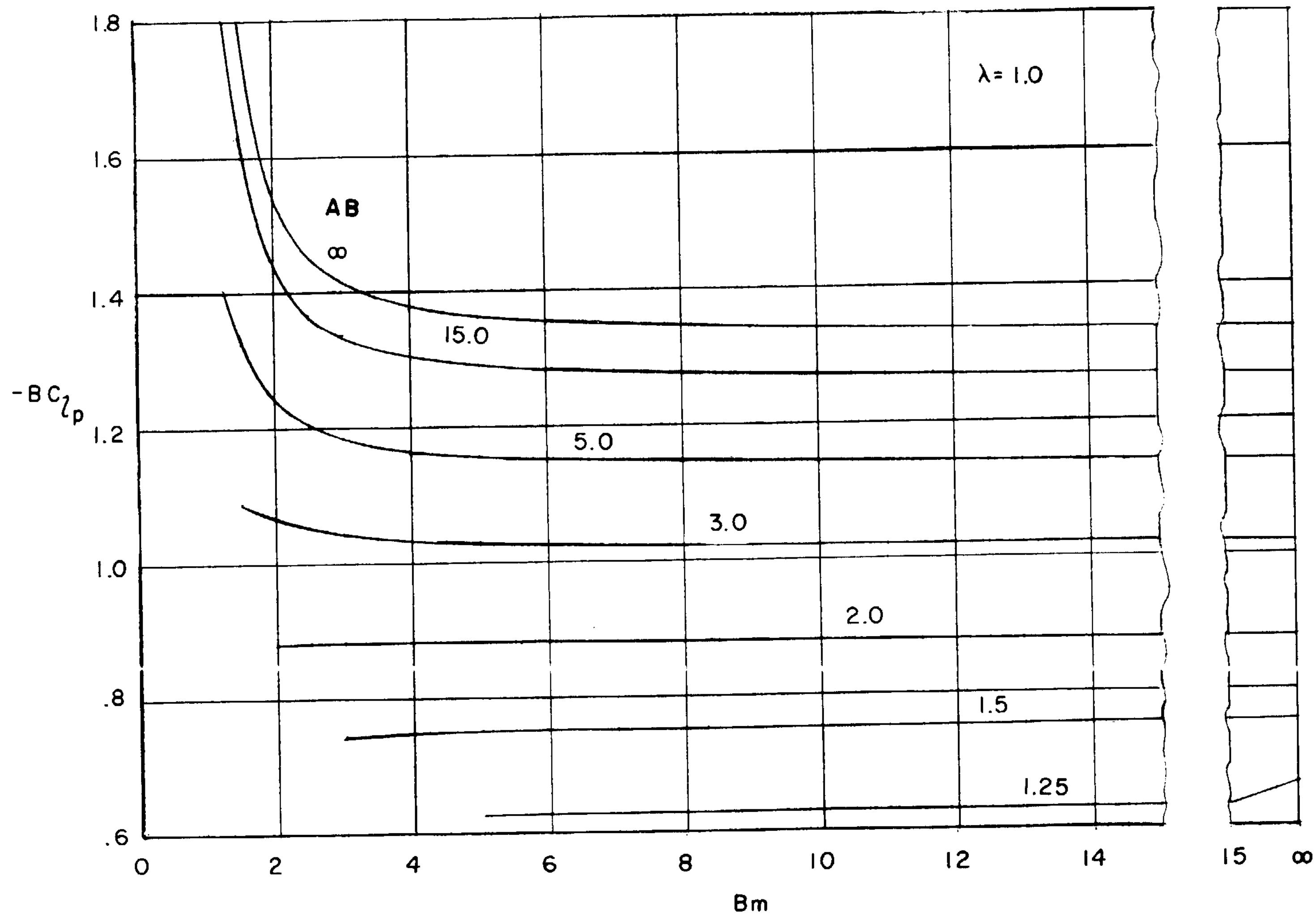

(f) Taper ratio, 1.0.

Figure 8.- Concluded.

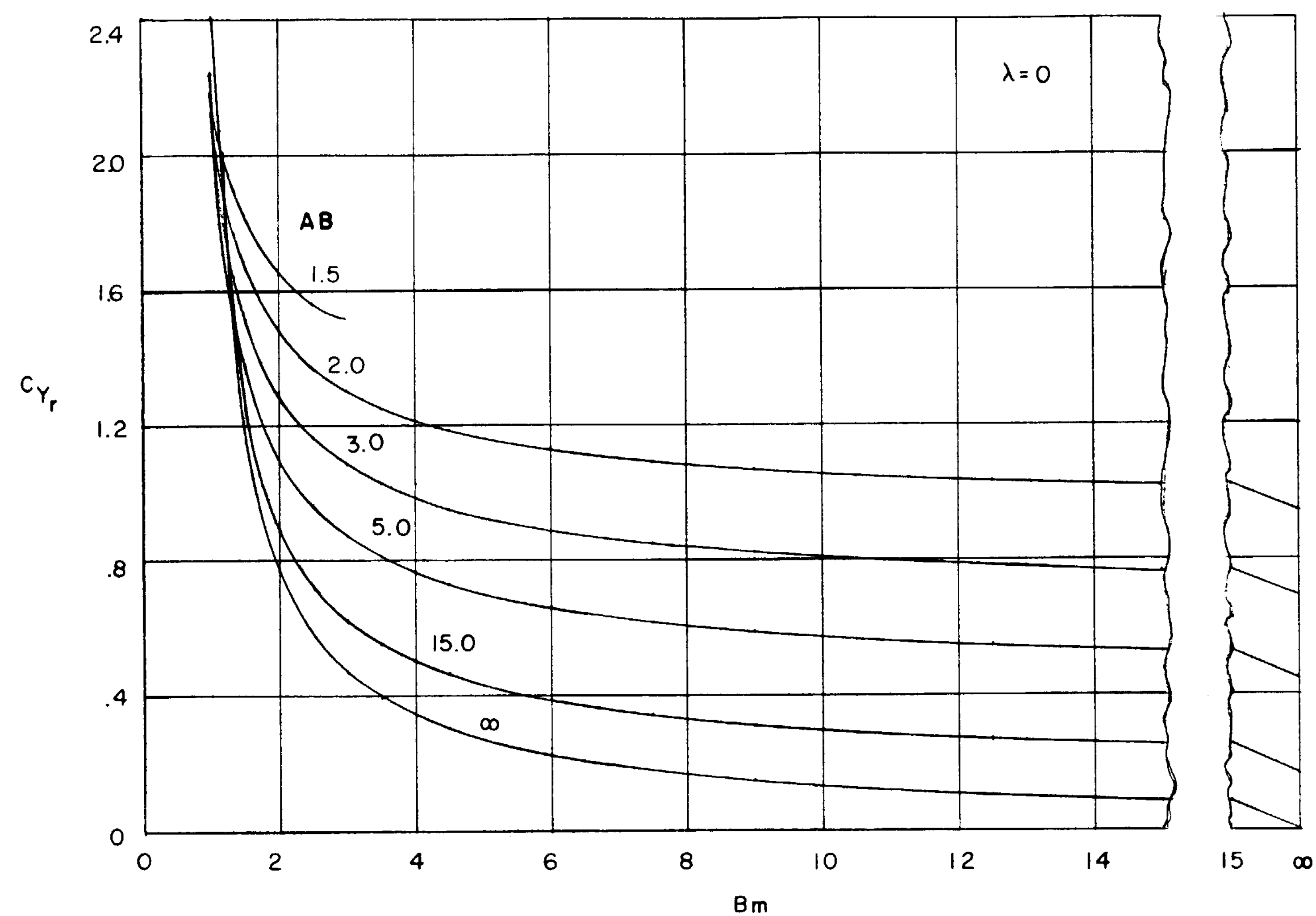

(a) Taper ratio, 0.

Figure 9.- Variation of C_{Y_r} with Mach number-geometry parameters.

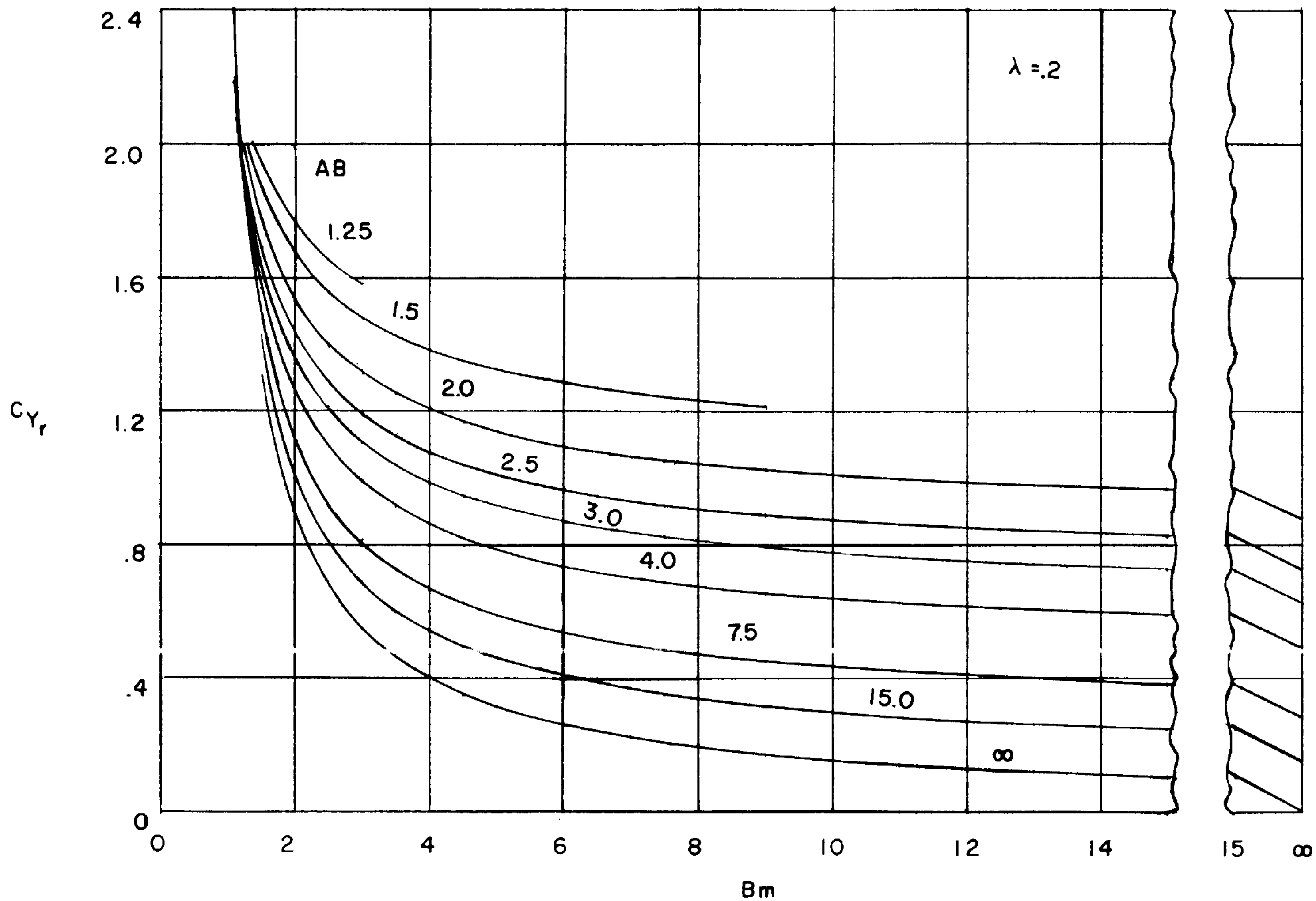

(b) Taper ratio, 0.2.

Figure 9.- Continued.

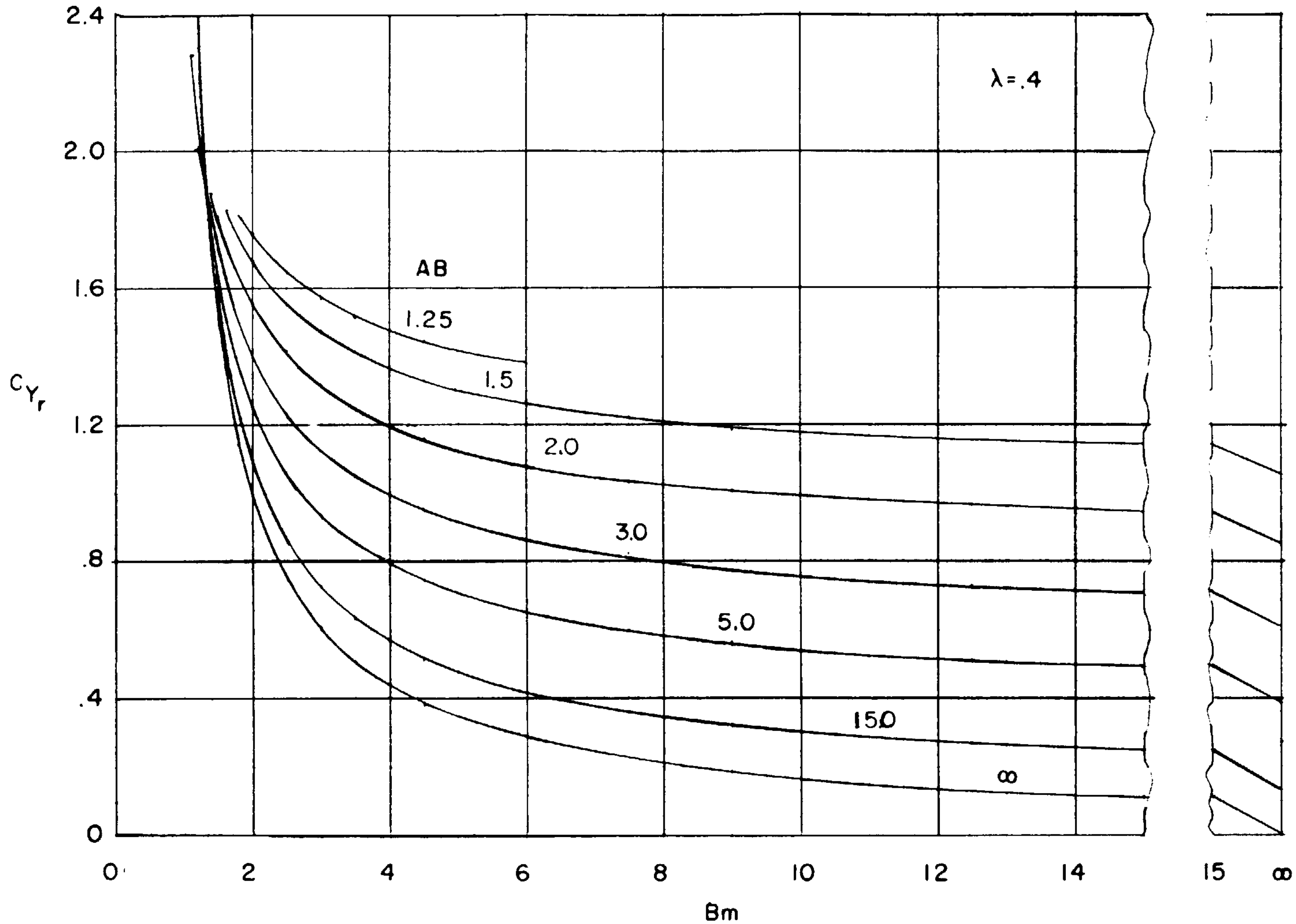

(c) Taper ratio, 0.4.

Figure 9.- Continued.

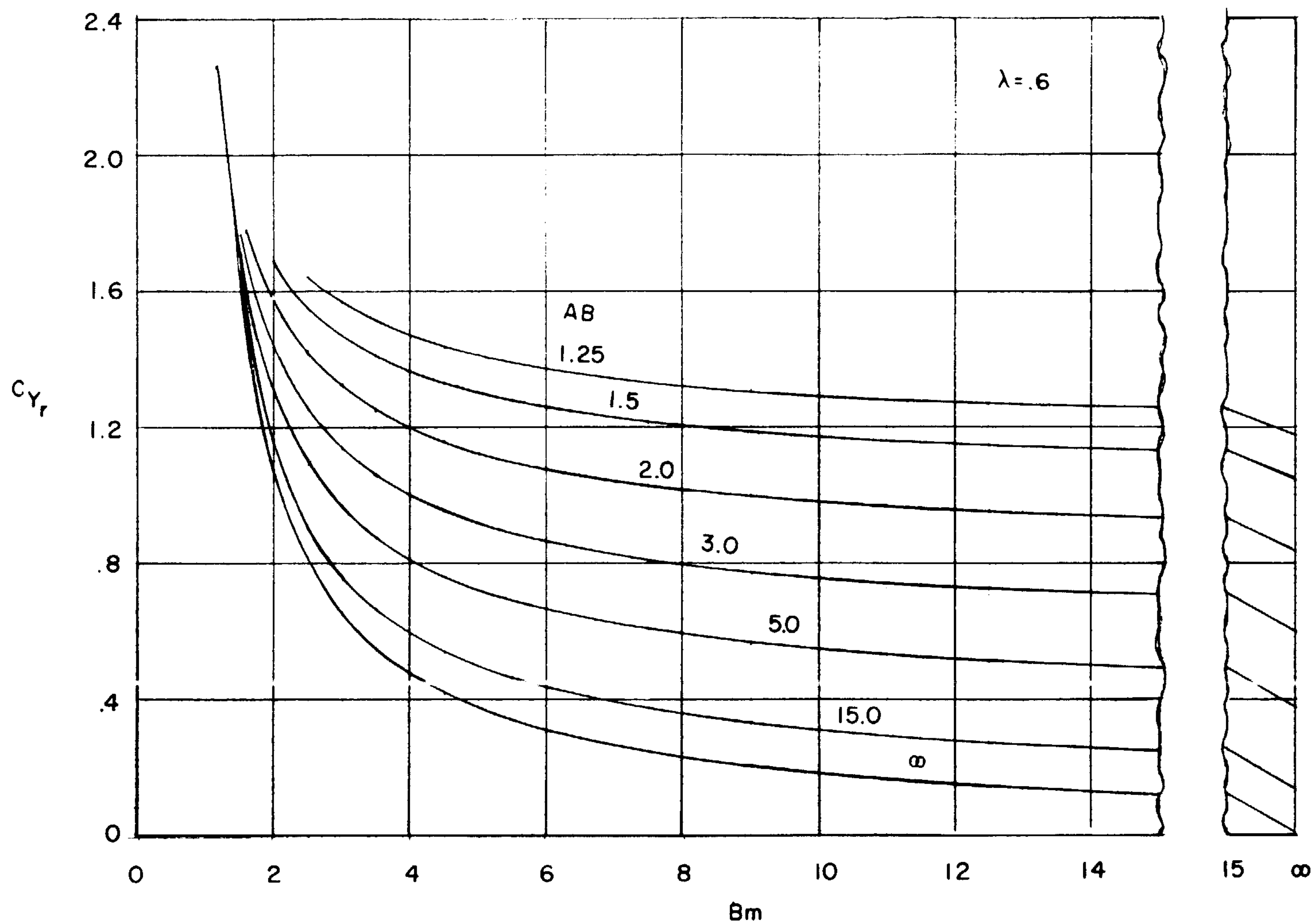

(d) Taper ratio, 0.6.

Figure 9.- Continued.

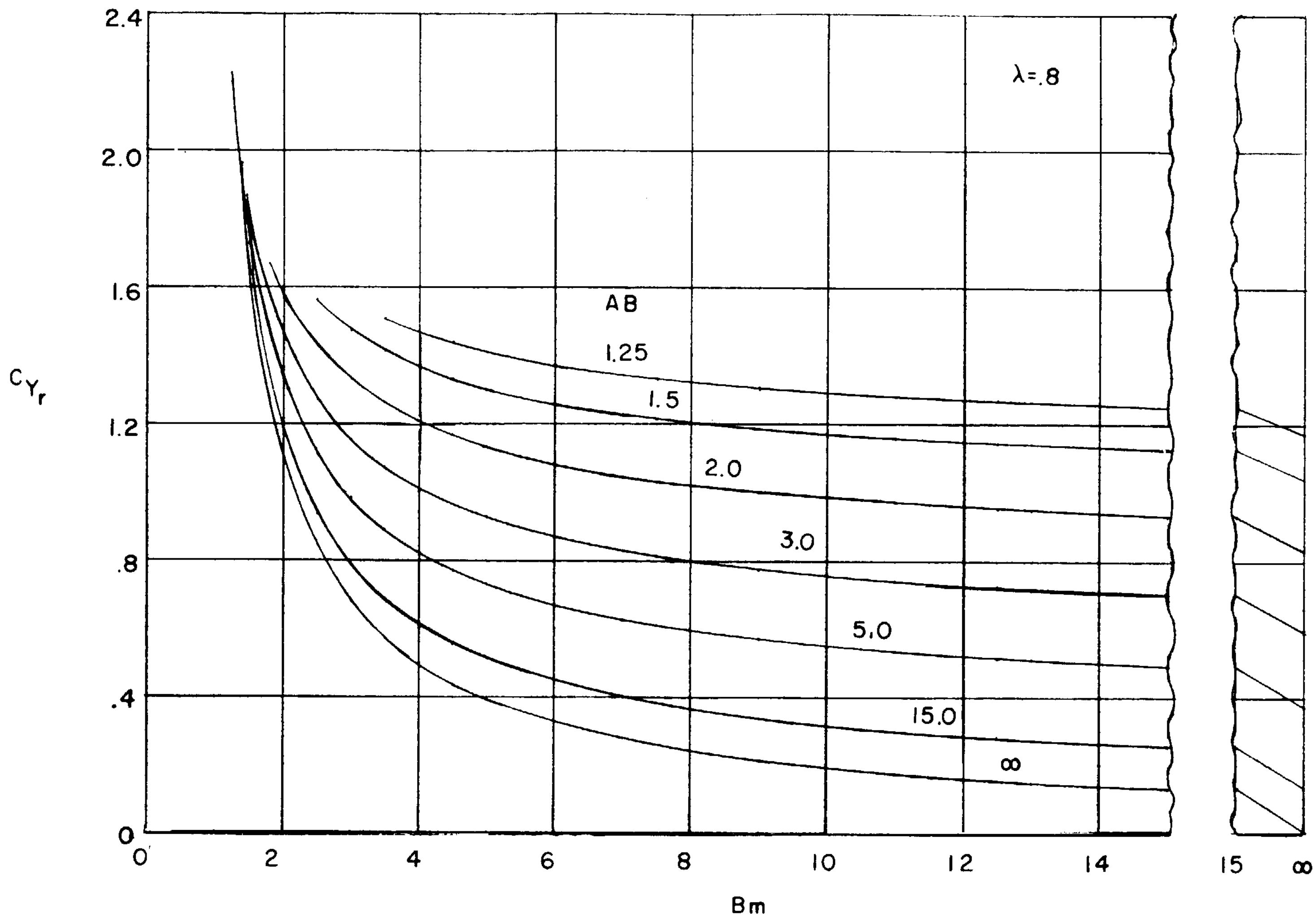

(e) Taper ratio, 0.8.

Figure 9.- Continued.

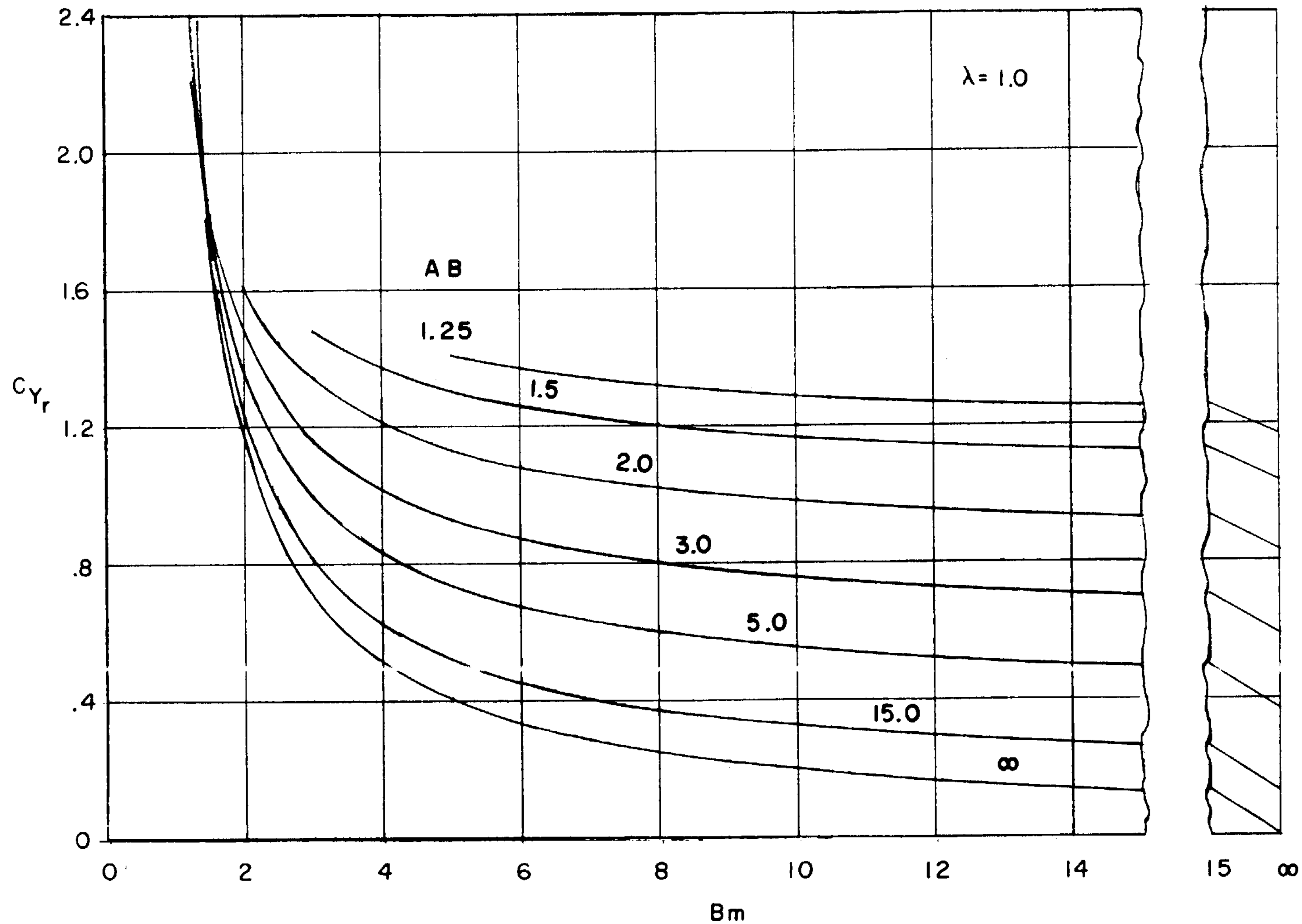

(f) Taper ratio, 1.0.

Figure 9.- Concluded.

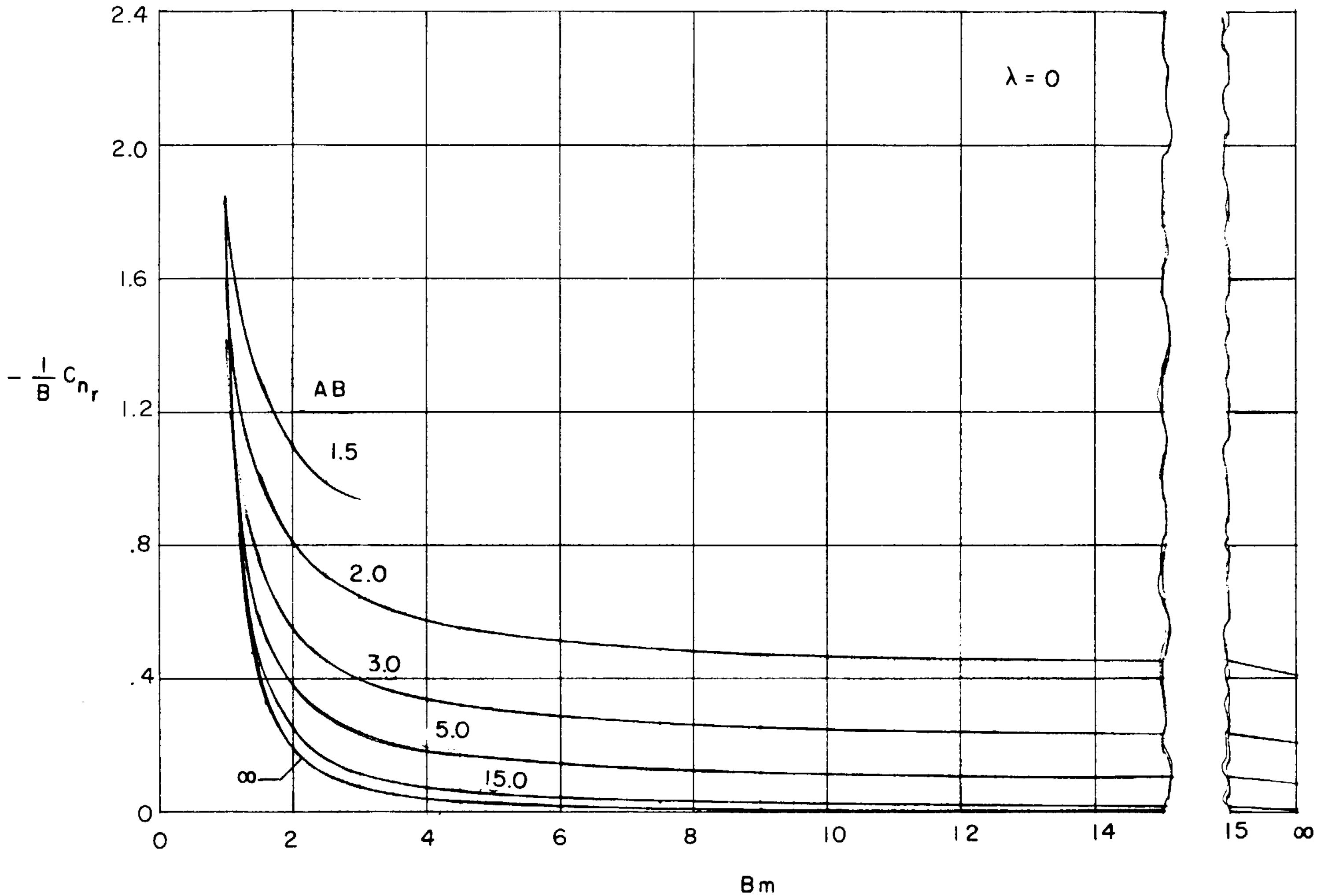

(a) Taper ratio, 0.

Figure 10.- Variation of $-\frac{1}{B}C_{n_r}$ with Mach number-geometry parameters.

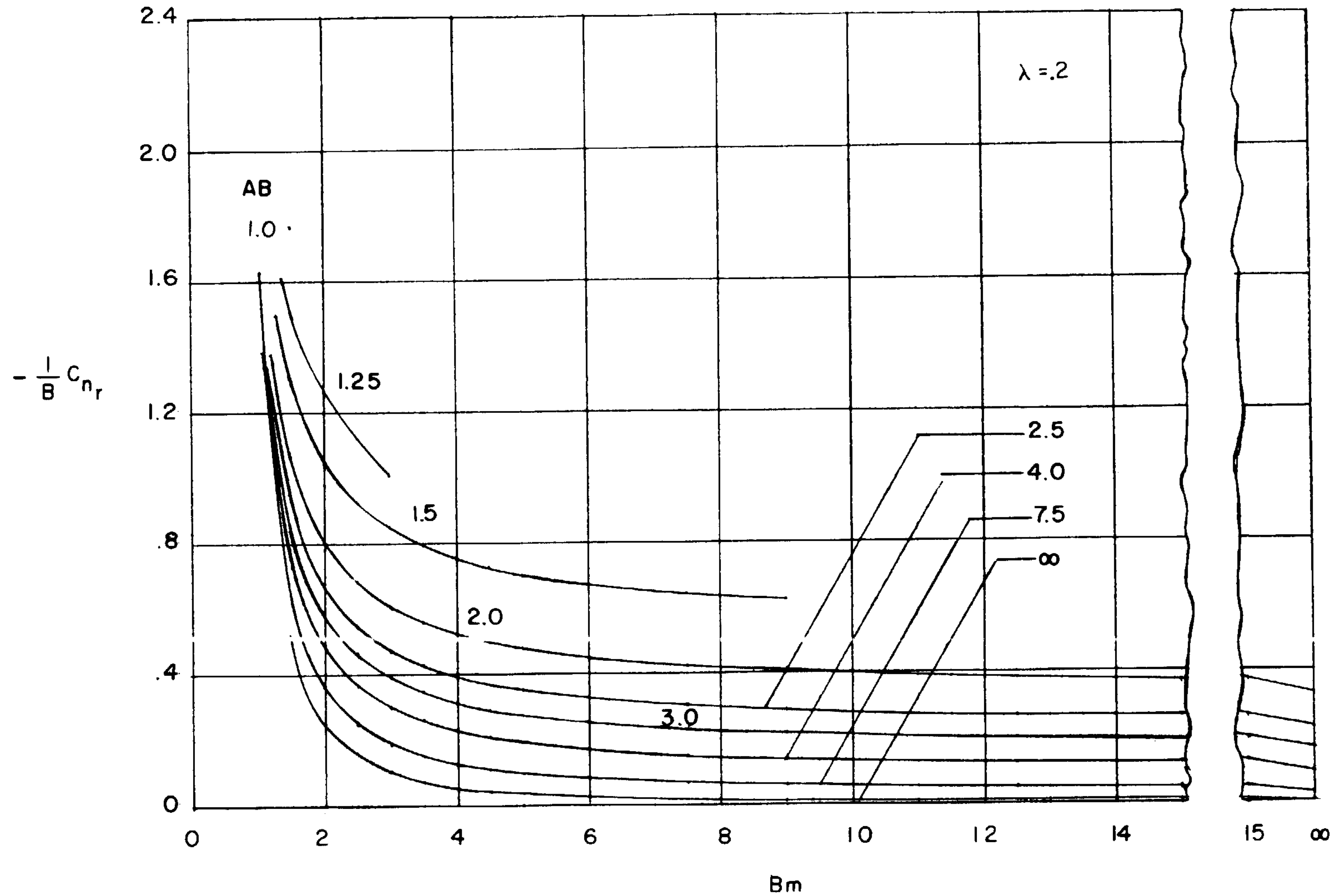

(b) Taper ratio, 0.2.

Figure 10.- Continued.

L-780

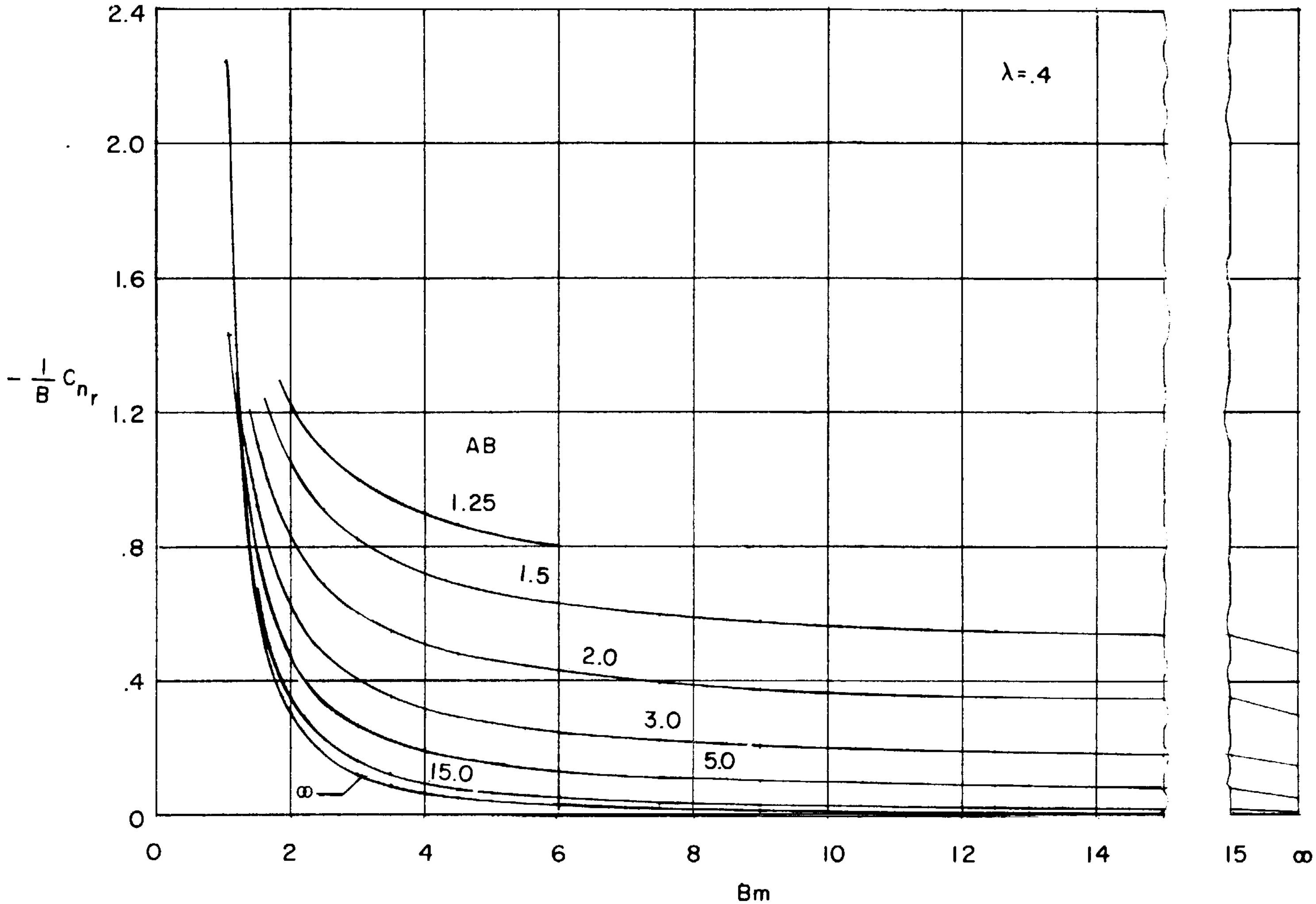

(c) Taper ratio, 0.4.

Figure 10.- Continued.

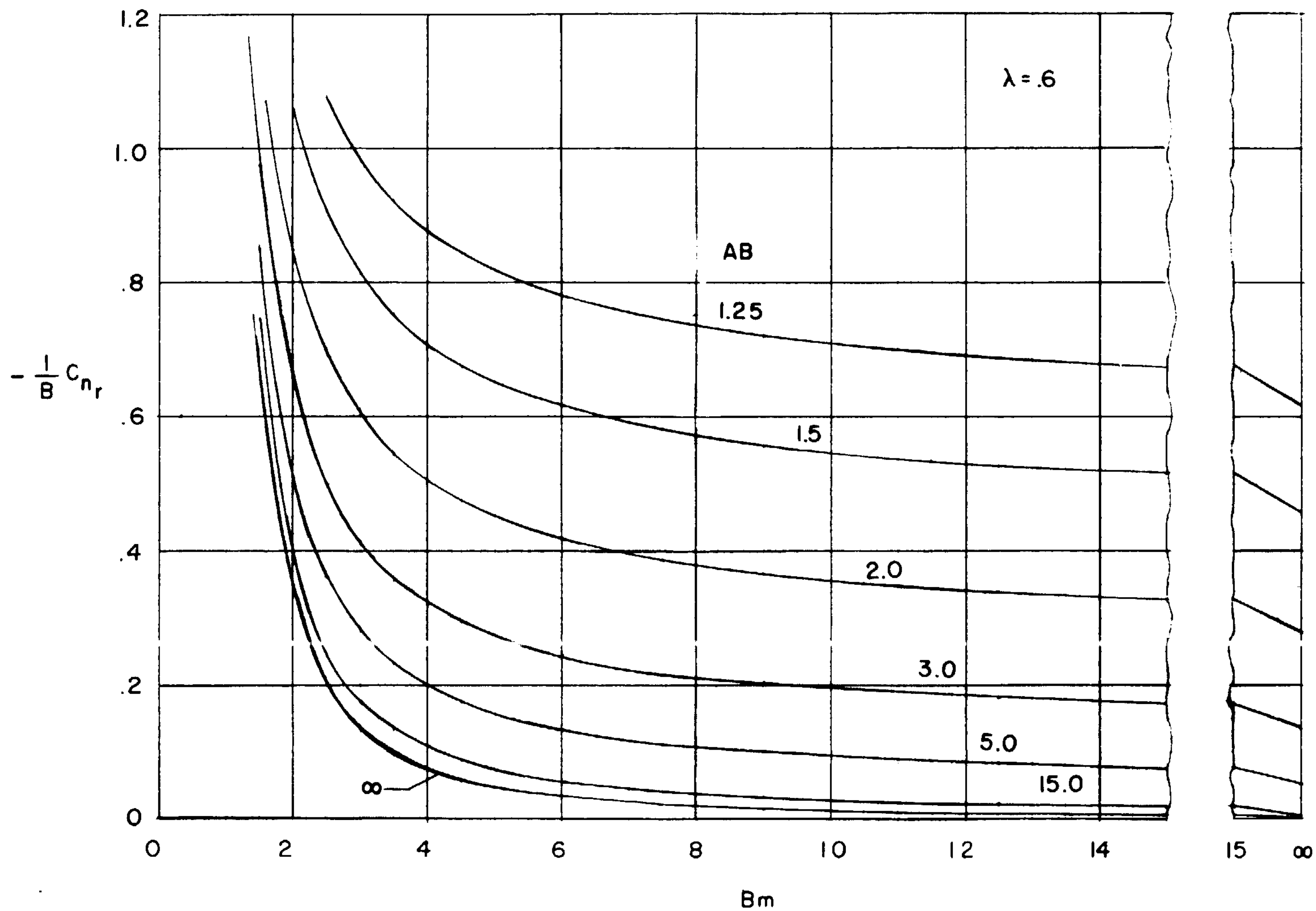

(d) Taper ratio, 0.6.

Figure 10.- Continued.

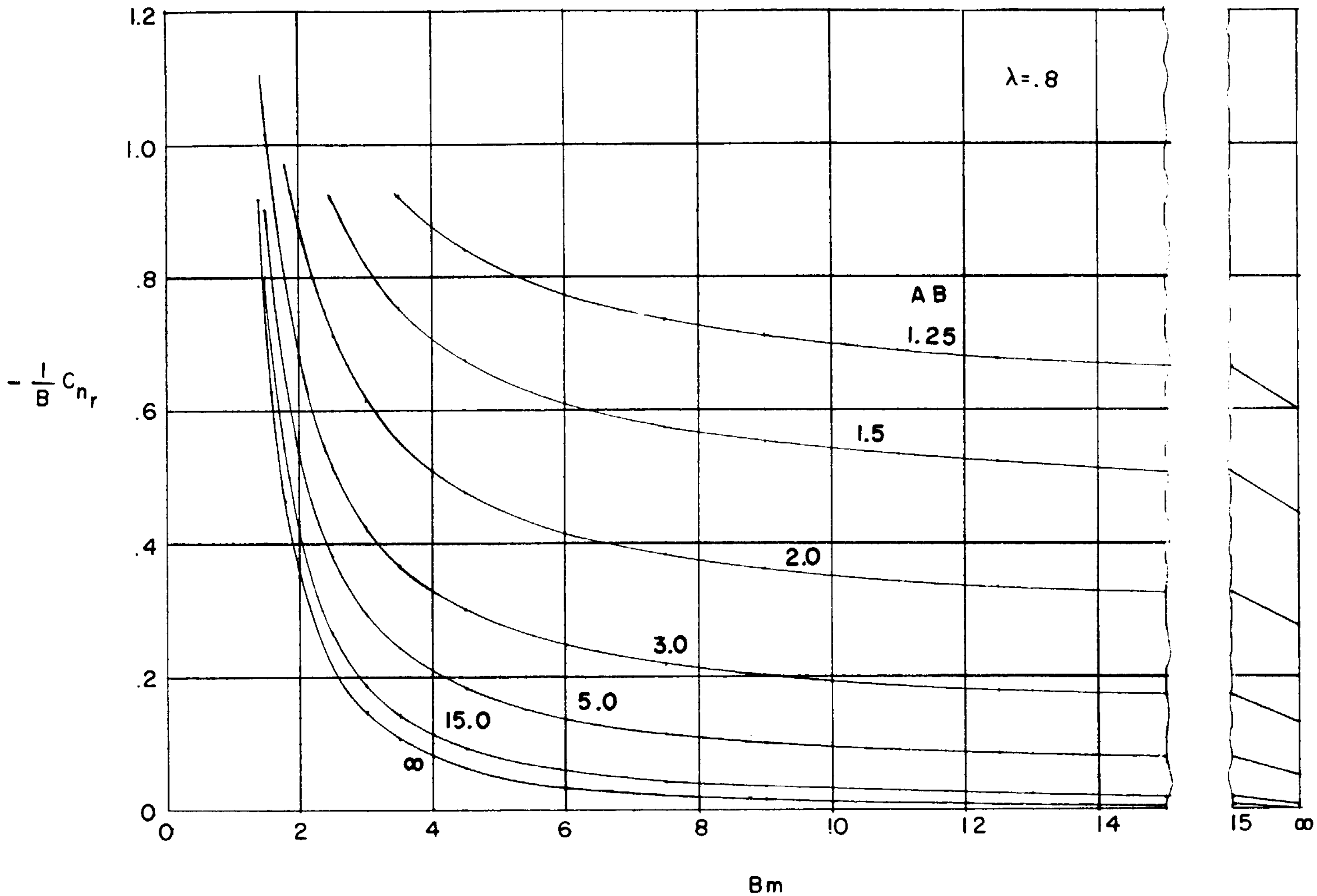

(e) Taper ratio, 0.8.

Figure 10.- Continued.

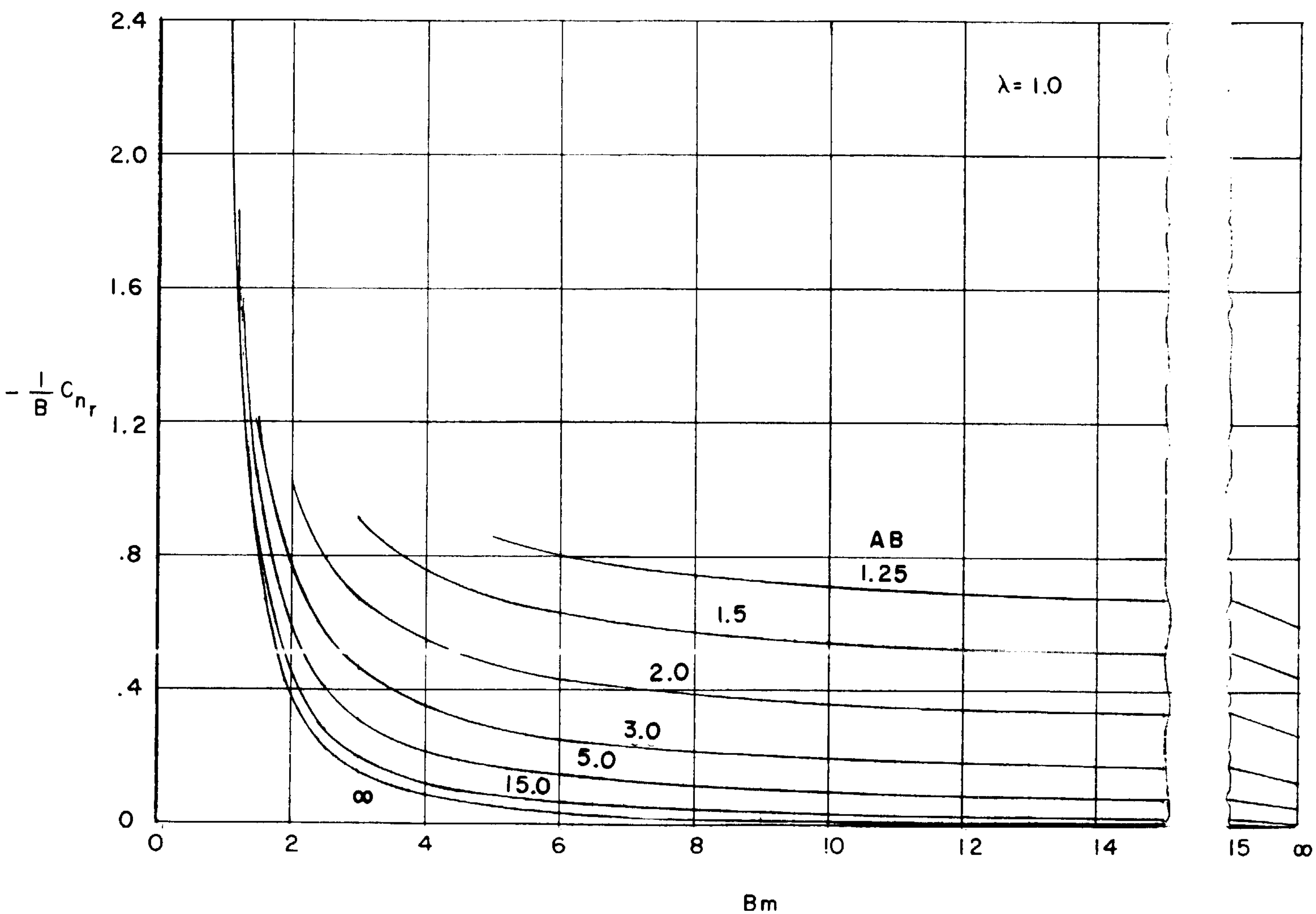

(f) Taper ratio, 1.0.

Figure 10.- Concluded.

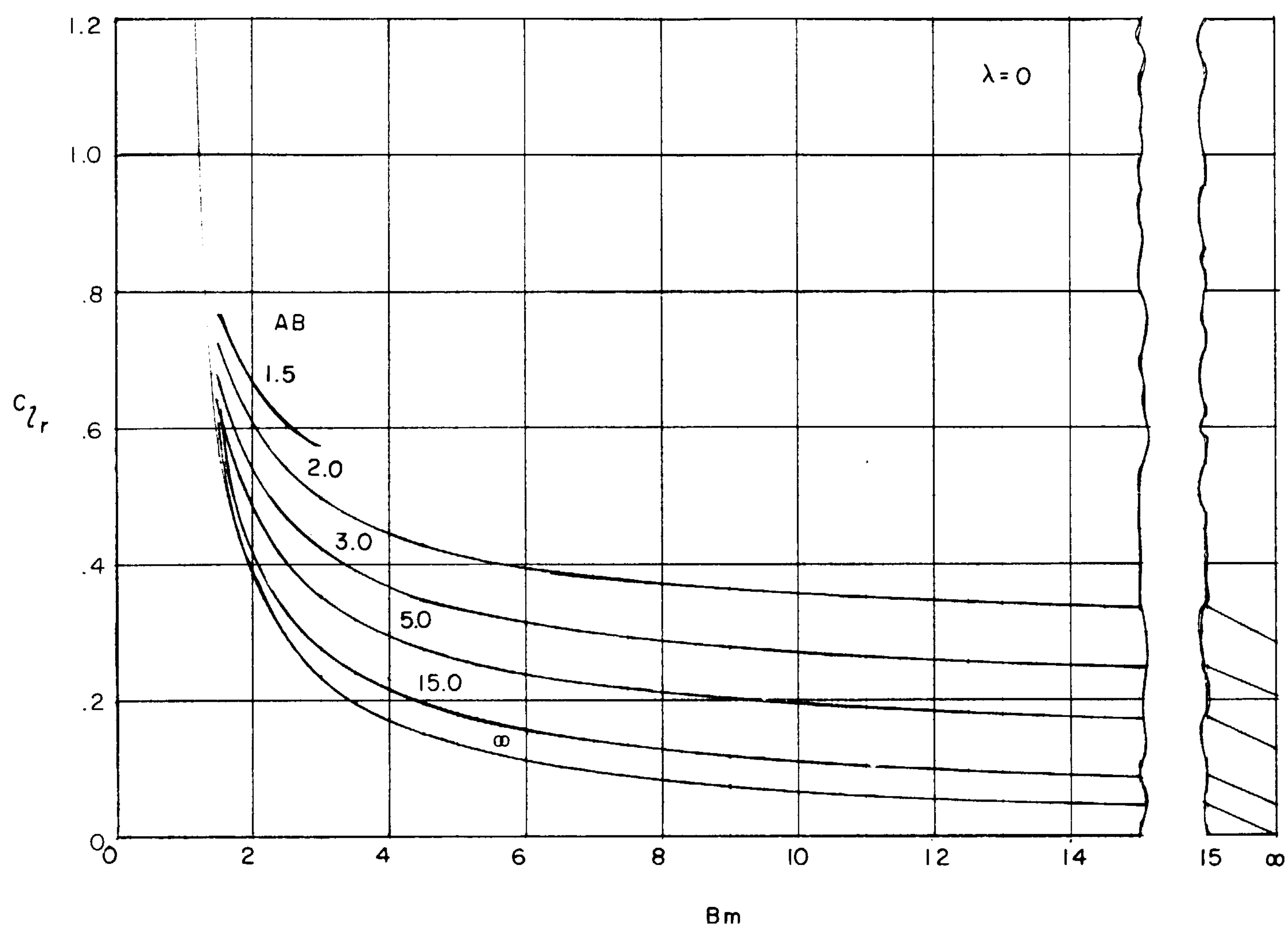

(a) Taper ratio, 0.

Figure 11.- Variation of C_{l_r} with Mach number-geometry parameters.

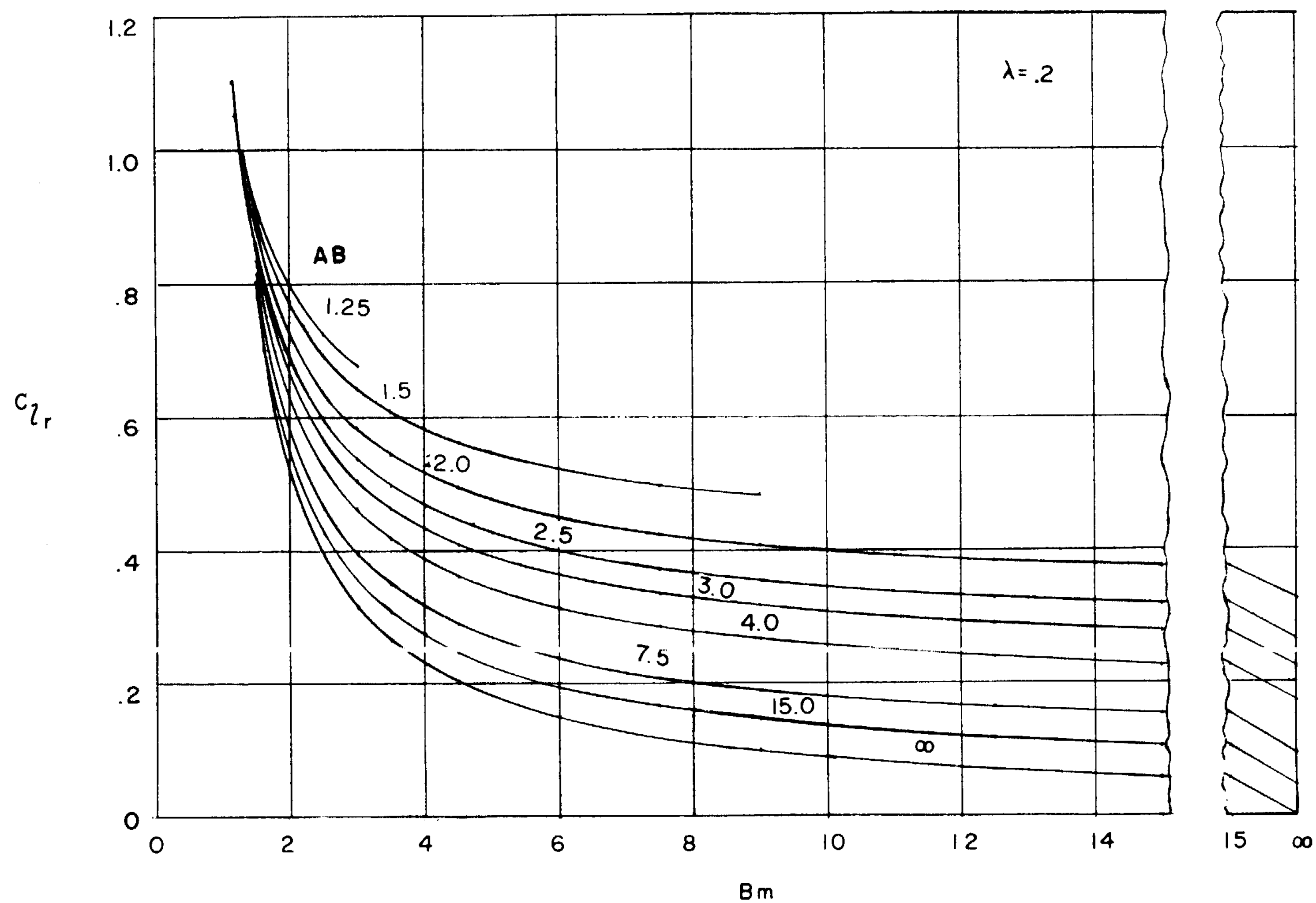

(b) Taper ratio, 0.2.

Figure 11.- Continued.

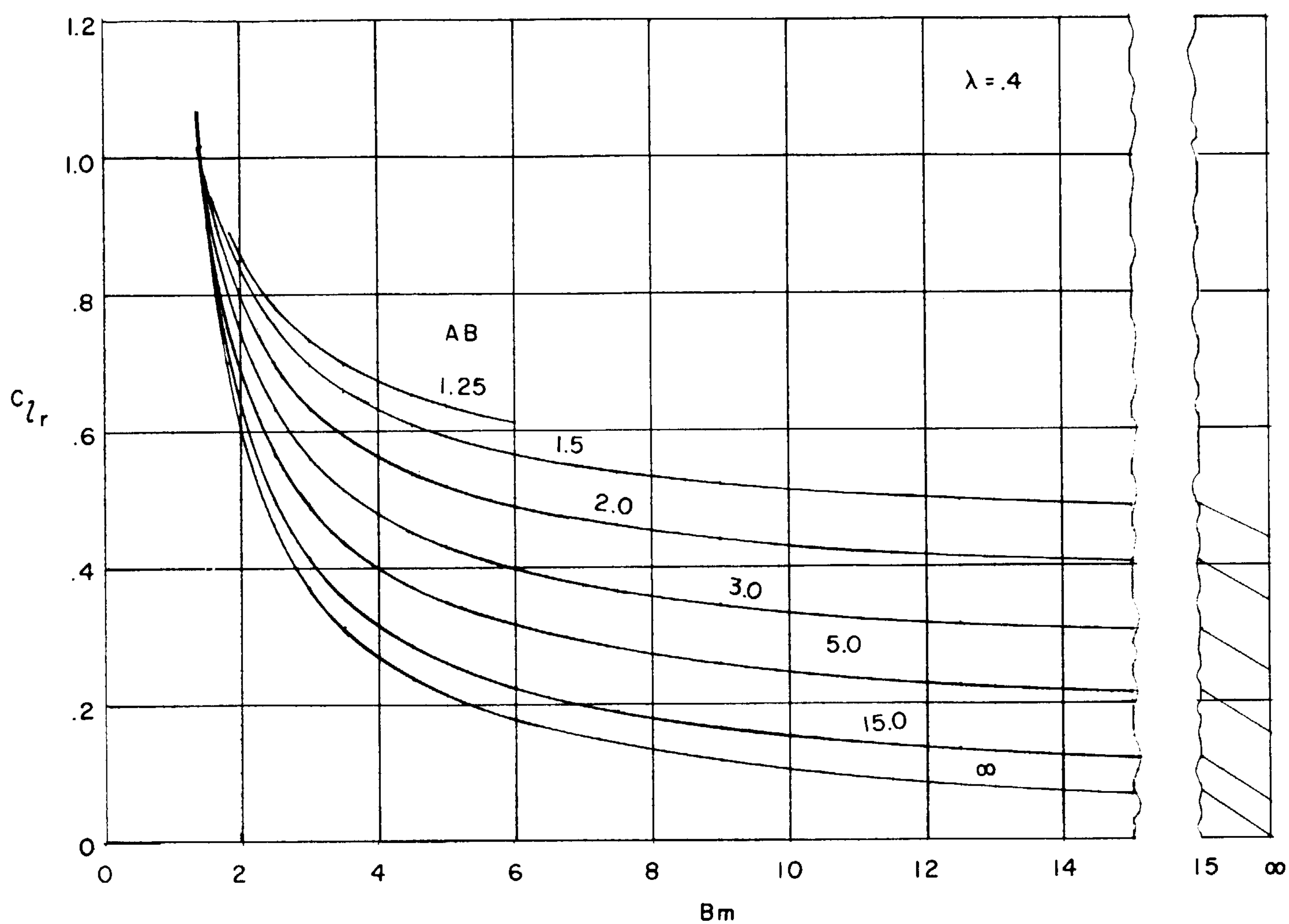

(c) Taper ratio, 0.4.

Figure 11.- Continued.

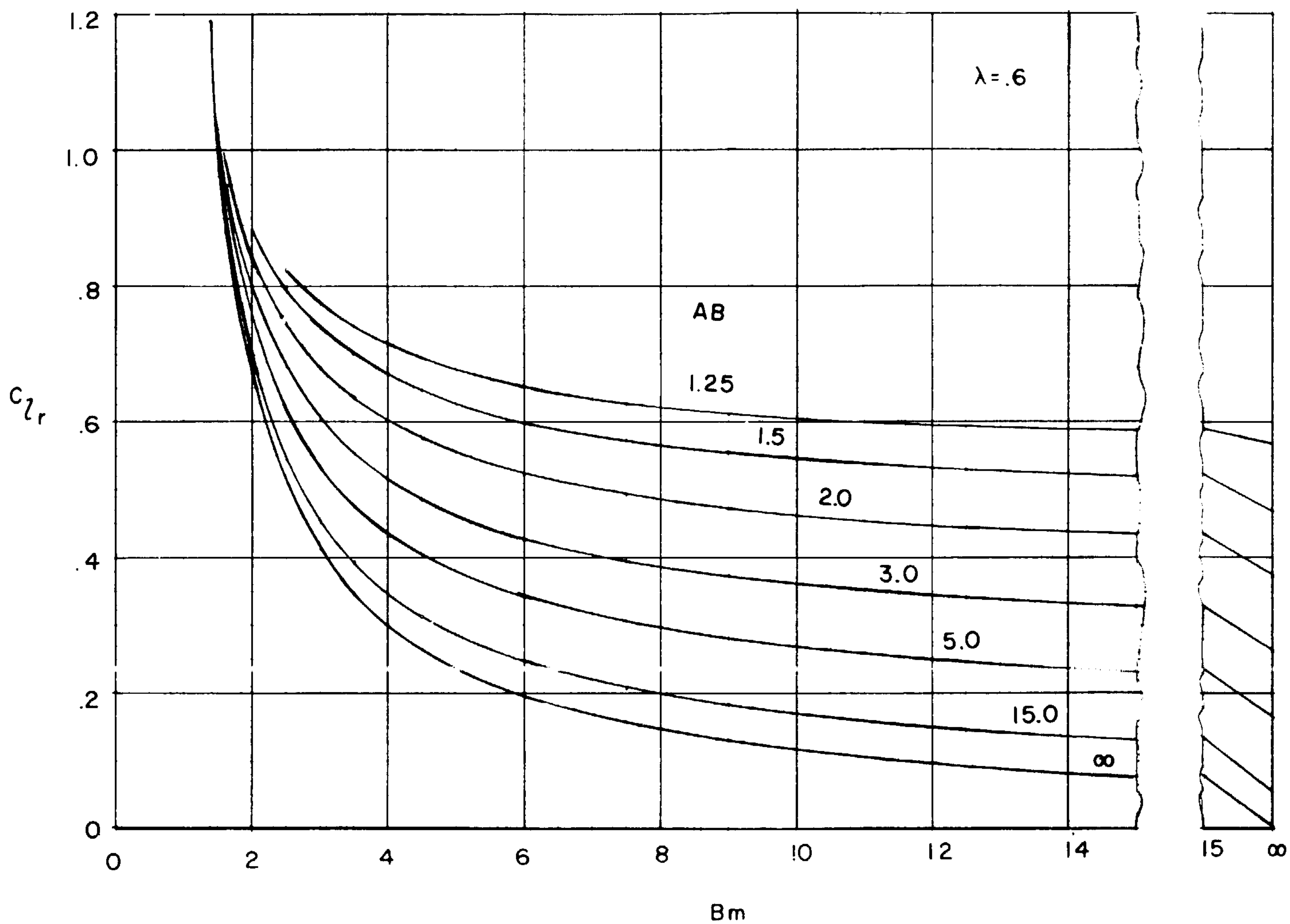

(d) Taper ratio, 0.6.

Figure 11.- Continued.

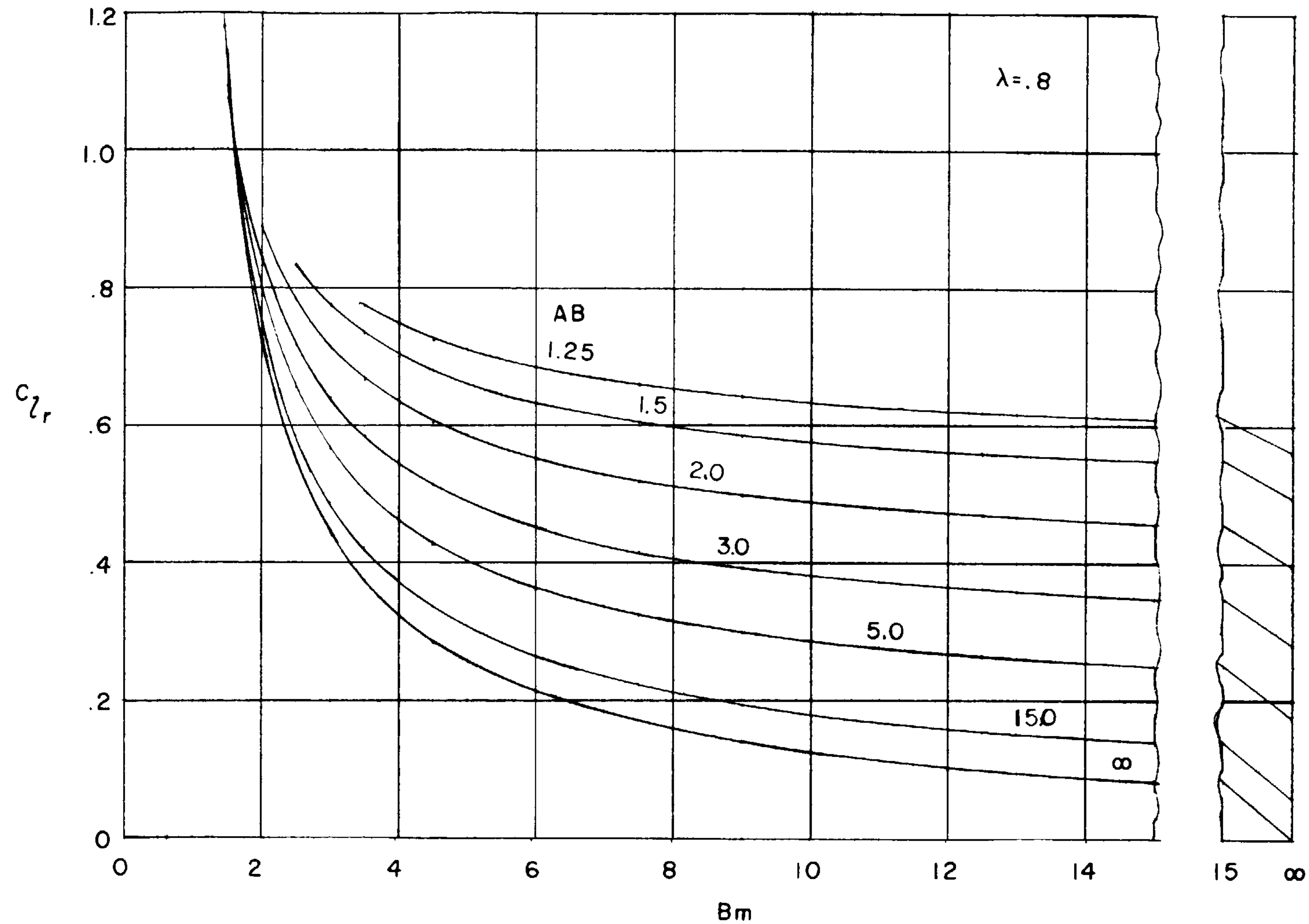

(e) Taper ratio, 0.8.

Figure 11.- Continued.

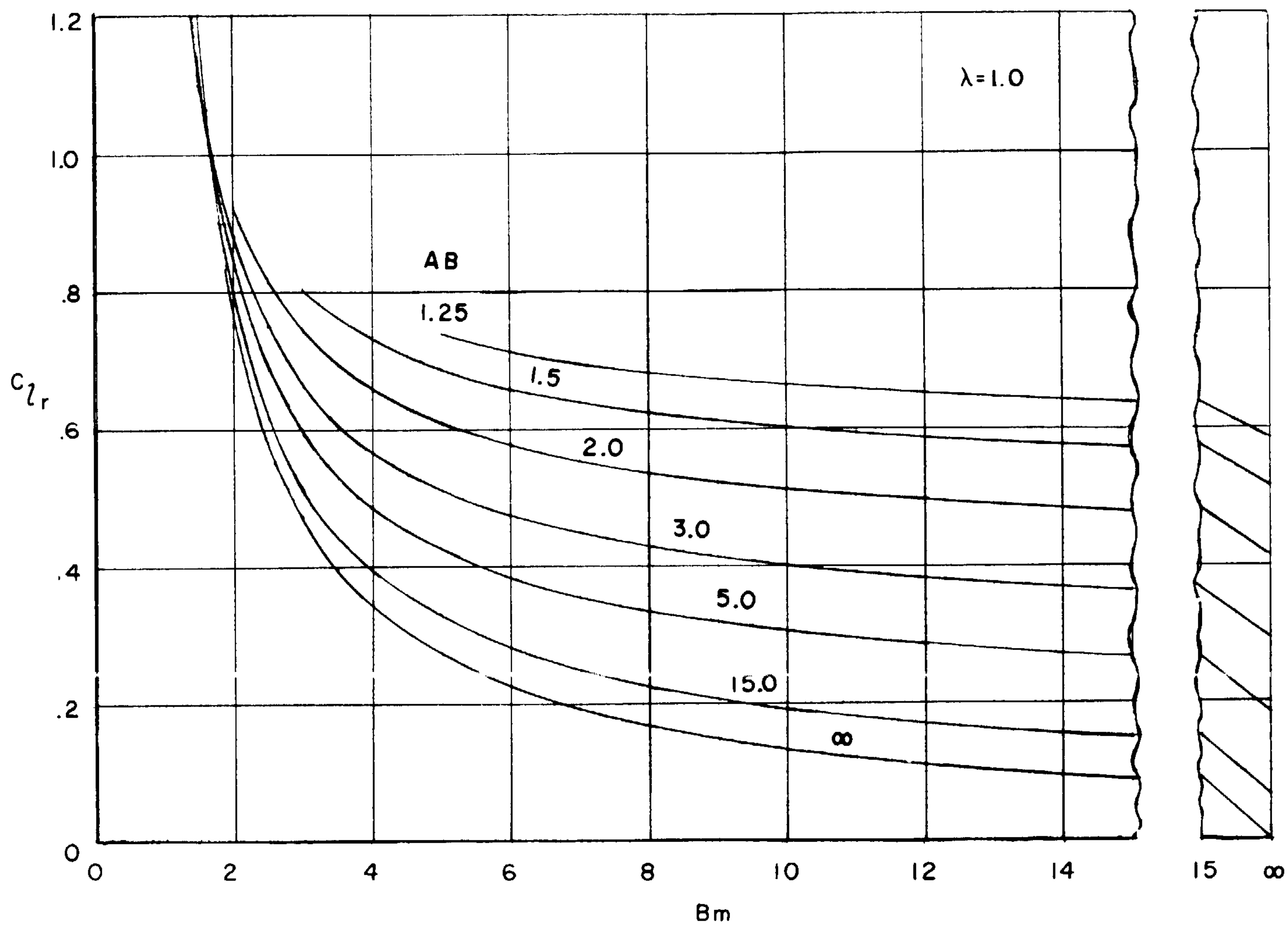

(f) Taper ratio, 1.0.

Figure 11.- Concluded.

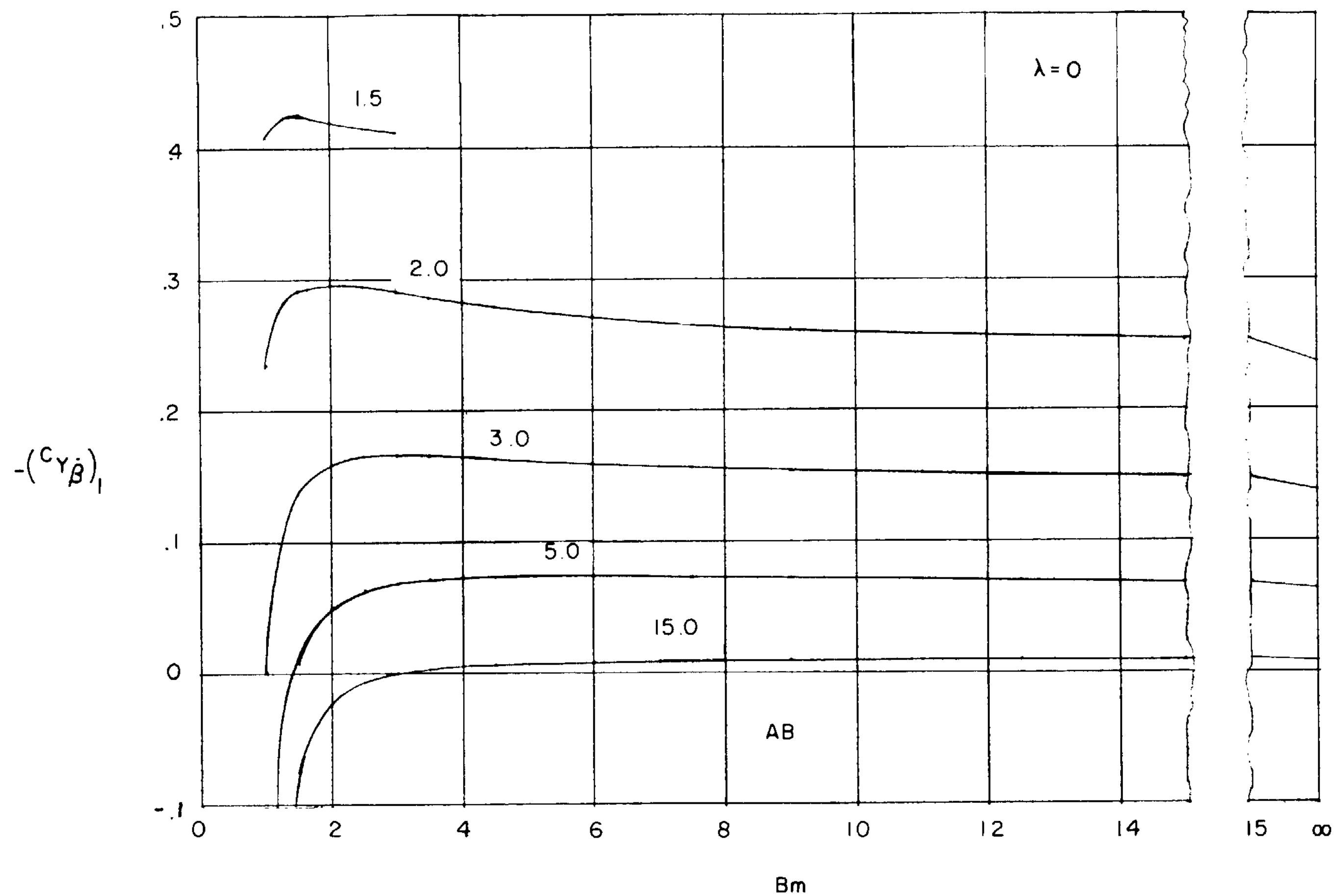

(a) Component $\left(C_{Y_{\dot{\beta}}}\right)_1$; taper ratio, 0.

Figure 12.- Variation of stability derivative $C_{Y_{\dot{\beta}}}$ with Mach number-geometry parameters. Note that $C_{Y_{\dot{\beta}}} = \left(C_{Y_{\dot{\beta}}}\right)_1 + \left(C_{Y_{\dot{\beta}}}\right)_2$.

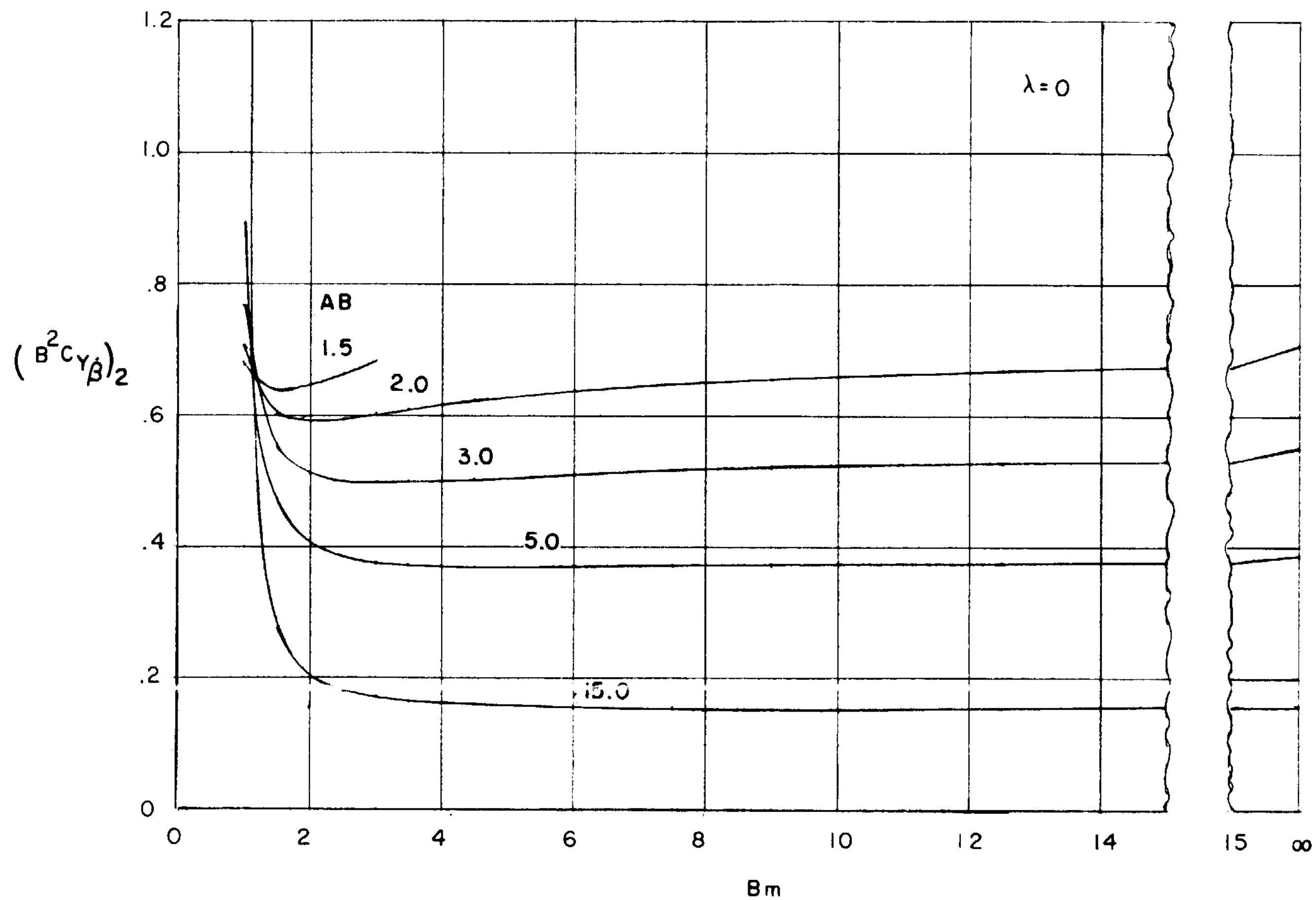

(b) Component $\left(C_{Y_{\dot{\beta}}}\right)_2$; taper ratio, 0.

Figure 12.- Continued.

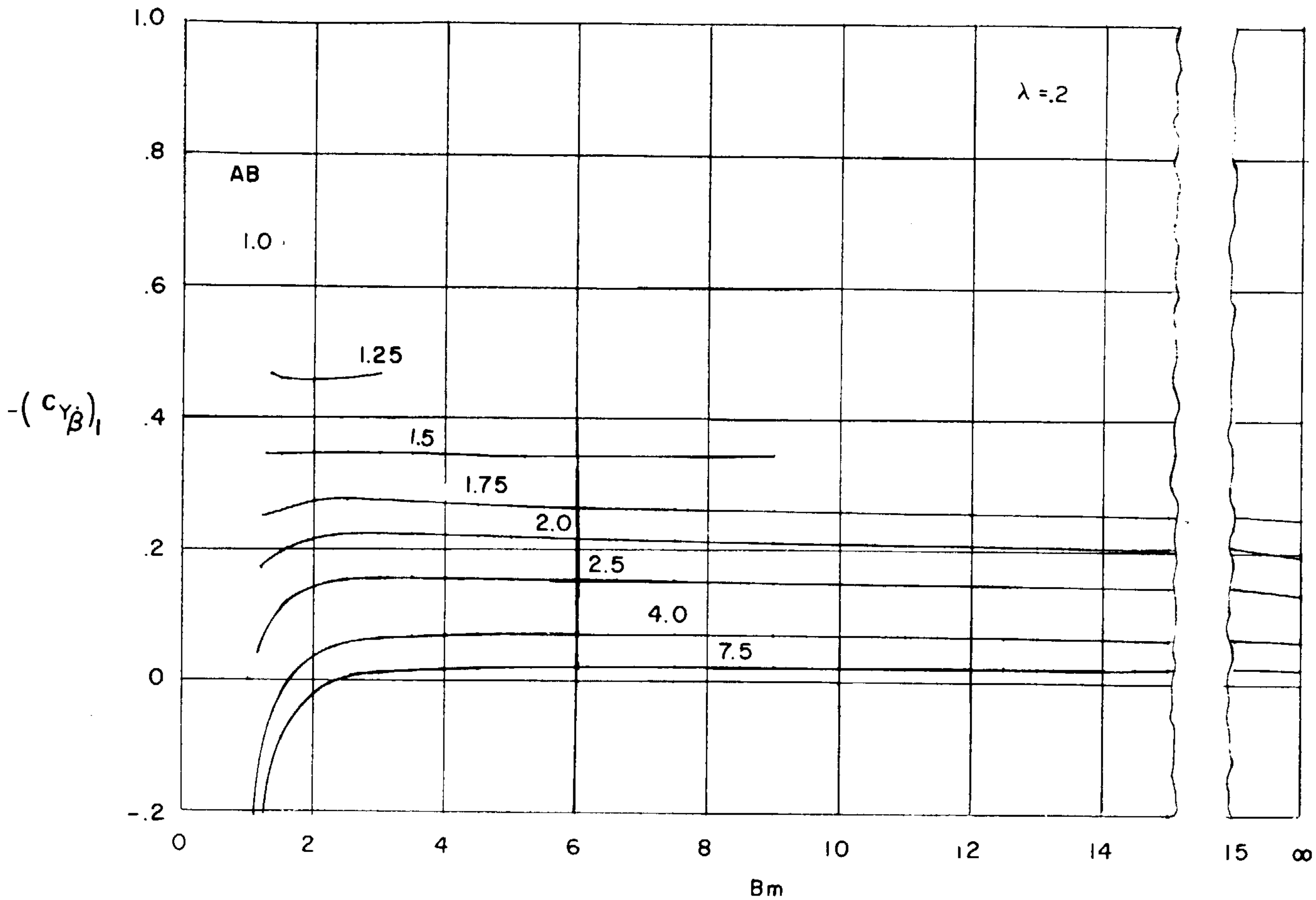

(c) Component $\left(C_{Y_{\dot{\beta}}}\right)_1$; taper ratio, 0.2.

Figure 12.- Continued.

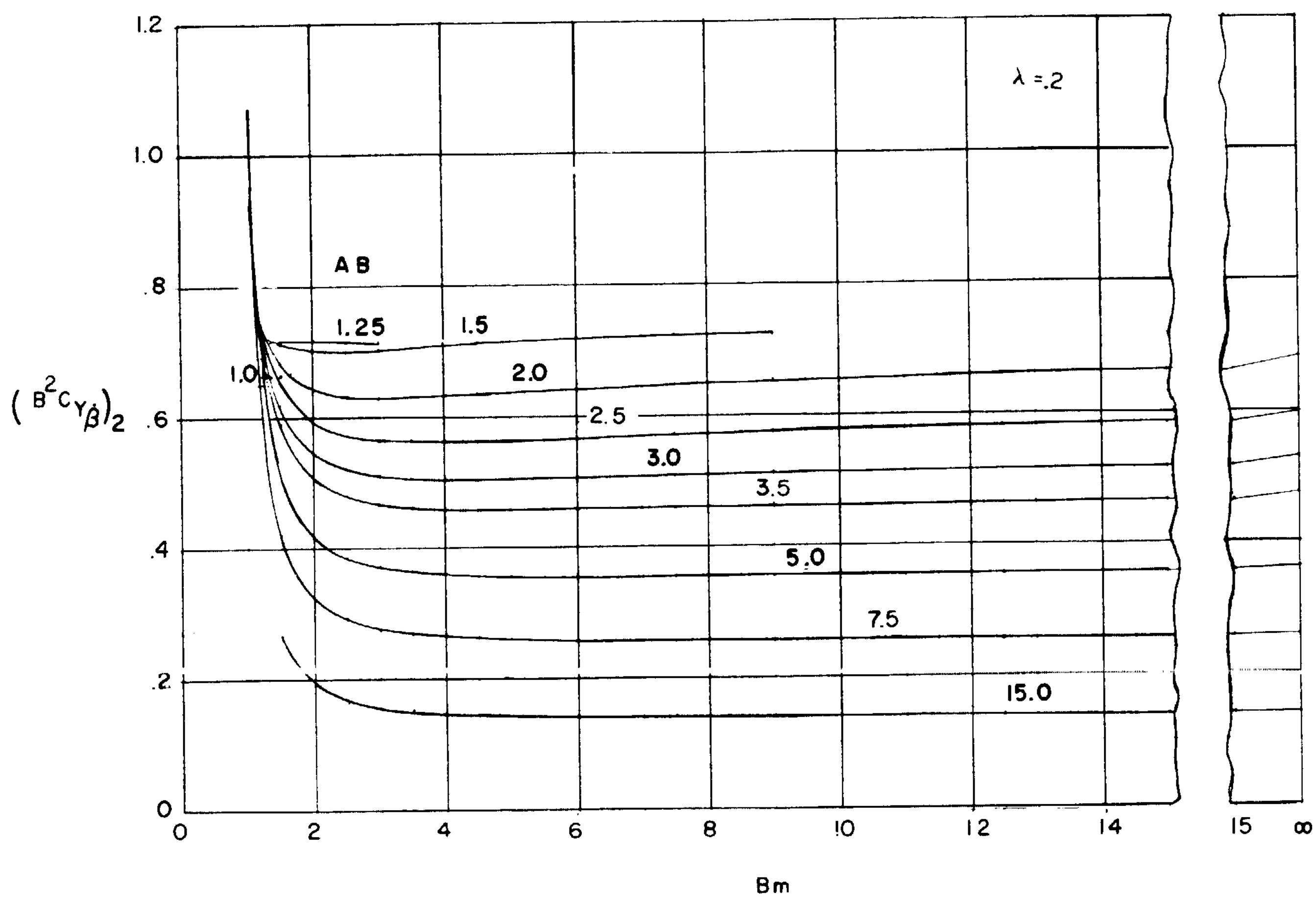

(d) Component $\left(C_{Y_{\dot{\beta}}}\right)_2$; taper ratio, 0.2.

Figure 12.- Continued.

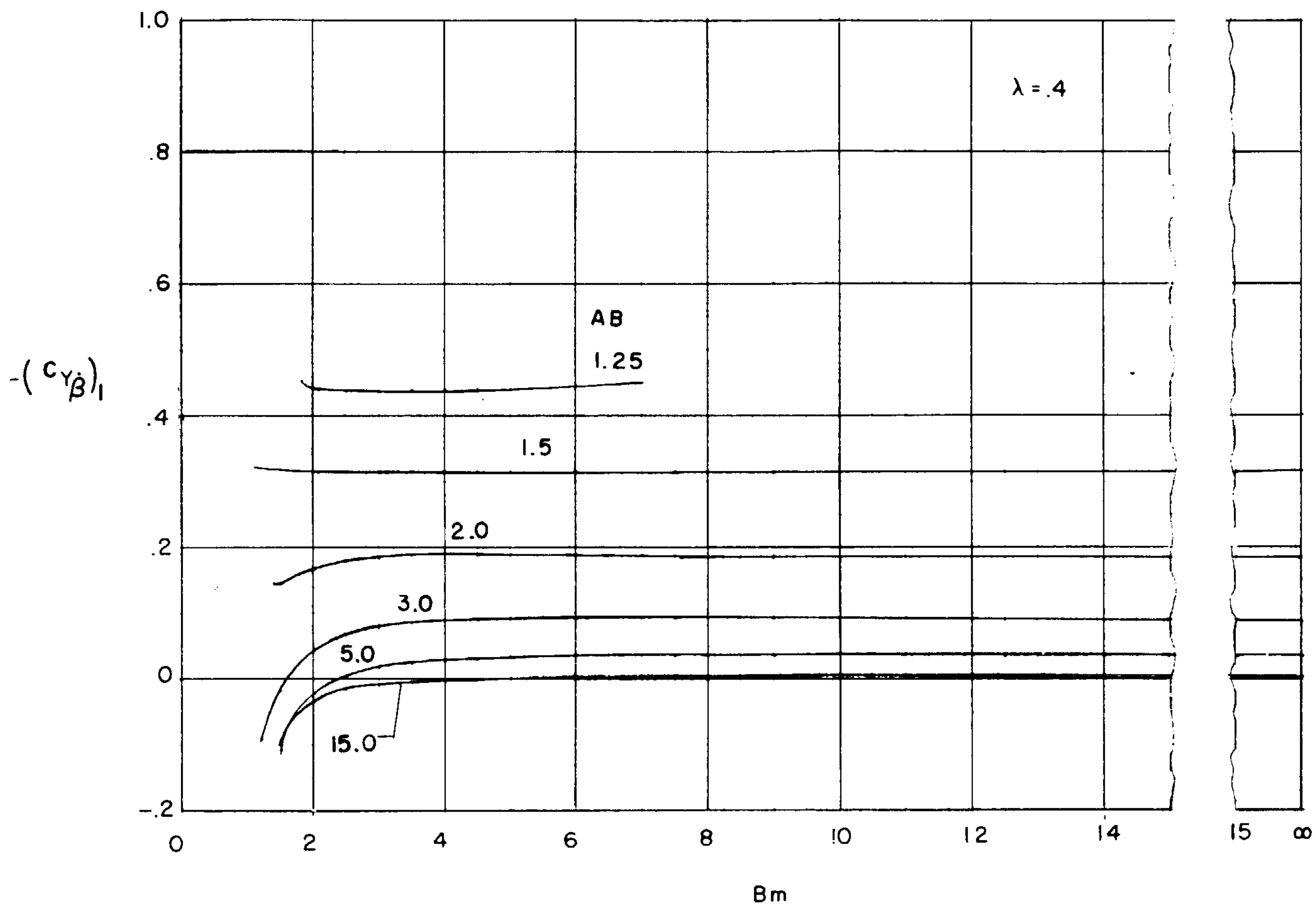

(e) Component $\left(C_{Y_{\dot{\beta}}}\right)_1$; taper ratio, 0.4.

Figure 12.- Continued.

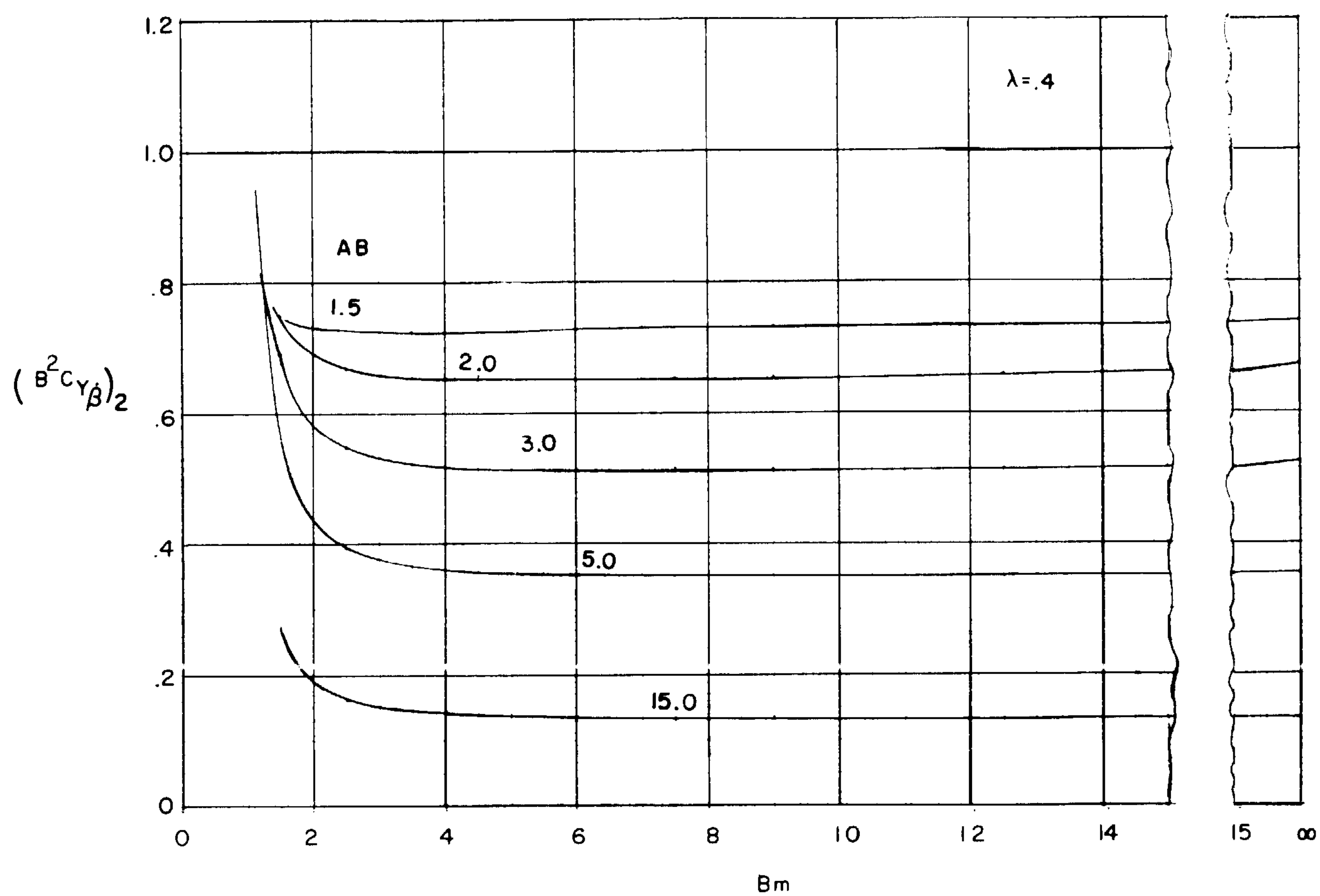

(f) Component $\left(C_{Y_{\dot{\beta}}}\right)_2$; taper ratio, 0.4.

Figure 12.- Continued.

L-780

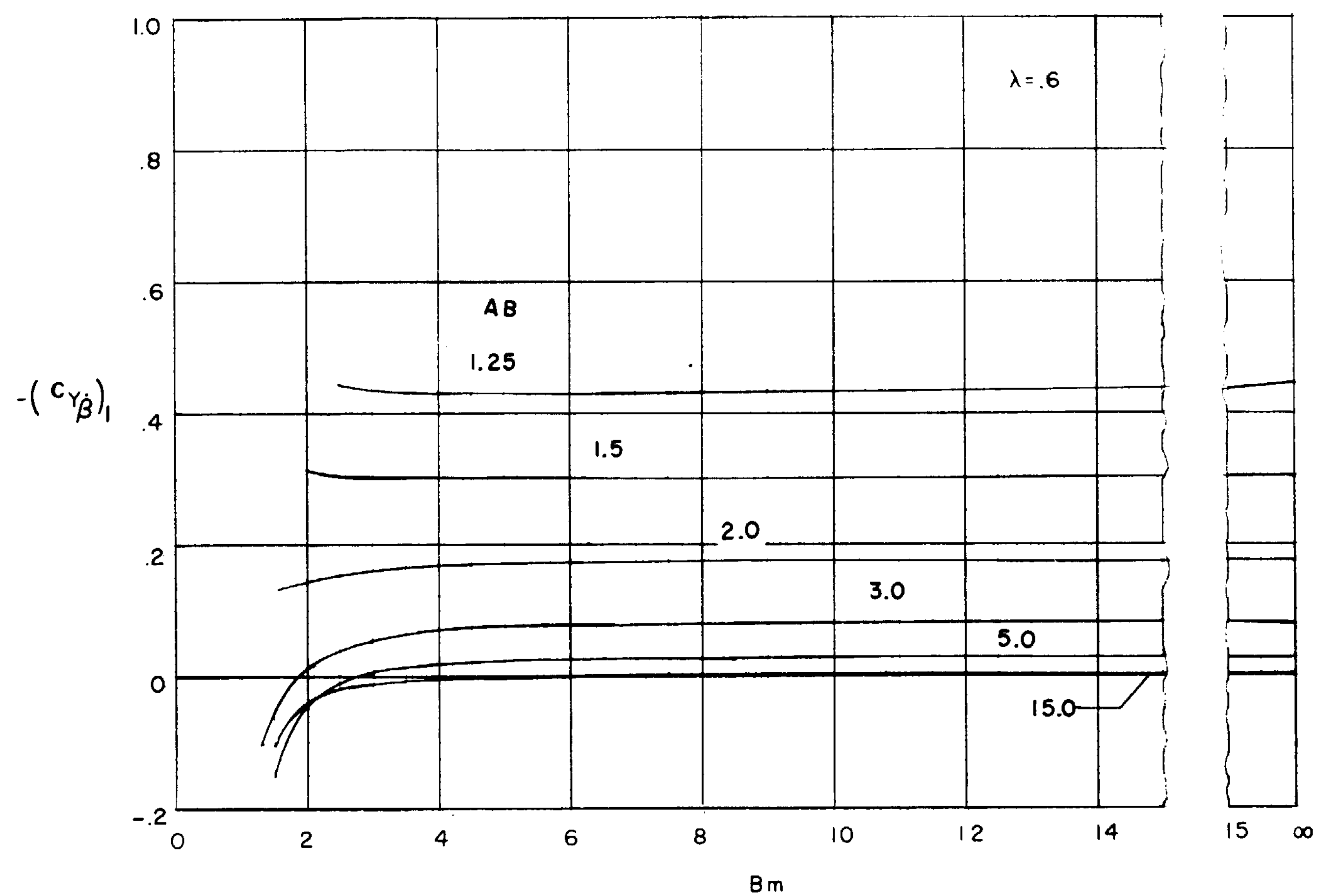

(g) Component $\left(C_{Y_{\dot{\beta}}}\right)_1$; taper ratio, 0.6.

Figure 12.- Continued.

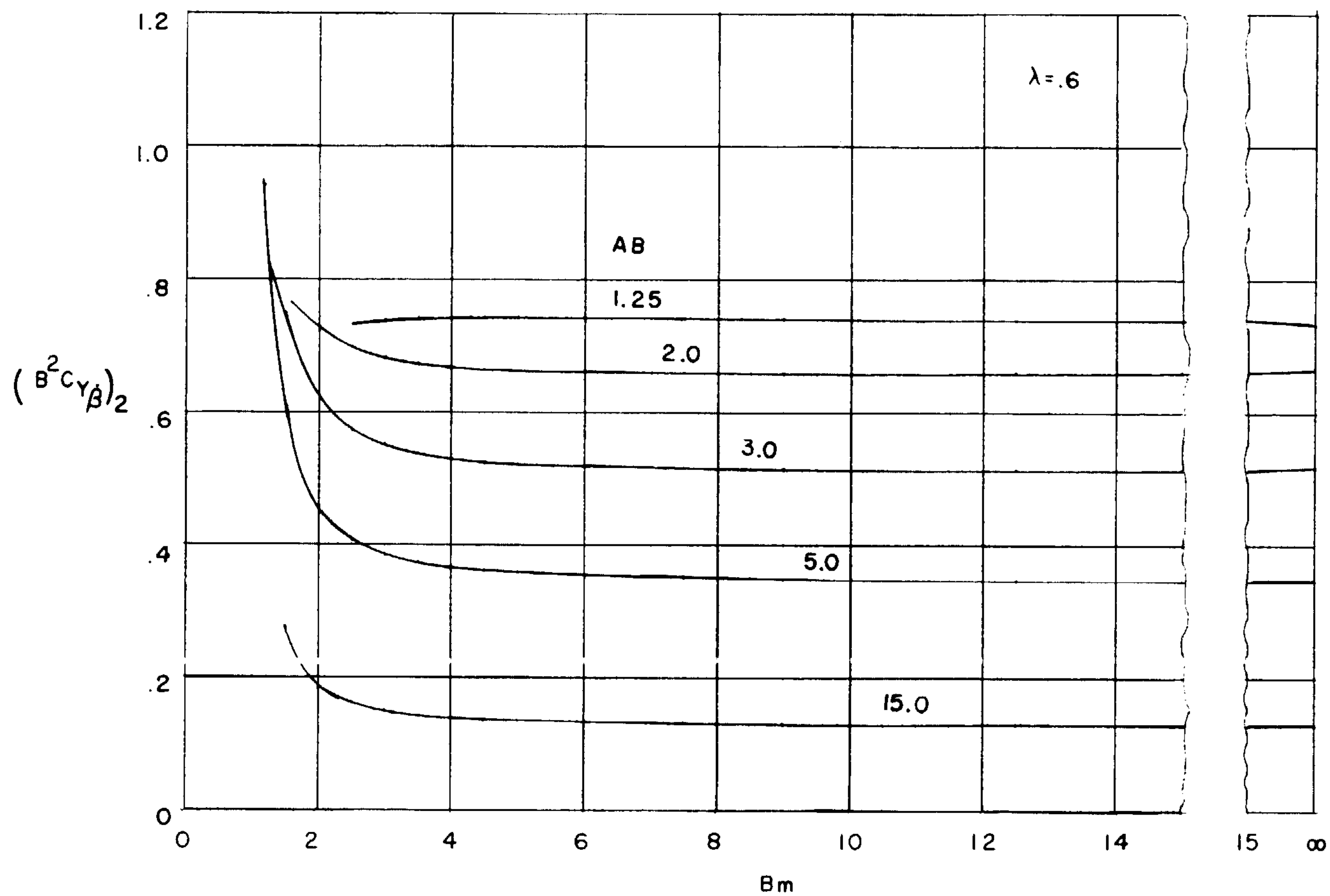

(h) Component $\left(C_{Y_{\dot{\beta}}}\right)_2$; taper ratio, 0.6.

Figure 12.- Continued.

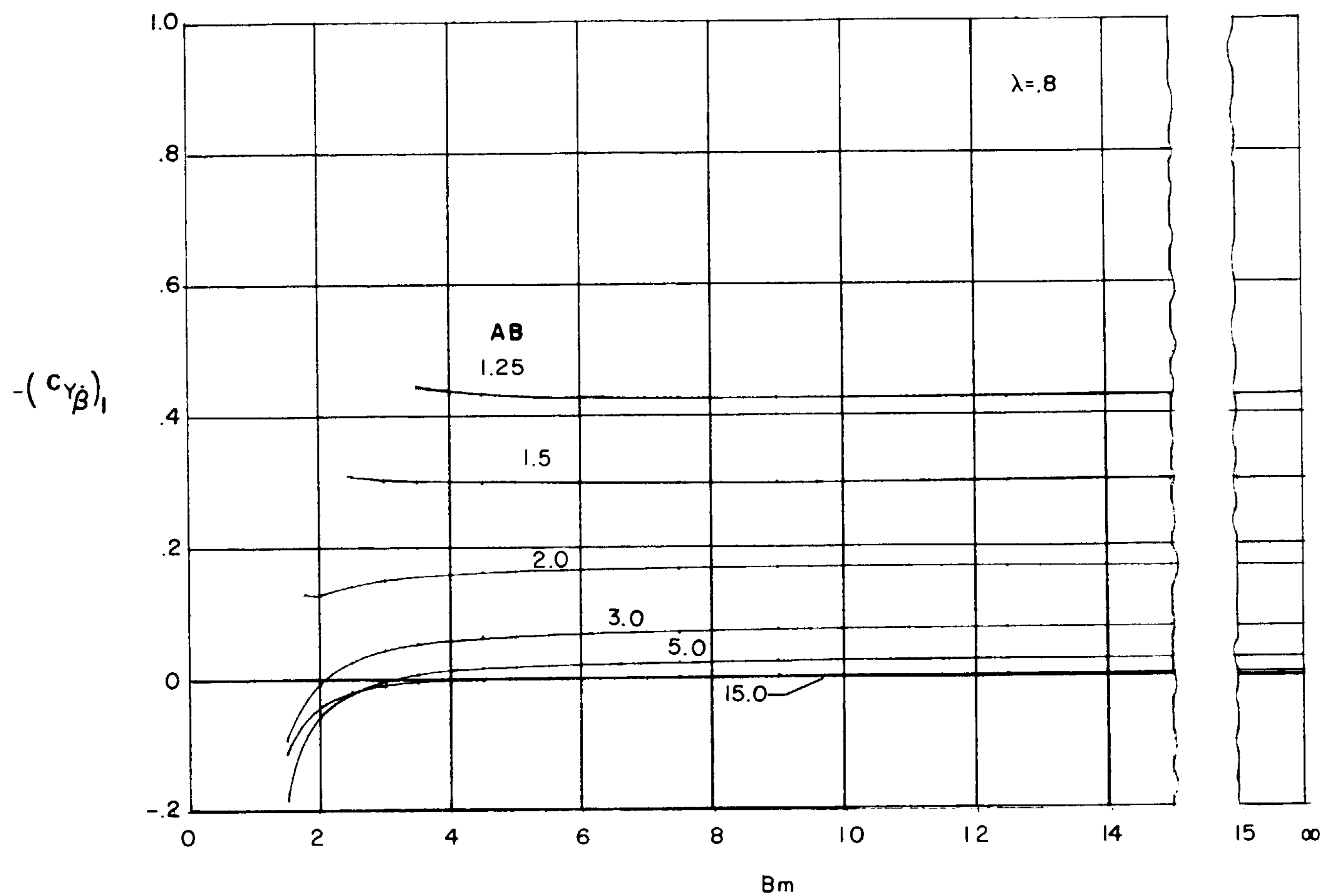

(i) Component $\left(C_{Y_{\dot{\beta}}}\right)_1$; taper ratio, 0.8.

Figure 12.- Continued.

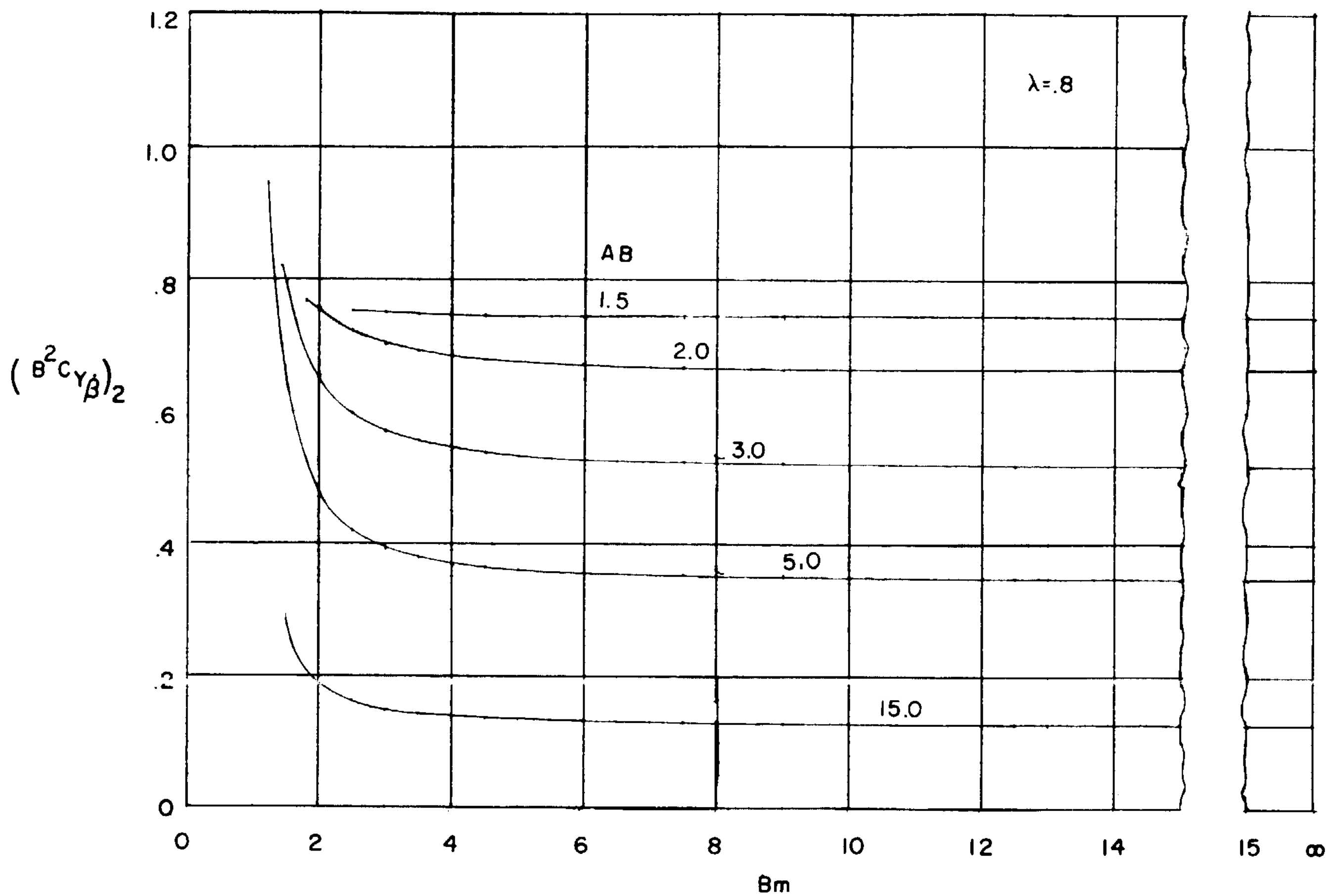

(j) Component $\left(C_{Y_{\dot{\beta}}}\right)_2$; taper ratio, 0.8.

Figure 12.- Continued.

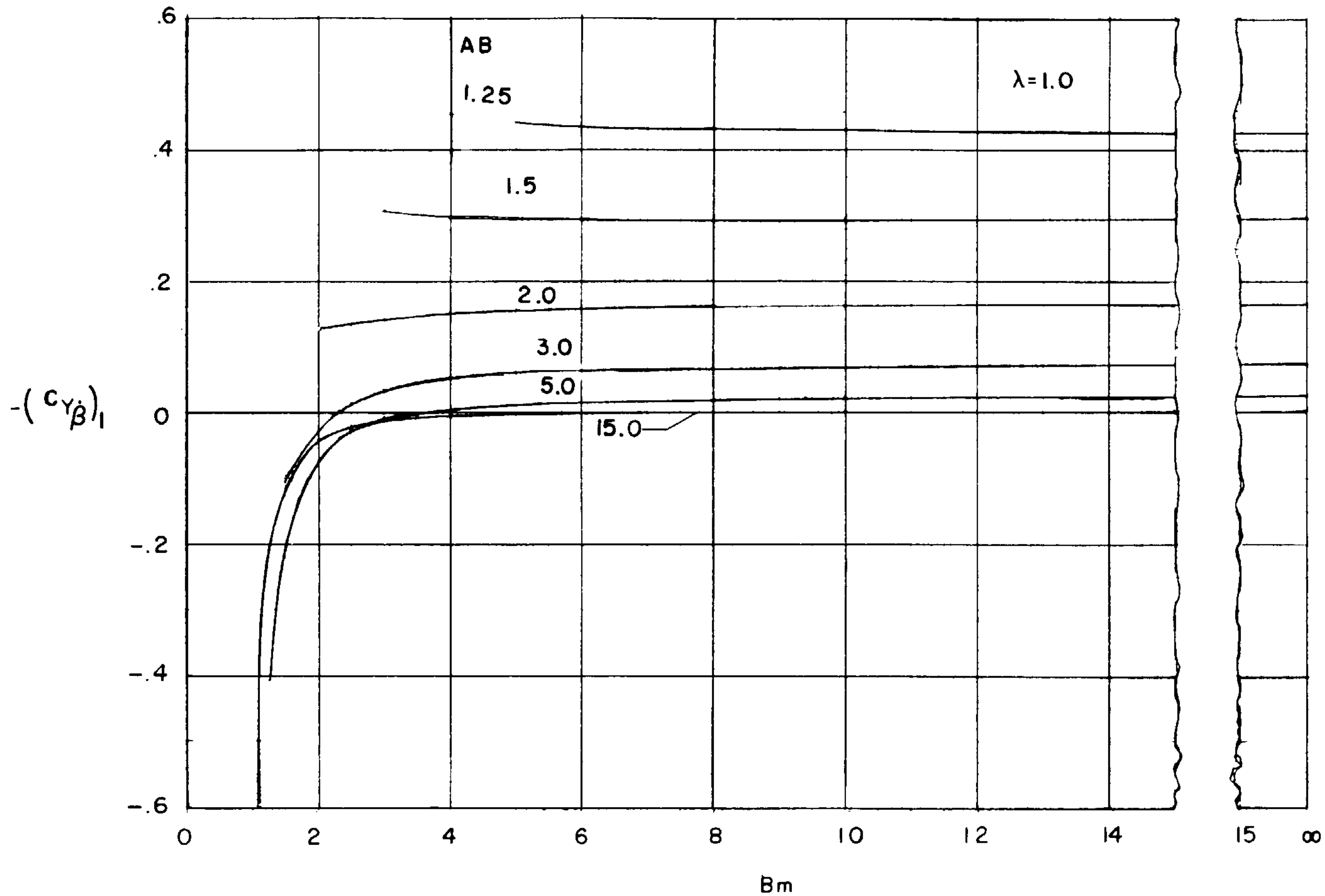

(k) Component $\left(C_{Y_{\dot{\beta}}}\right)_1$; taper ratio, 1.0.

Figure 12.- Continued.

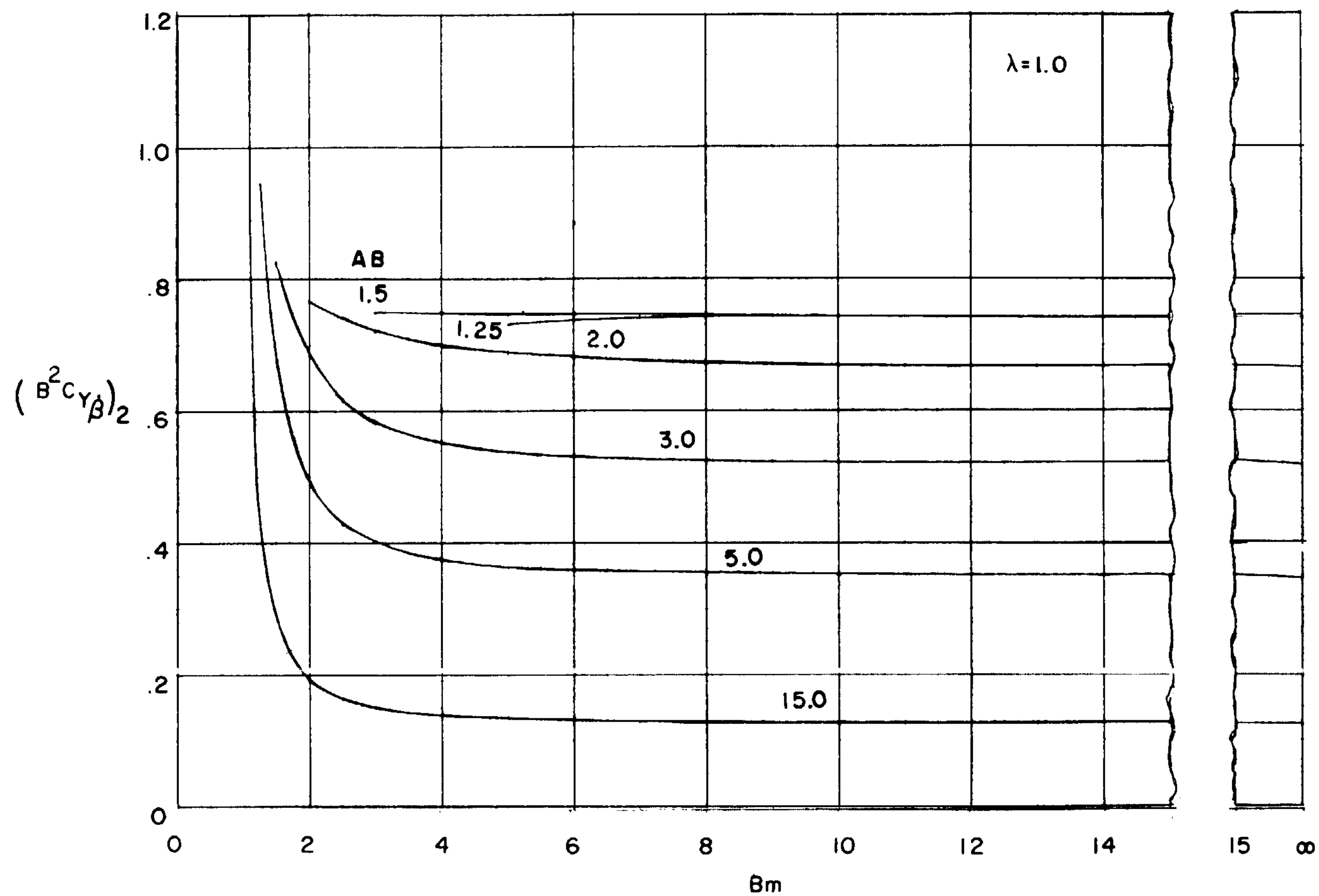

(l) Component $\left(C_{Y_{\dot{\beta}}}\right)_2$; taper ratio, 1.0.

Figure 12.- Concluded.

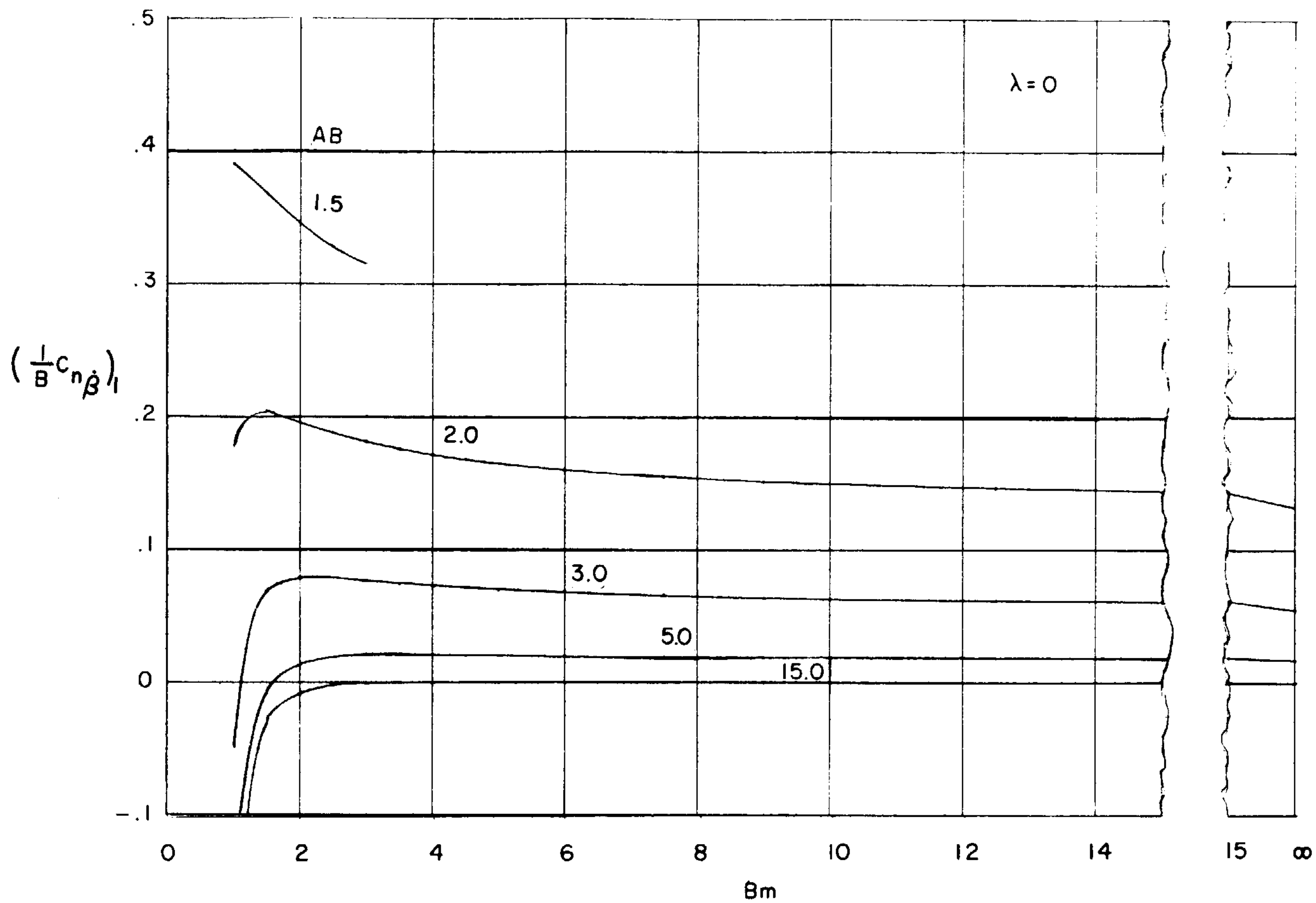

(a) Component $\left(C_{n_{\dot{\beta}}}\right)_1$; taper ratio, 0.

Figure 13.- Variation of stability derivative $C_{n_{\dot{\beta}}}$ with Mach number-geometry parameters. Note that $C_{n_{\dot{\beta}}} = \left(C_{n_{\dot{\beta}}}\right)_1 + \left(C_{n_{\dot{\beta}}}\right)_2$.

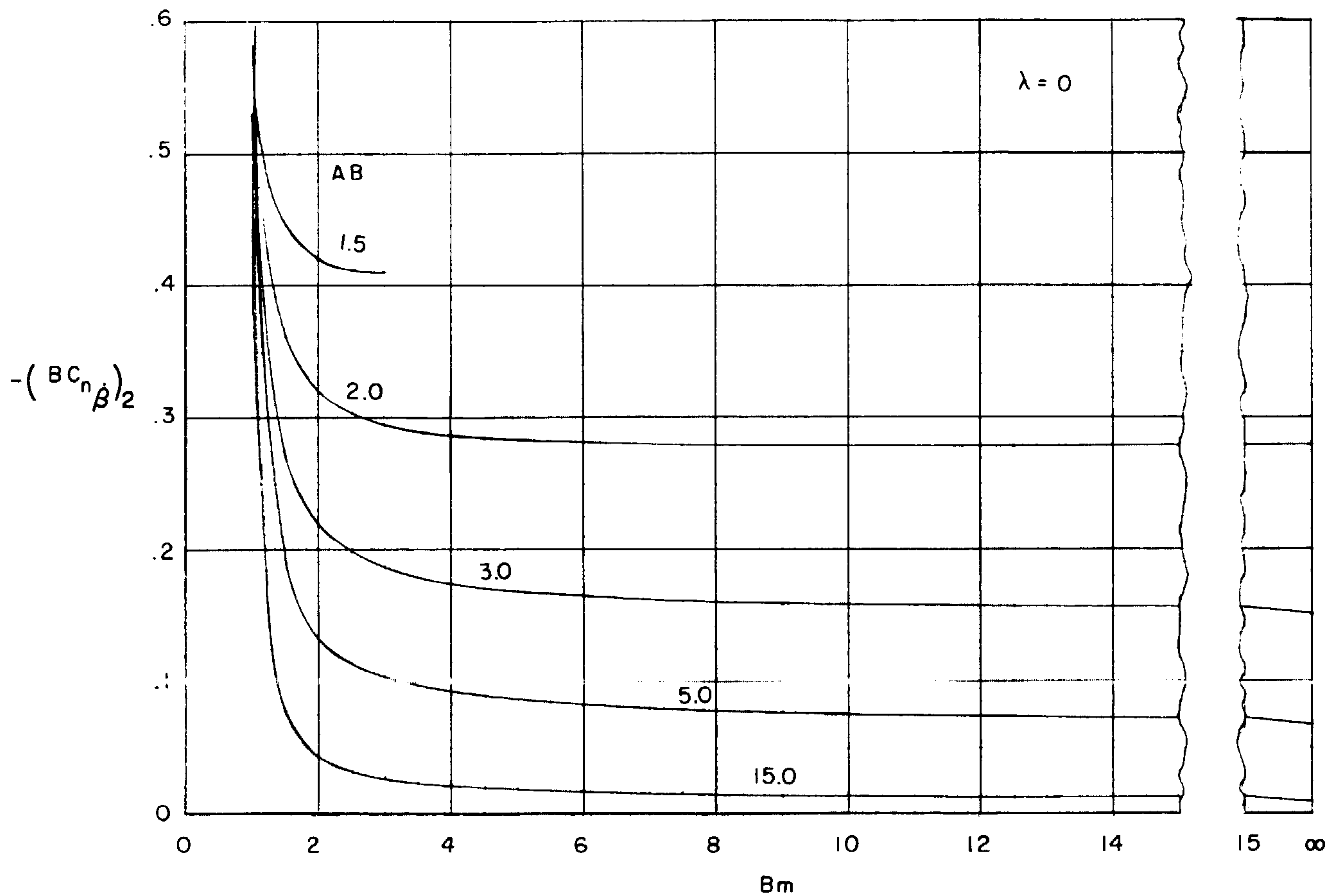

(b) Component $\left(C_{n_{\dot{\beta}}}\right)_2$; taper ratio, 0.

Figure 13.- Continued.

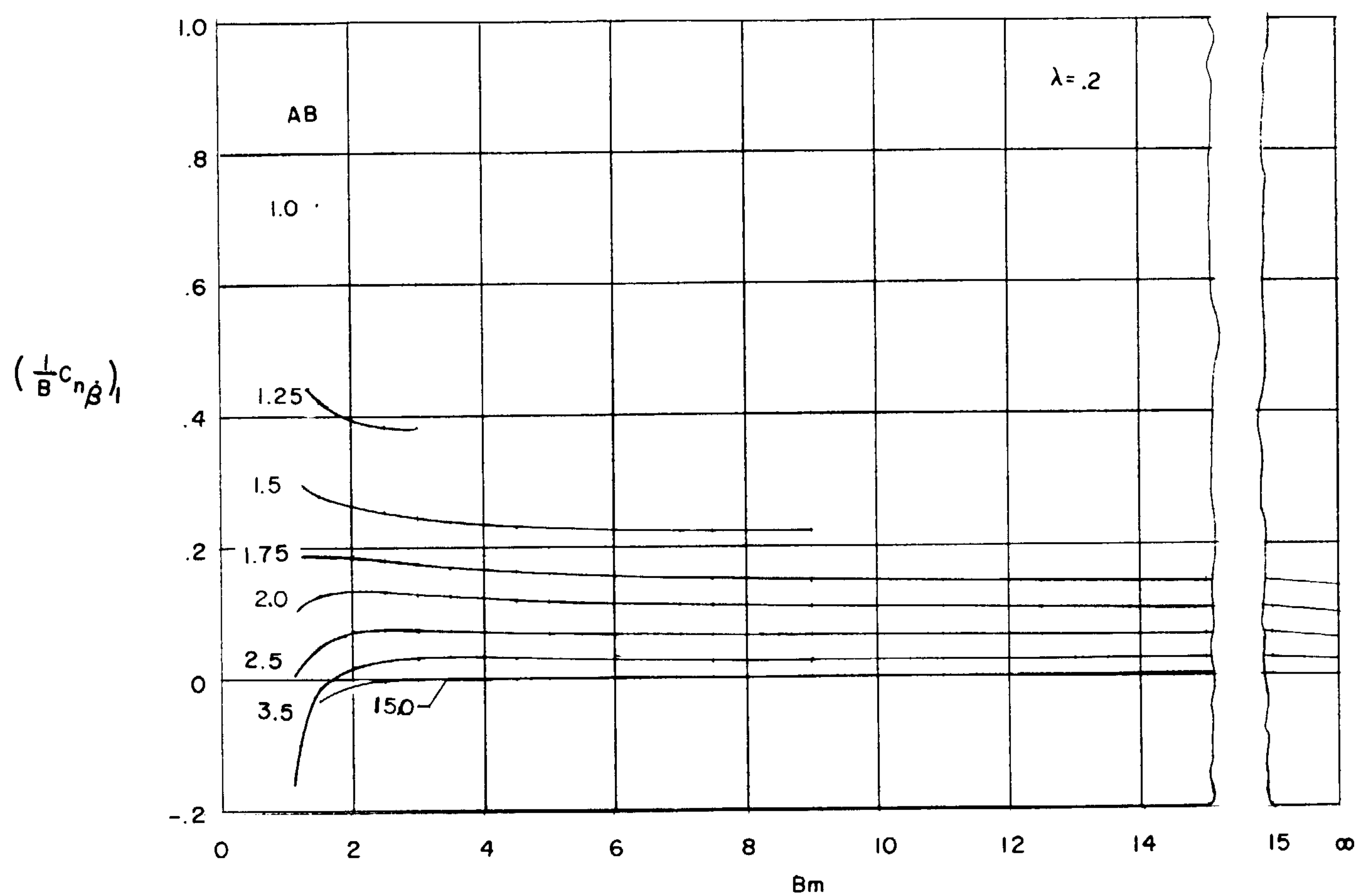

(c) Component $\left(C_{n_{\dot{\beta}}}\right)_1$; taper ratio, 0.2.

Figure 13.- Continued.

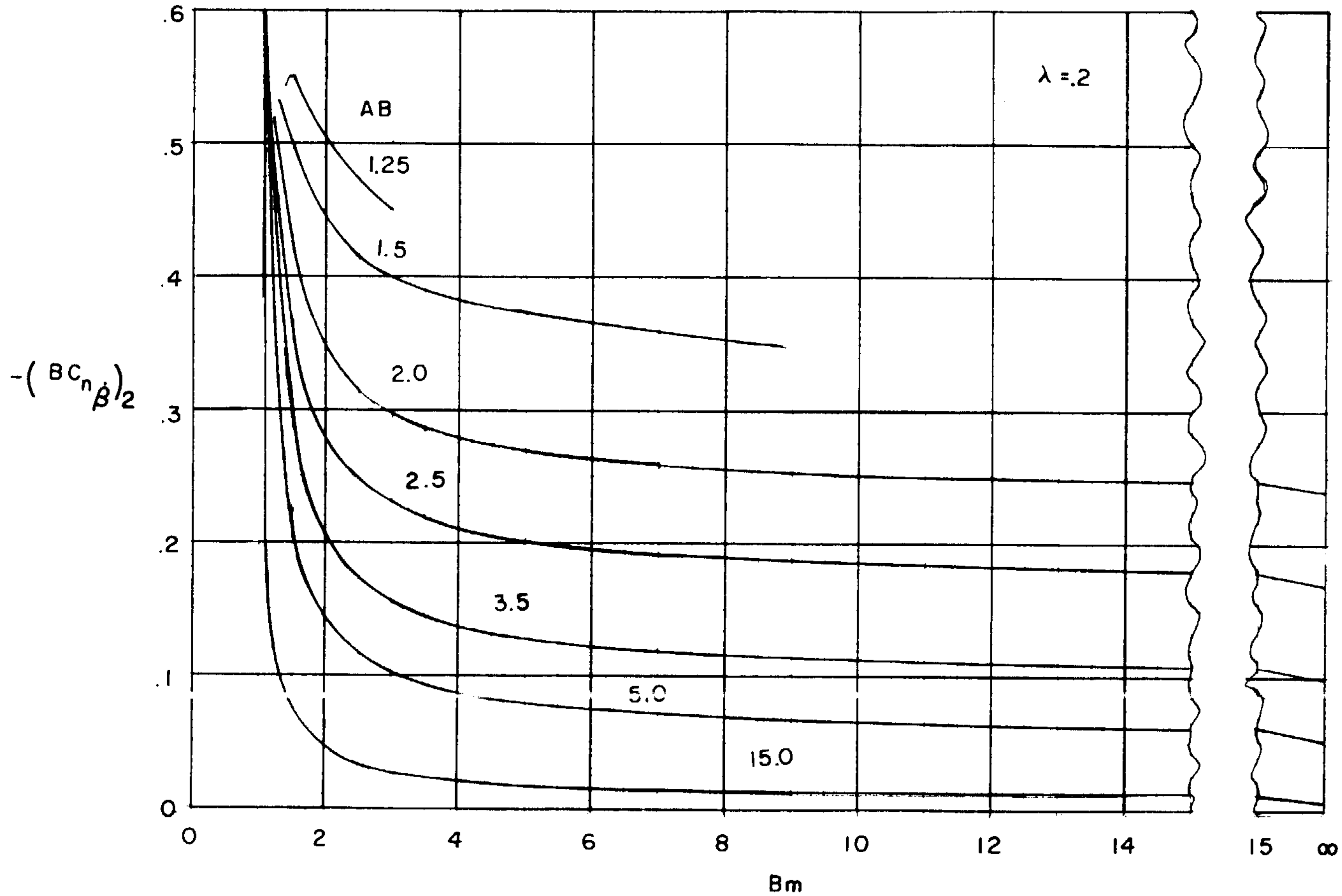

(d) Component $\left(C_{n_{\dot{\beta}}}\right)_2$, taper ratio, 0.2.

Figure 13.- Continued.

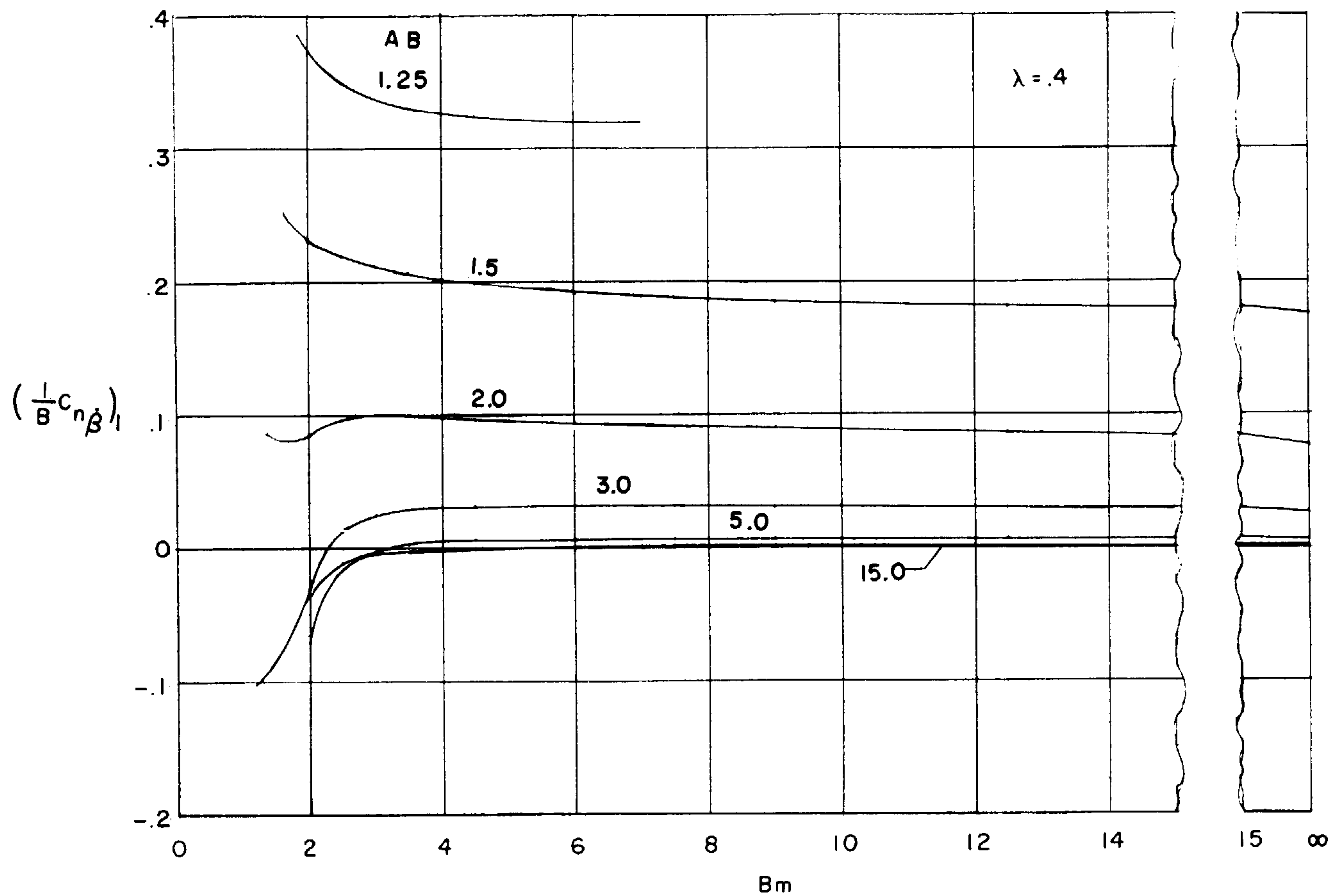

(e) Component $\left(C_{n_{\dot{\beta}}}\right)_1$; taper ratio, 0.4.

Figure 13.- Continued.

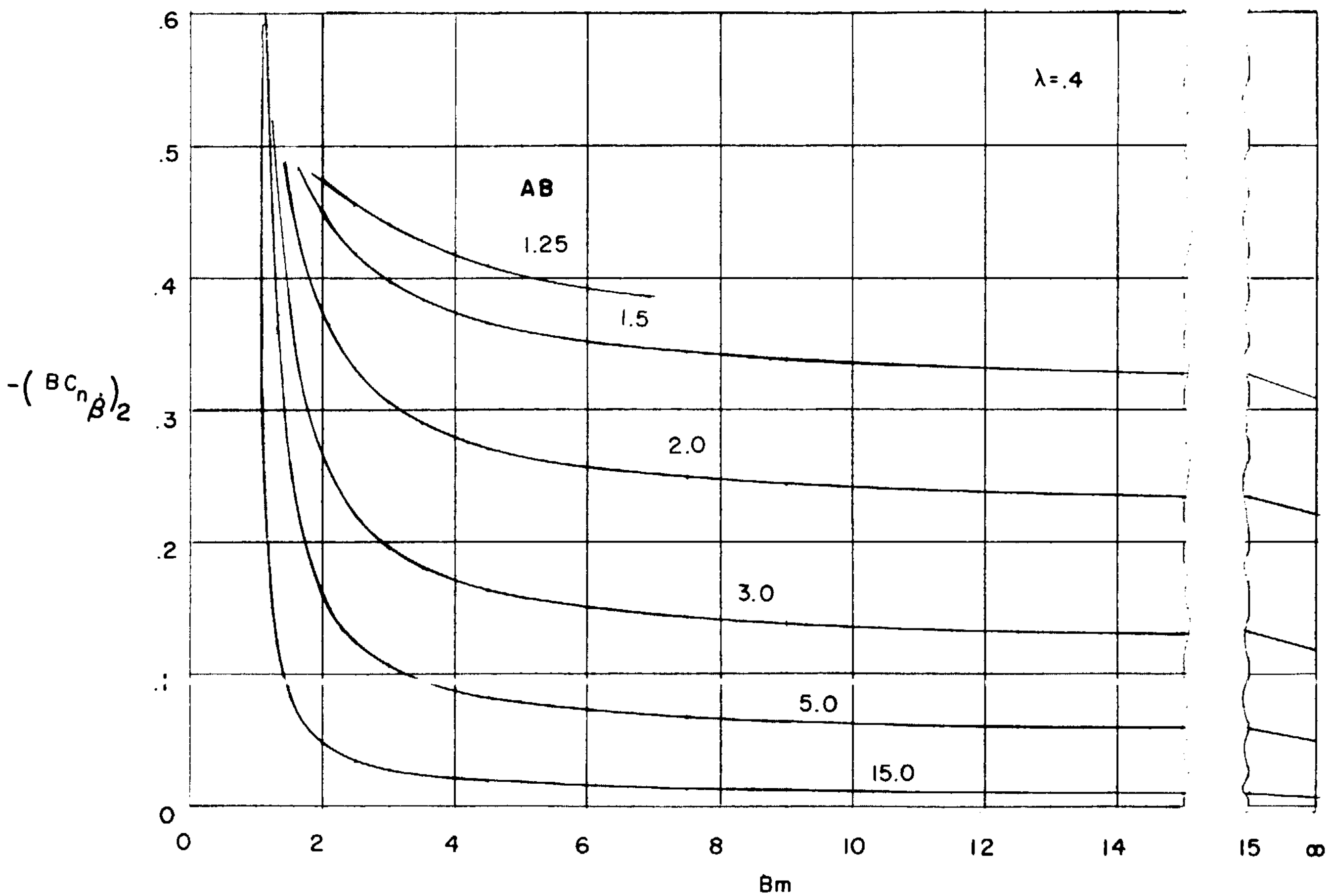

(f) Component $\left(C_{n_{\dot{\beta}}}\right)_2$; taper ratio, 0.4.

Figure 13.- Continued.

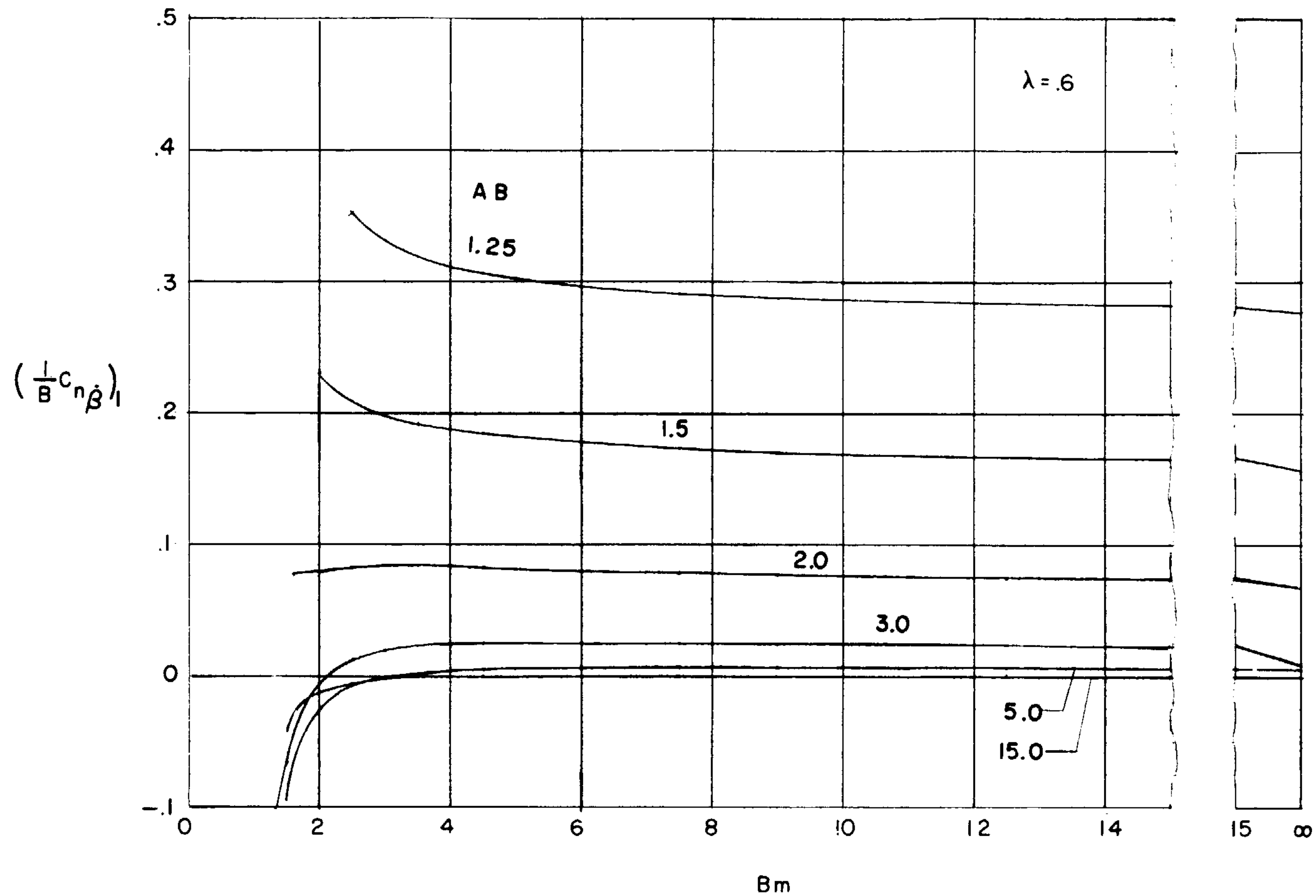

(g) Component $\left(C_{n_{\dot{\beta}}}\right)_1$; taper ratio, 0.6.

Figure 13.- Continued.

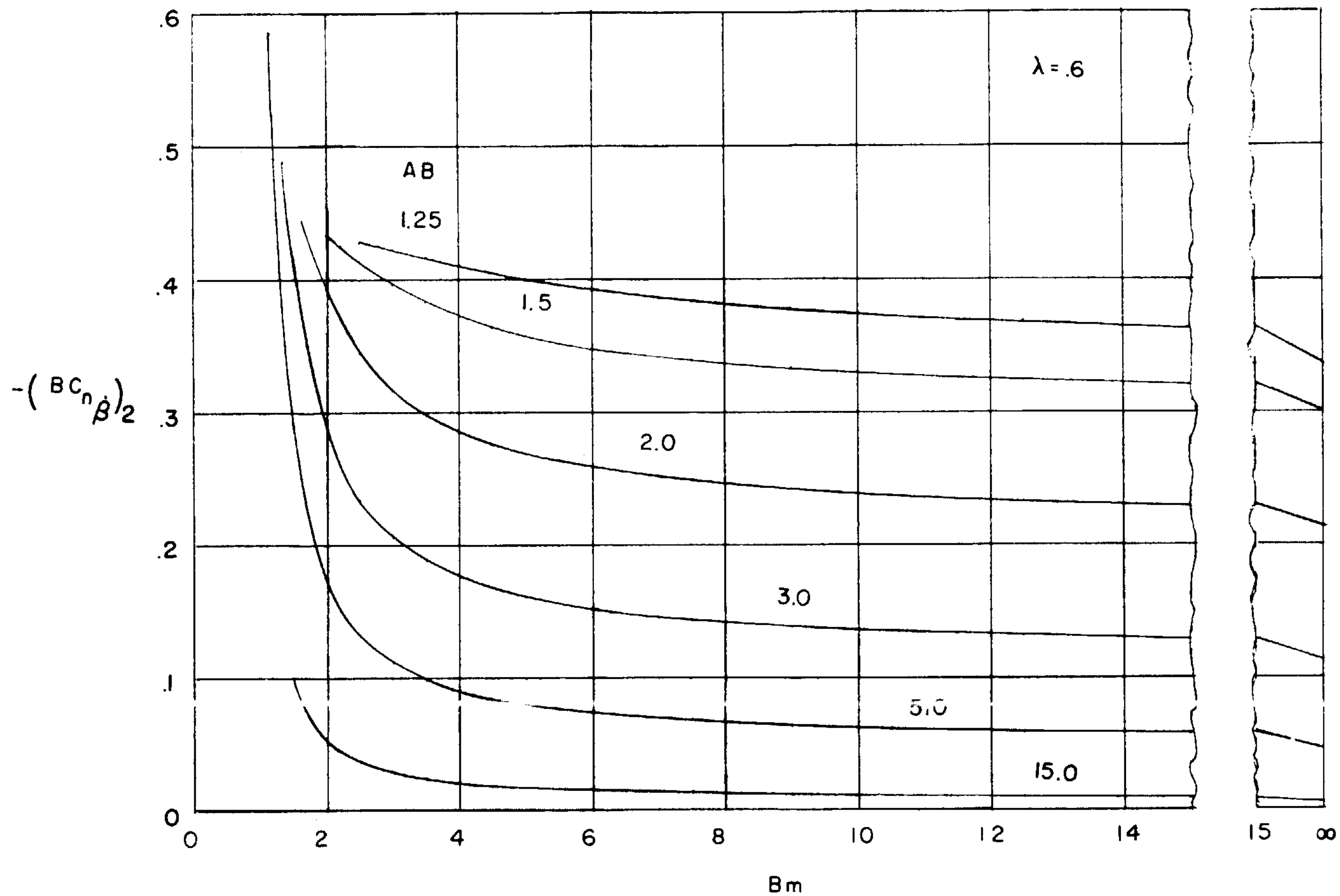

(h) Component $\left(C_{n_{\dot{\beta}}}\right)_2$; taper ratio, 0.6.

Figure 13.- Continued.

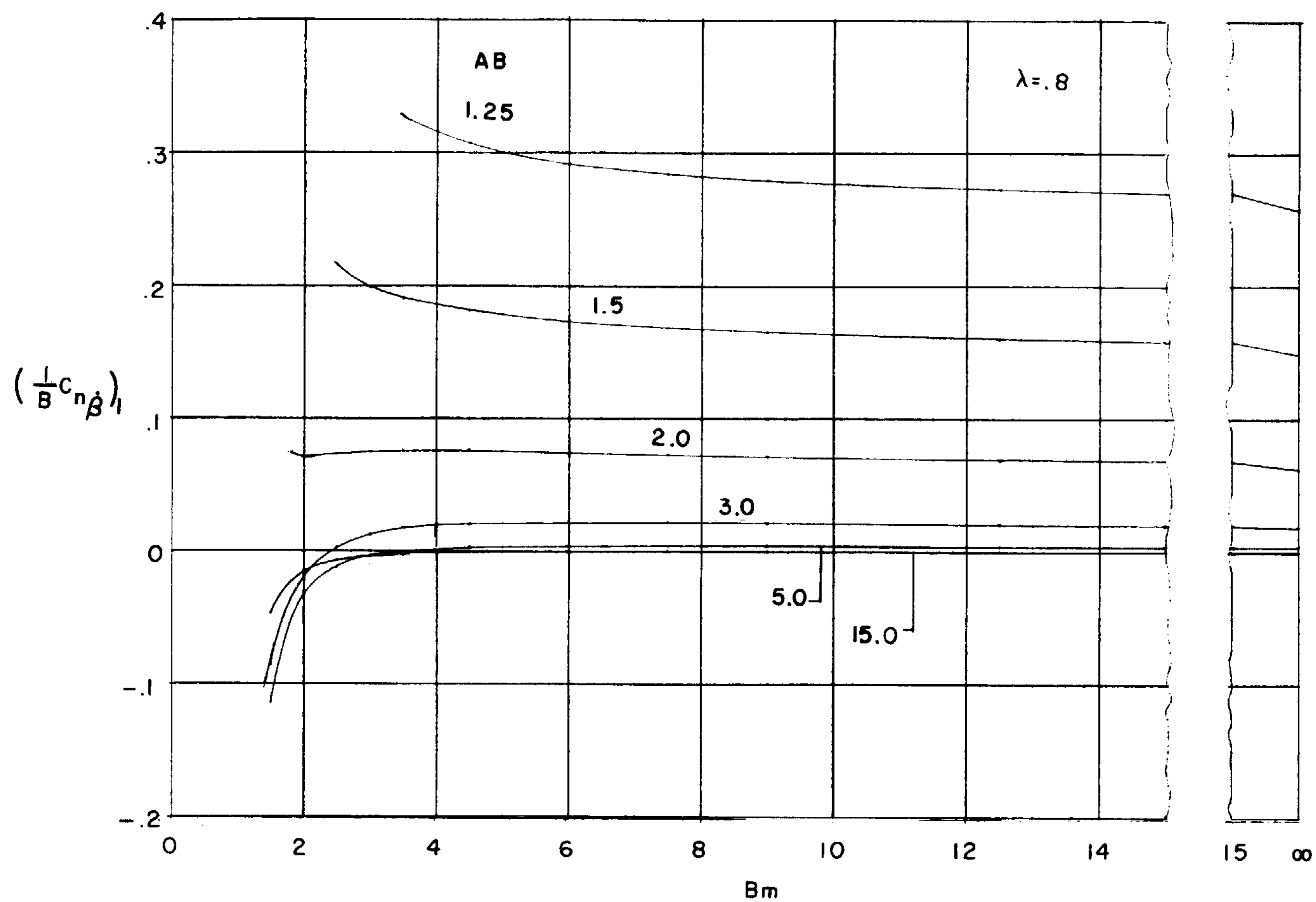

(i) Component $\left(C_{n_{\dot{\beta}}}\right)_1$; taper ratio, 0.8.

Figure 13.- Continued.

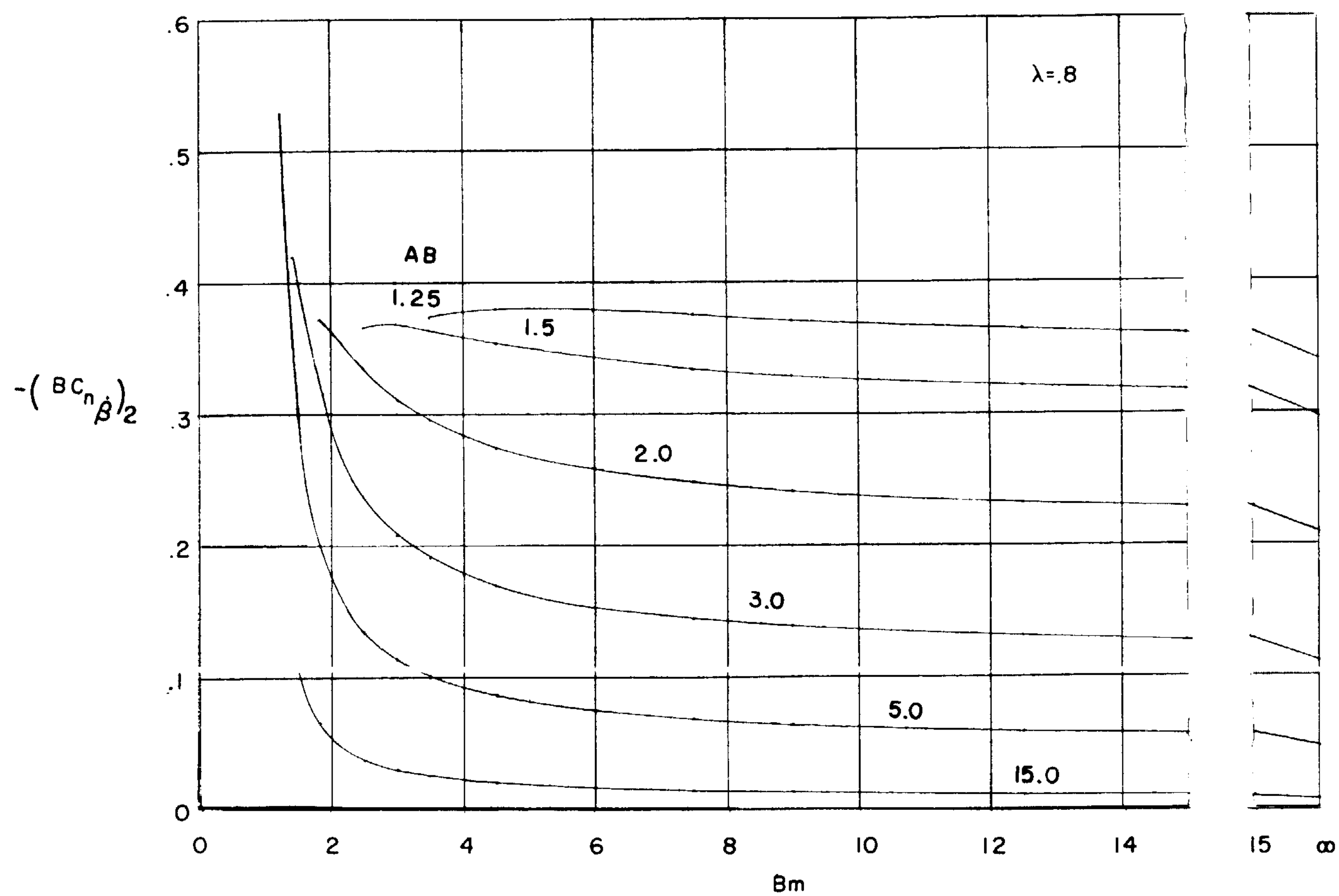

(j) Component $\left(C_{n_{\dot{\beta}}}\right)_2$; taper ratio, 0.8.

Figure 13.- Continued.

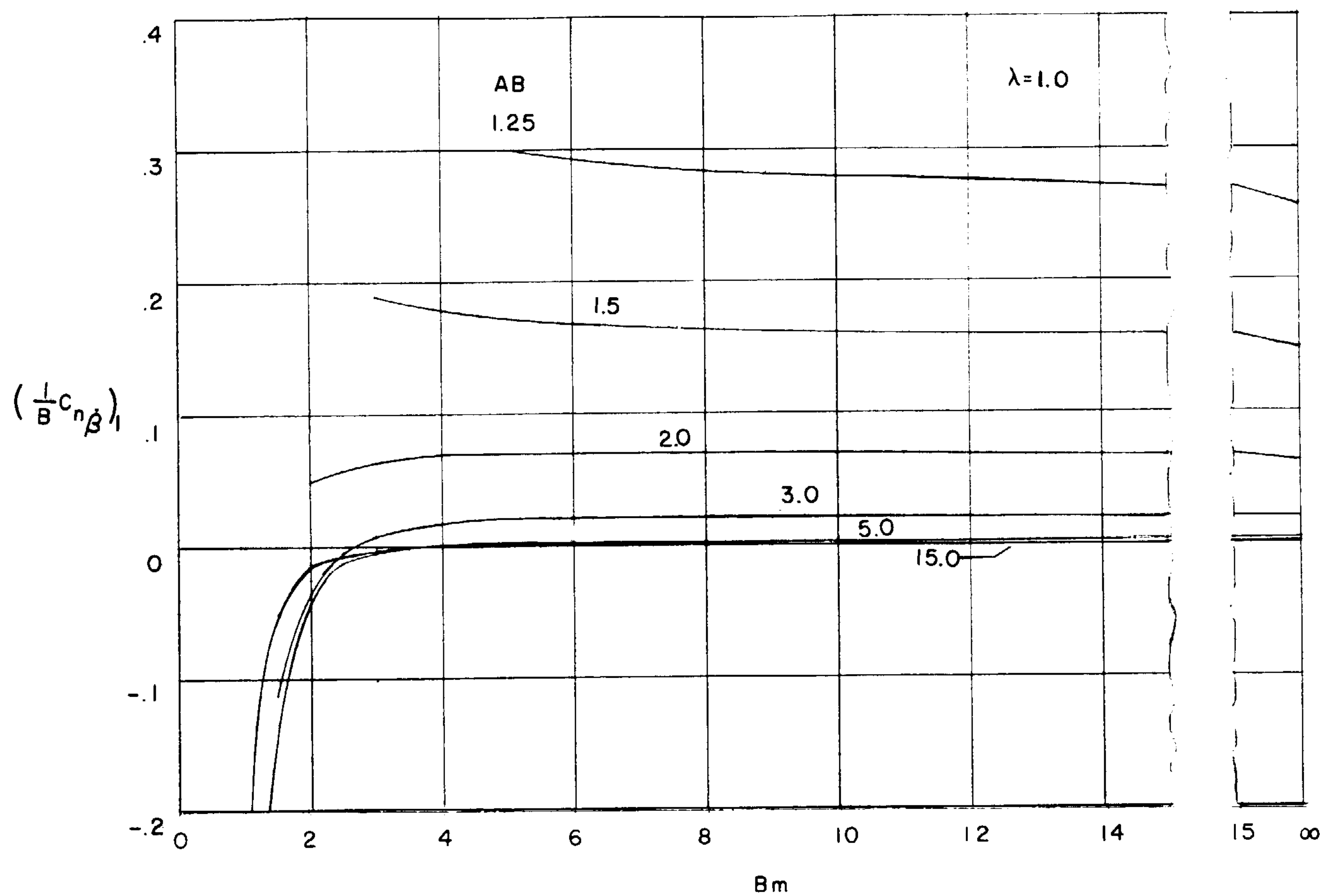

(k) Component $\left(C_{n_{\dot{\beta}}}\right)_1$; taper ratio, 1.0.

Figure 13.- Continued.

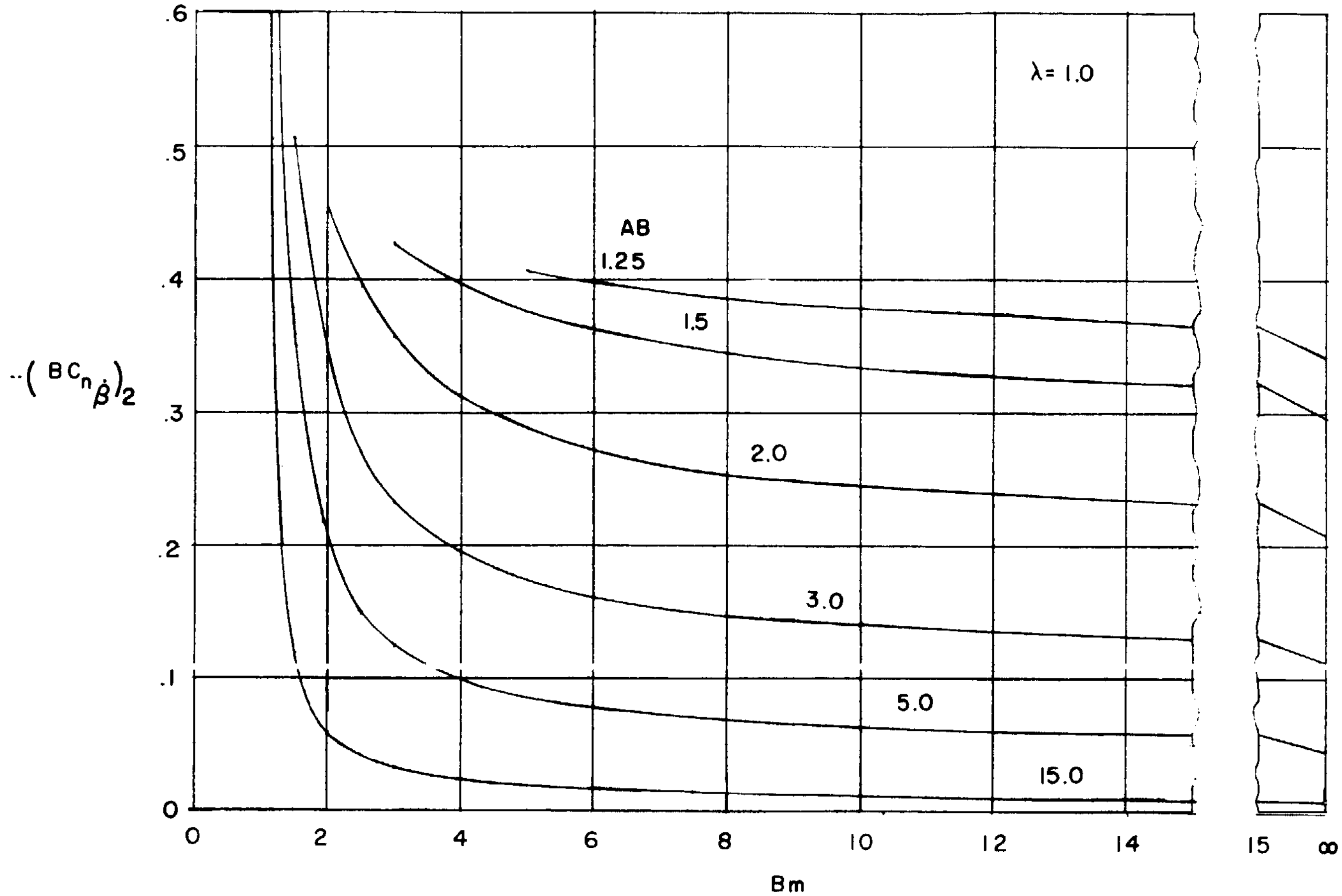

(l) Component $\left(C_{n_{\dot{\beta}}}\right)_2$; taper ratio, 1.0.

Figure 13.- Concluded.

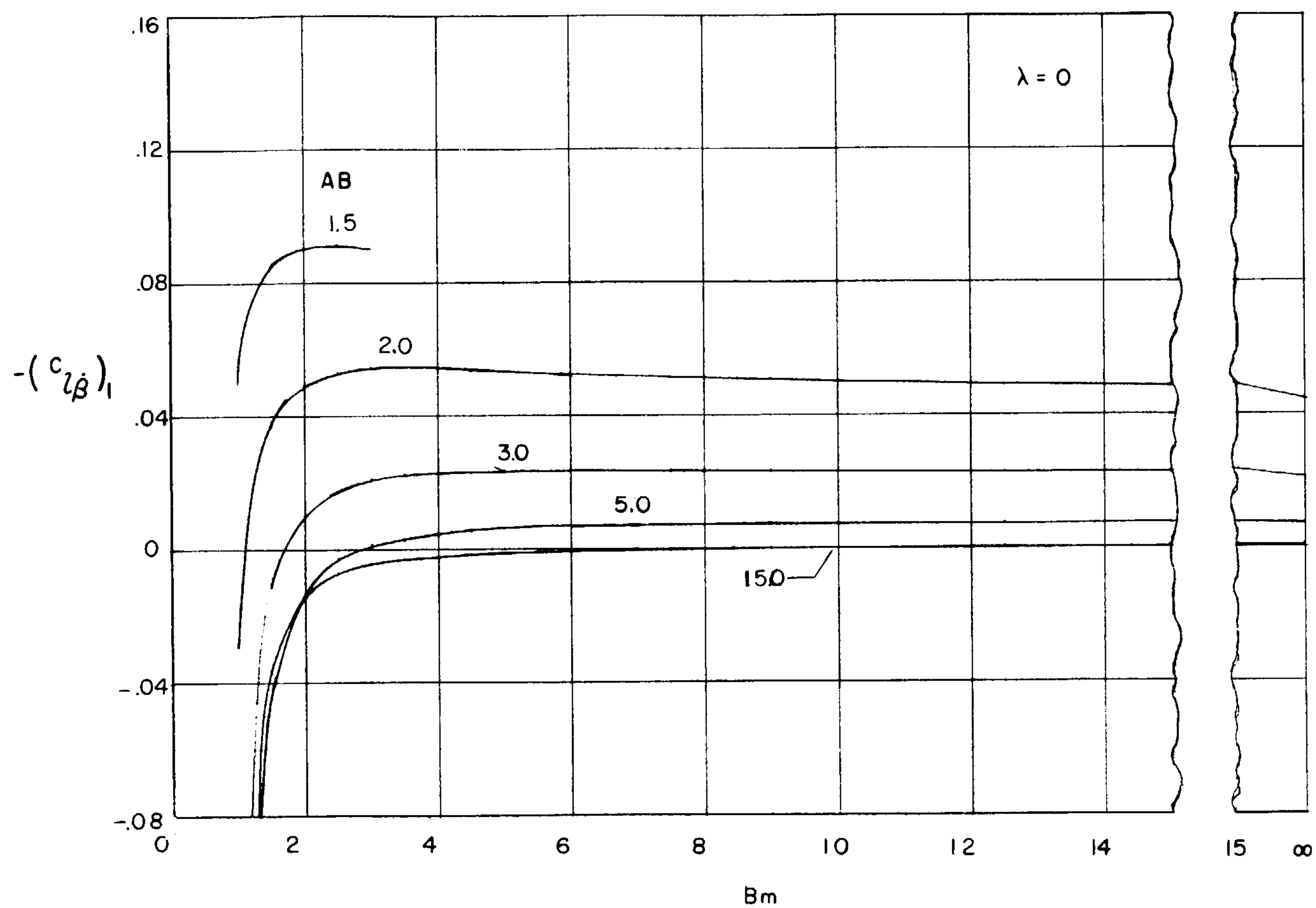

(a) Component $\left(C_{l_{\dot{\beta}}}\right)_1$; taper ratio, 0.

Figure 14.- Variation of stability derivative $C_{l_{\dot{\beta}}}$ with Mach number-geometry parameters. Note that $C_{l_{\dot{\beta}}} = \left(C_{l_{\dot{\beta}}}\right)_1 + \left(C_{l_{\dot{\beta}}}\right)_2$.

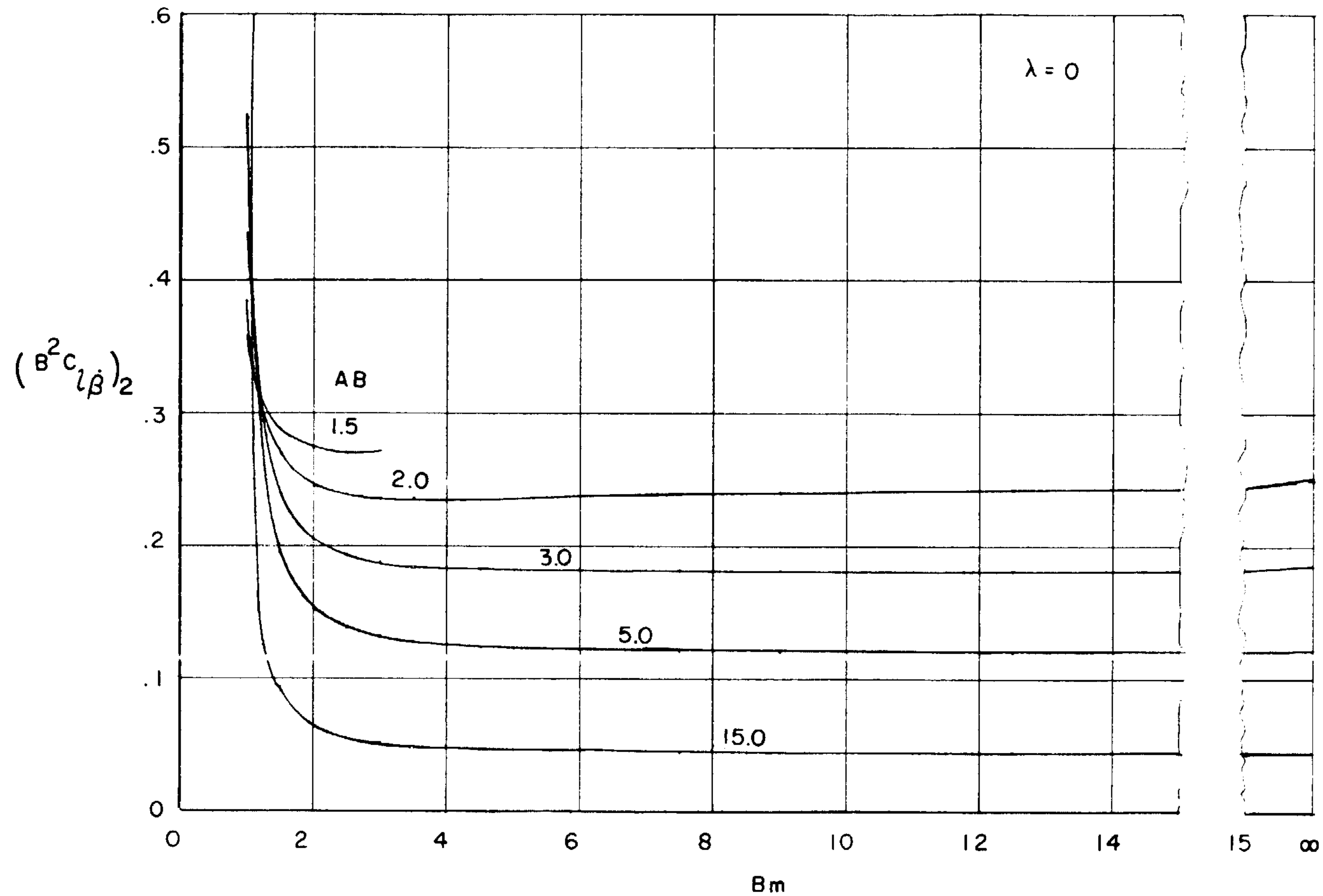

(b) Component $\left(C_{l_{\dot{\beta}}}\right)_2$; taper ratio, 0.

Figure 14.- Continued.

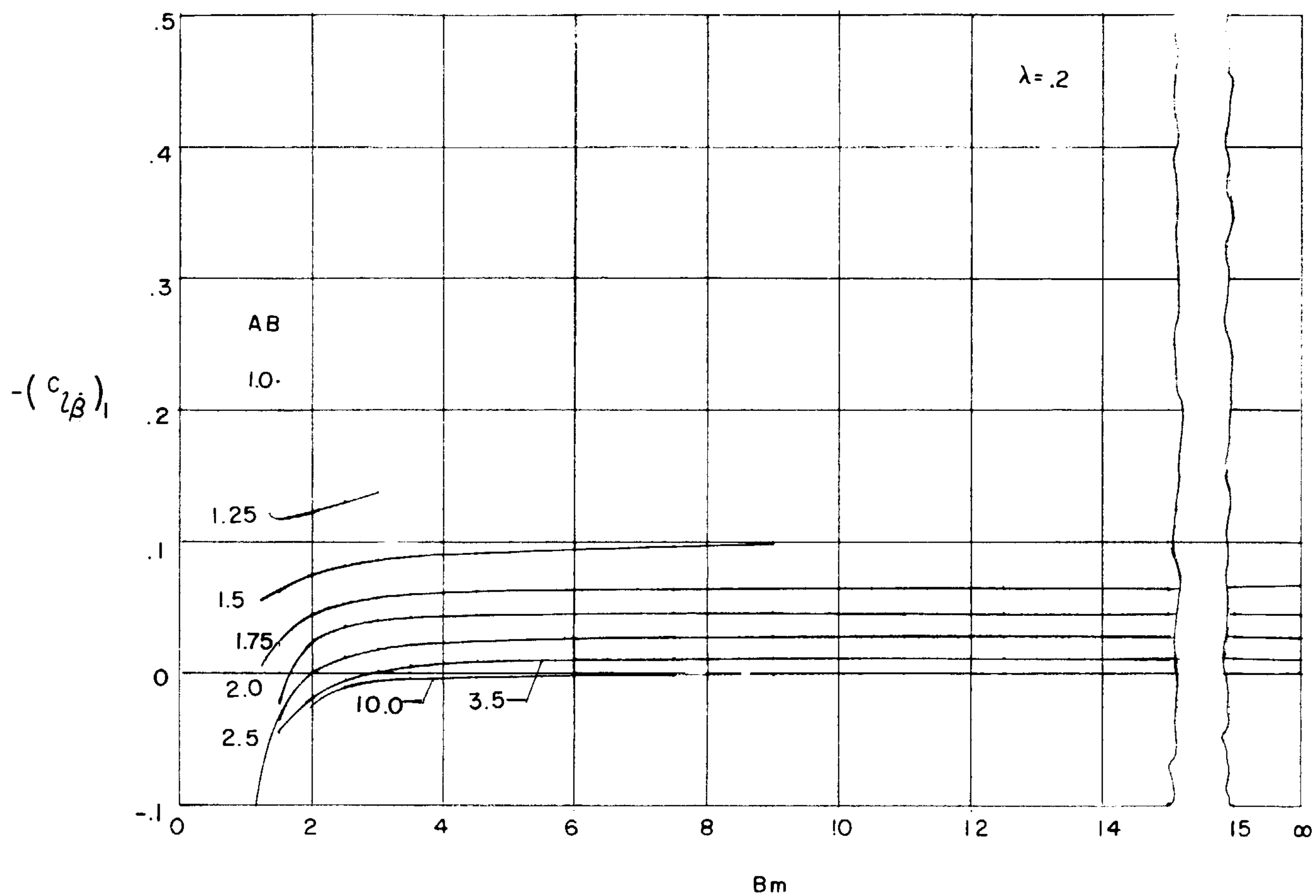

(c) Component $\left(C_{l_{\dot{\beta}}}\right)_1$; taper ratio, 0.2.

Figure 14.- Continued.

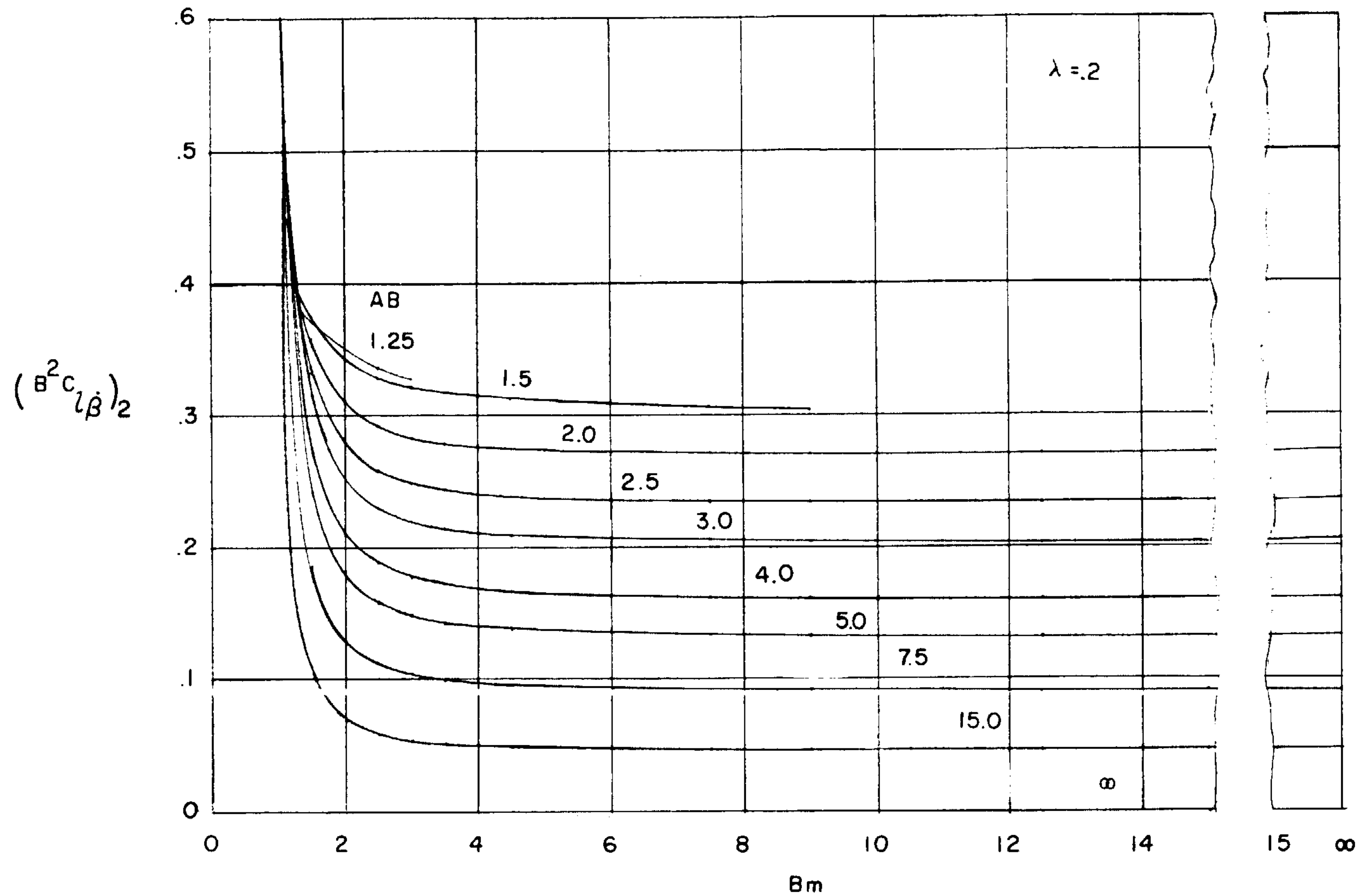

(d) Component $\left(C_{l_{\dot{\beta}}}\right)_2$; taper ratio, 0.2.

Figure 14.- Continued.

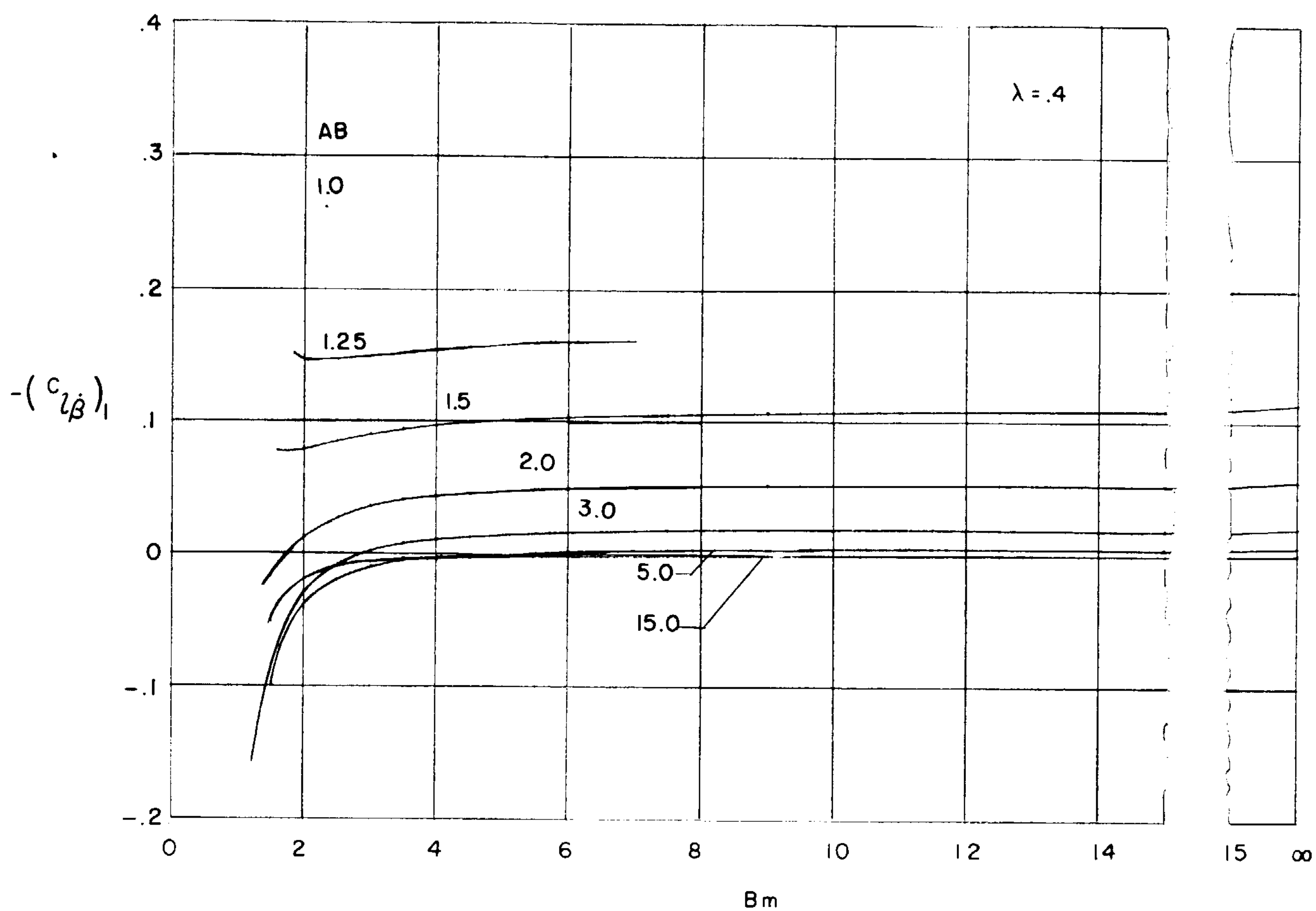

(e) Component $\left(C_{l_{\dot{\beta}}}\right)_1$; taper ratio, 0.4.

Figure 14.- Continued.

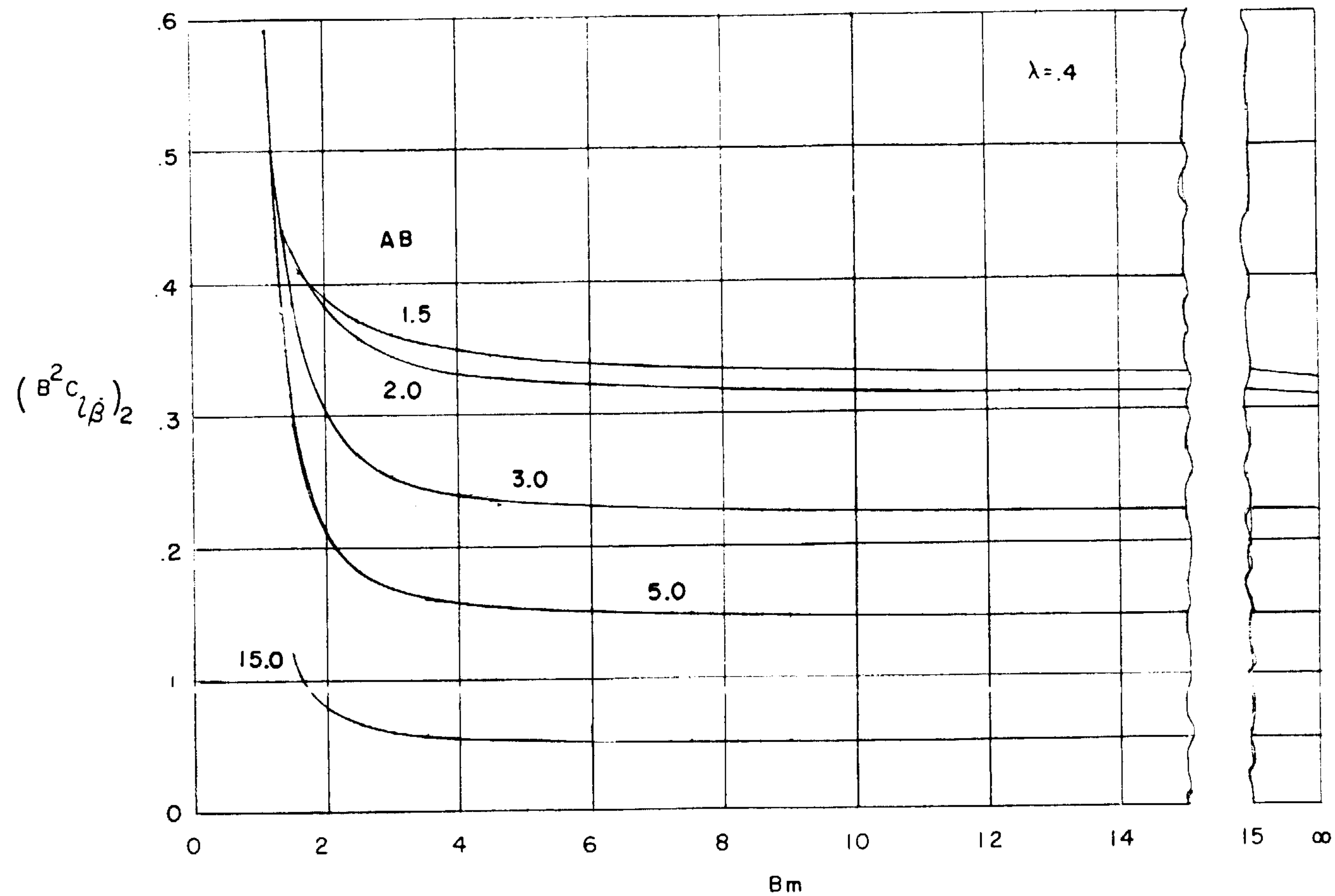

(f) Component $\left(C_{l_{\dot{\beta}}}\right)_2$; taper ratio, 0.4.

Figure 14.- Continued.

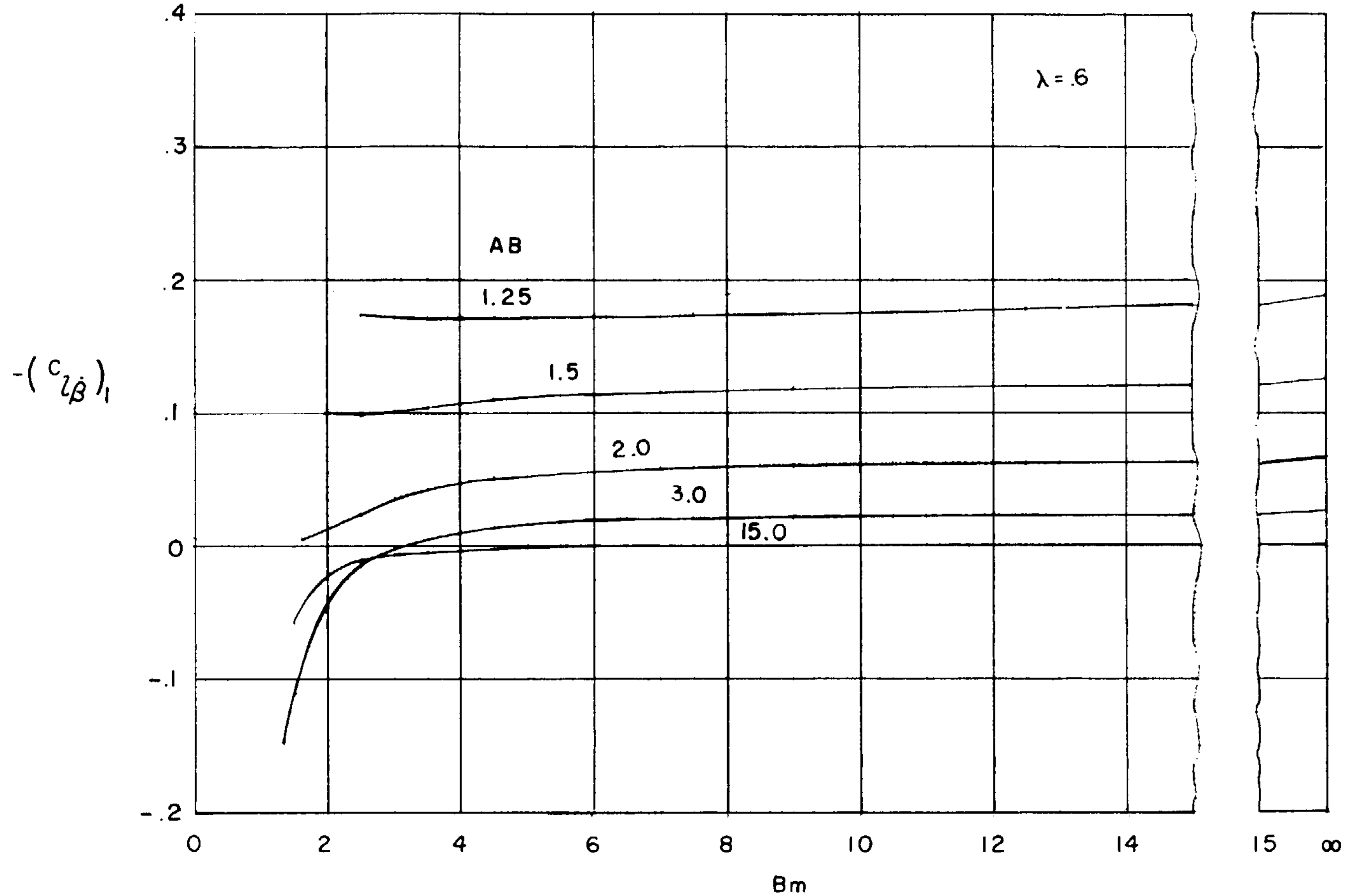

(g) Component $\left(C_{l_{\dot{\beta}}}\right)_1$; taper ratio, 0.6.

Figure 14.- Continued.

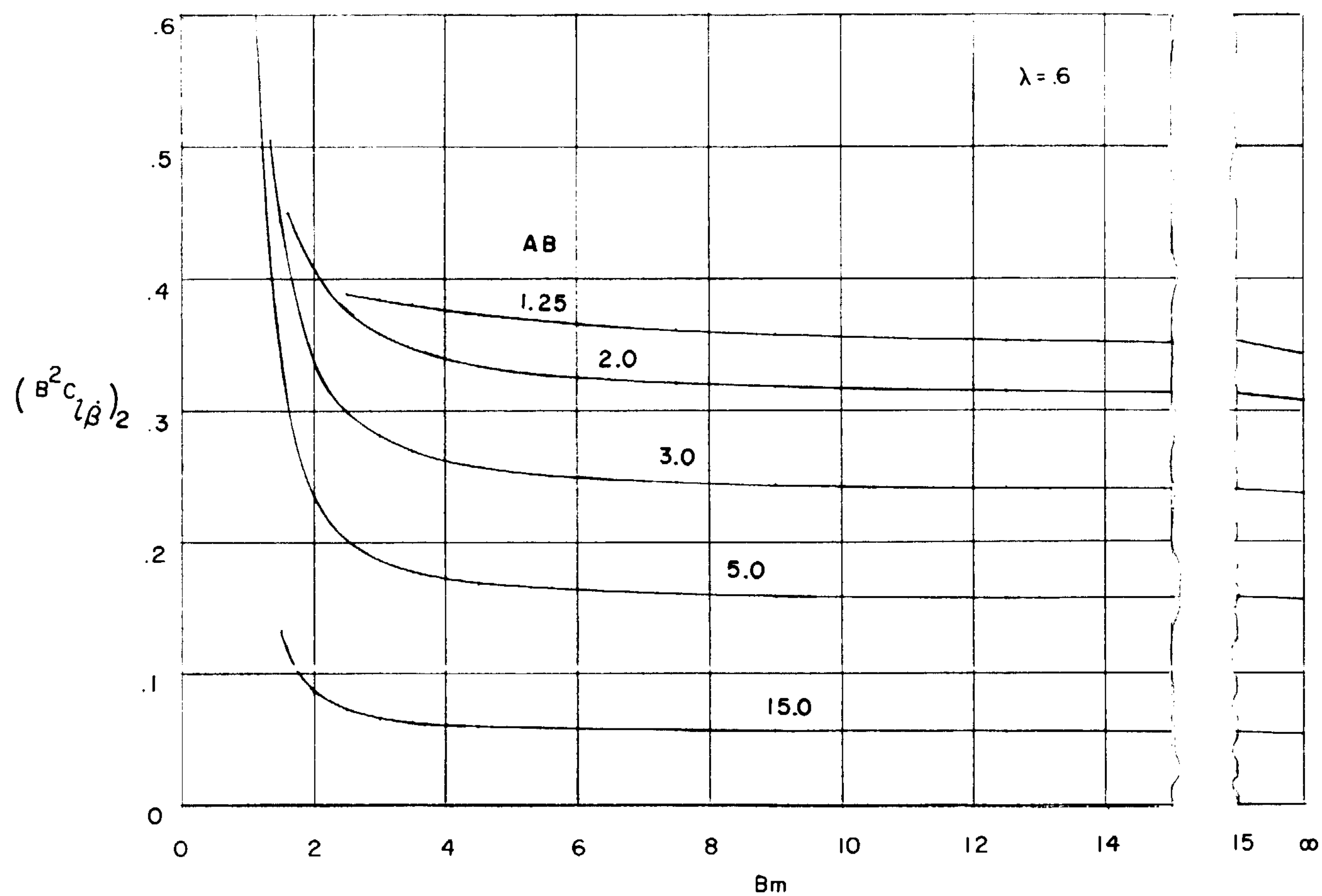

(h) Component $\left(C_{l_{\dot{\beta}}}\right)_2$; taper ratio, 0.6.

Figure 14.- Continued.

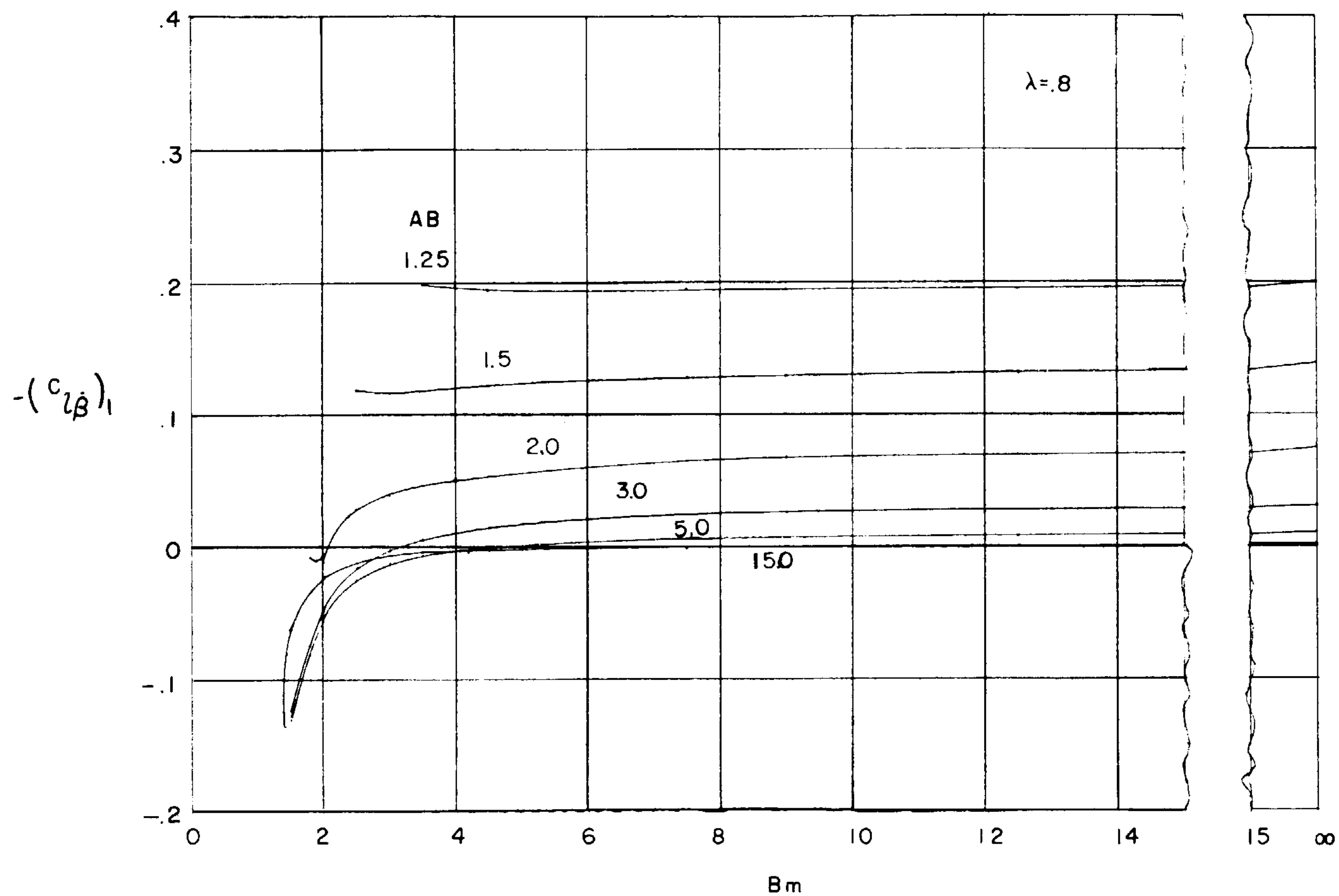

(i) Component $\left(C_{l_{\dot{\beta}}}\right)_1$; taper ratio, 0.8.

Figure 14.- Continued.

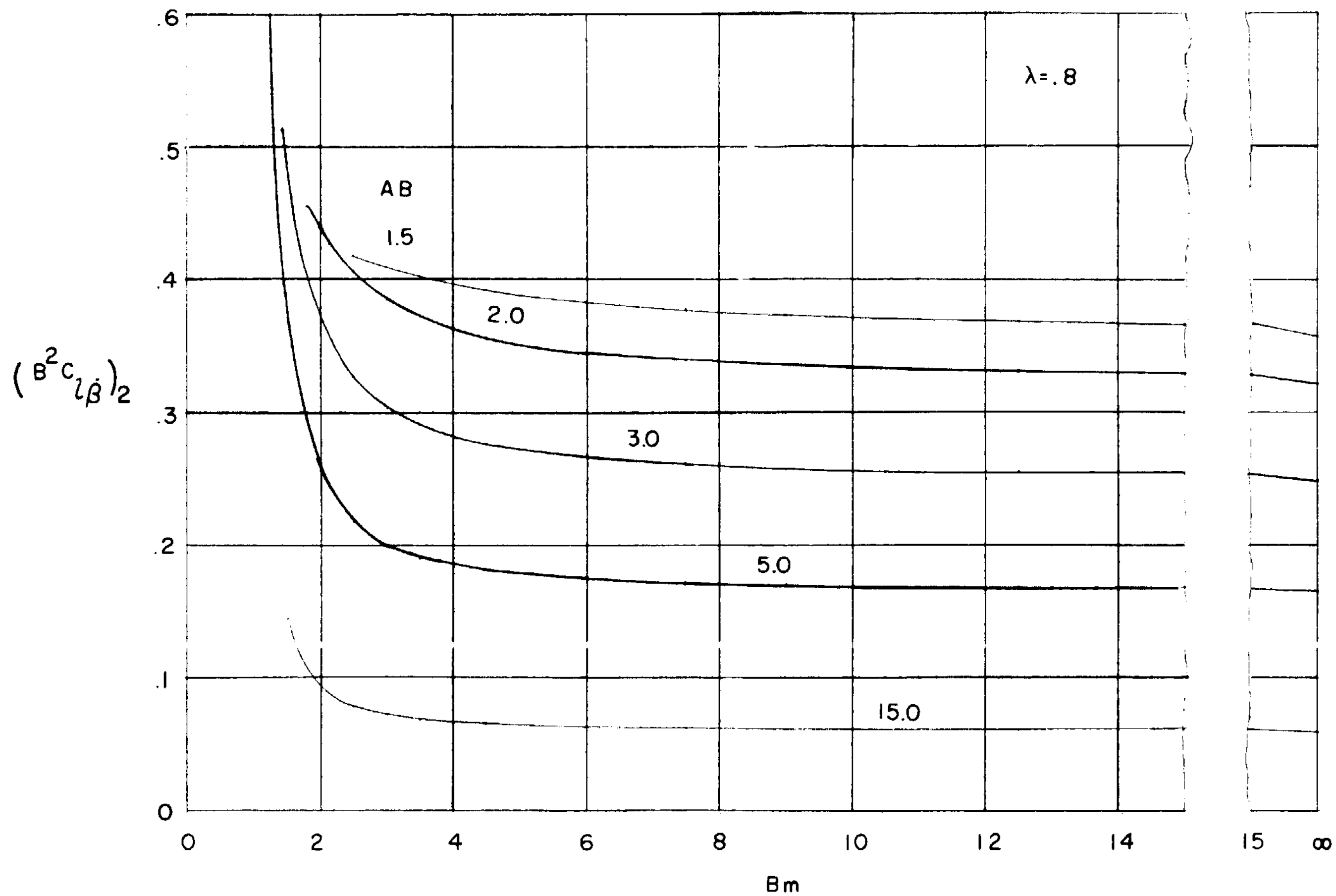

(j) Component $\left(C_{l_{\dot{\beta}}}\right)_2$; taper ratio, 0.8.

Figure 14.- Continued.

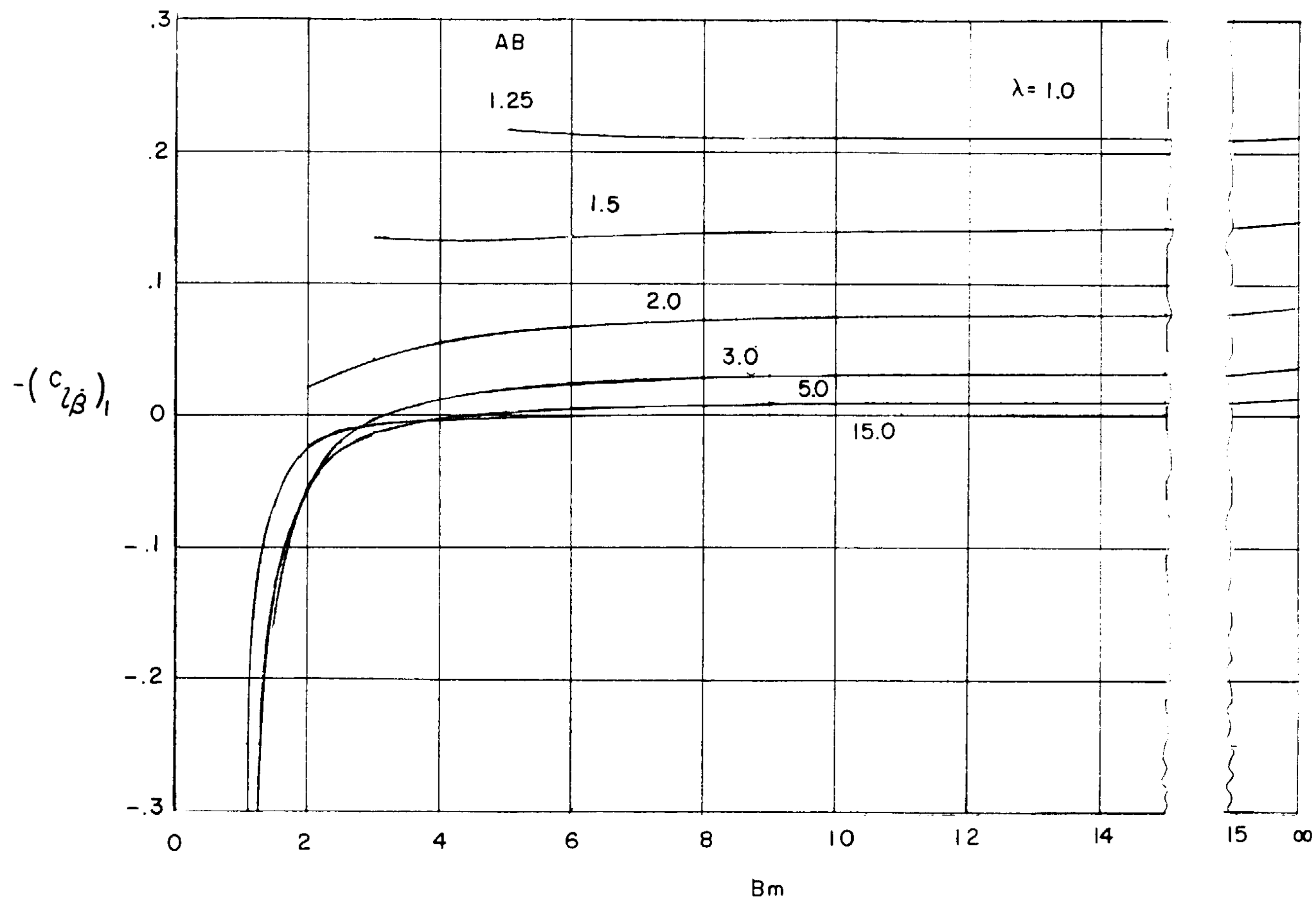

(k) Component $\left(C_{l_{\dot{\beta}}}\right)_1$; taper ratio, 1.0.

Figure 14.- Continued.

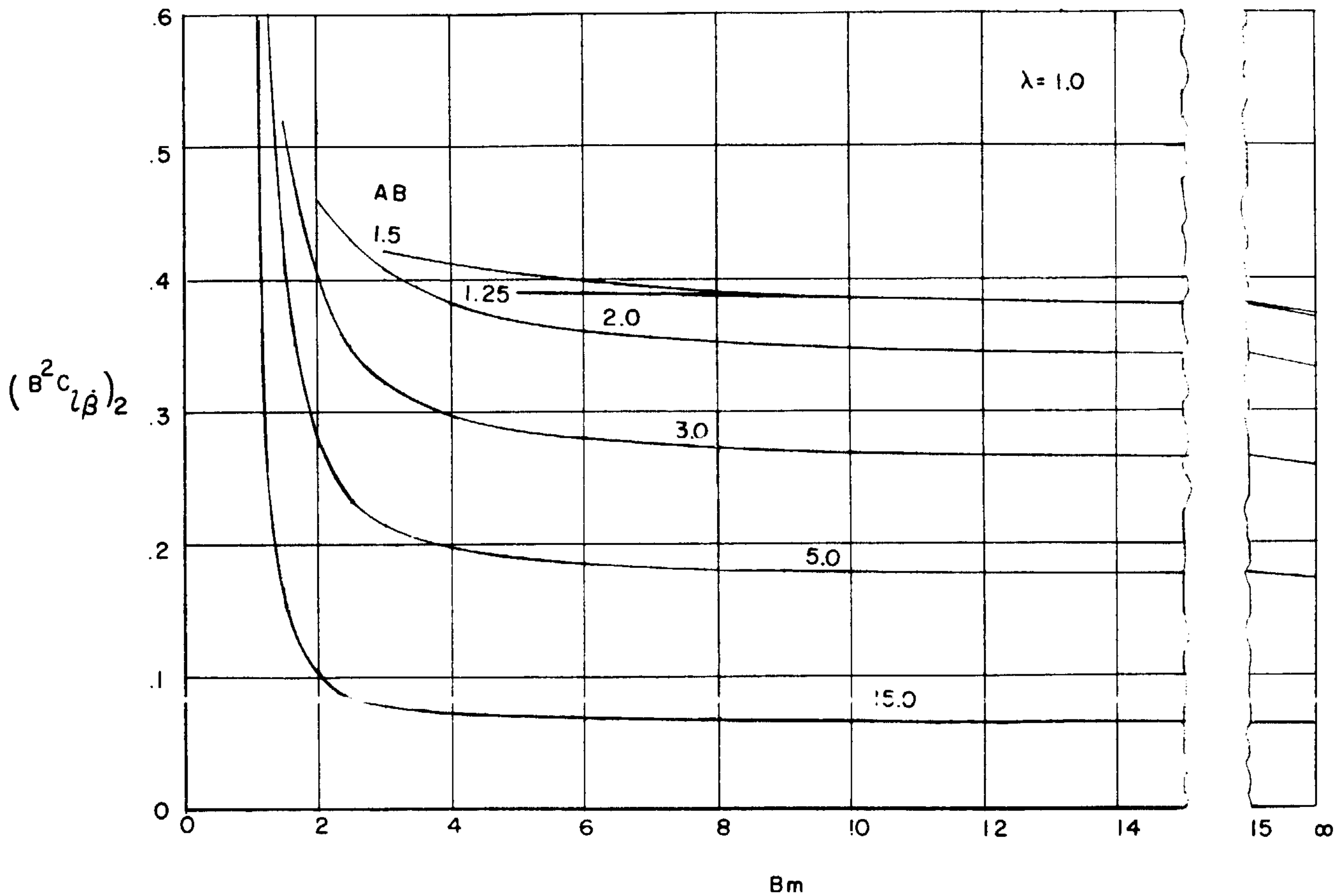

(l) Component $\left(C_{l_{\dot{\beta}}}\right)_2$; taper ratio, 1.0.

Figure 14.- Concluded.

NASA - Langley Field, Va. L-780